UNIVERSITEIT VAN PRETORIA
UNIVERSITY OF PRETORIA
YUNIBESITHI YA PRETORIA

Assessing the effects of two plants containing psychoactive compounds on the SH-SY5Y Parkinson's disease neuroblastoma cell model

by

Tidimalo Mogale

A dissertation submitted in fulfilment of the requirements for the degree

Magister Scientiae

in

Pharmacology

in the

Faculty of Health Sciences

University of Pretoria

Supervisor: Prof V Steenkamp

Co-supervisor: Mr AD de Beer

December 2024

Declaration

University of Pretoria

Faculty of Health Sciences

Department of Pharmacology

Student name: Tidimalo Mogale

Student number: 19236612

Dissertation title: Assessing the effects of two plants containing psychoactive compounds on the SH-SY5Y Parkinson's disease neuroblastoma cell model

Declaration

1. I understand what plagiarism is and I am aware of the University's policy in this regard.

2. I declare that this dissertation is my own original work. Where other people's work has been used (either from a printed source, Internet or any other source), this has been properly acknowledged and referenced in accordance with departmental requirements.

3. I have not used work previously produced by another student or any other person to hand in as my own.

4. I have not allowed and will not allow anyone to copy my work with the intention of passing it off as his or her own work.

Signature: 

Date: 06/12/24

Abstract

Parkinson's disease is an incurable, progressive disorder characterised by the loss of dopaminergic neurons in the brain's substantia nigra, primarily due to oxidative stress and mitochondrial dysfunction. Current treatments focus on symptomatic relief, by increasing endogenous dopamine levels, mimicking dopamine's function, and slowing oxidative metabolism, but do not prevent disease progression. Medicinal plants are widely used to treat neurological disorders. The aim of this study was to evaluate the effects of crude and fractionated extracts of *Catha edulis* and *Datura stramonium*, plants known for their psychoactive properties and traditional use in treating neurological disorders, on 6-hydroxydopamine (6-OHDA)-induced cytotoxicity in the SH-SY5Y human neuroblastoma cell line, a model for Parkinson's disease.

Catha edulis (leaves) and *Datura stramonium* (leaf/root mixture) crude extracts were prepared using dichloromethane/methanol (50/50). Fractionation of the extract was conducted using semi-automated C8 solid phase extraction. Ultra performance liquid chromatography mass spectrometry analysis was employed to determine the presence of chemotaxonomic markers of the plants. Inherent cytotoxicity, of the crude extract and fractions (1, 3.1, and 10 µg/mL per fraction) and the cytoprotective ability of the crude extract and fractions against SH-SY5Y cells after 6-OHDA-induced cytotoxicity (72.83 µM), was assessed using the sulforhodamine B (SRB) assay after 48 h exposure. The half maximal inhibitory concentration (IC_{50}) values of commercially purchased pure compounds (atropine and scopolamine) and their cytoprotective effects against SH-SY5Y cells were assessed using the SRB assay after 48 h exposure. Cell morphology was visualised using phase contrast microscopy. Intracellular reactive oxygen species (ROS) levels were determined using the diacetyl dichlorofluorescein assay (H_2DCFDA). Mechanistic assays were performed using a single concentration (3.1 µg/mL) due to the inconsistent dose-dependent responses and unclear results in the cytoprotection and intracellular ROS assays at lower and higher concentrations. Caspase 3/7 activity was determined by the Acetyl-Asp-Glu-Val-Asp-7-amido-4-methylcoumarin Ac-DEVD-AMC) cleavage assay and mitochondrial membrane integrity using the mitochondrial staining assay. *In silico* analysis was performed to assess the binding affinities and interactions of chemotaxonomic markers identified in the plant crude extracts with dopamine 1 and 2 (D1 and D2) receptors.

Chemotaxonomic markers detected in *C. edulis* were cathine and norephedrine, while atropine, hyoscyamine, and noradrenaline, were identified in *D. stramonium*. After 48 h treatment, both

plant extracts and fractions exhibited minimal cytotoxicity. The crude extract and all fractions of *C. edulis* provided cytoprotection of between 5.8 and 10.07%, with fraction 1 displaying the highest cytoprotection. All fractions and the crude extract of *D. stramonium* provided cytoprotection ranging from 22.56 to 34.28%, with fraction 4 exhibiting the highest cytoprotection. The IC_{50} of the pure compounds, atropine and scopolamine, was determined as 49.48 µM and 48.26 µM, respectively. Atropine increased cell density by 30.69%, and scopolamine by 27.83%, indicating cytoprotective activity for both compounds. Microscopic analysis confirmed these results. 6-Hydroxydopamine reduced the cell density by approximately 18.62%, increased intracellular ROS generation by 2.82-fold, increased caspase 3/7 activation by 4.17-fold, and increased the ratio of healthy mitochondria to cell density by 0.5 relative to the negative control. All fractions of *C. edulis* and *D. stramonium* reduced intracellular ROS levels between 1.21 to 2.66-fold and 1.12 to 1.82-fold, respectively. Additionally, all fractions significantly ($p < 0.0001$) reduced caspase 3/7 activation, with *C. edulis* and *D. stramonium* reducing this parameter by approximately 1.35-fold and 3.24-fold, respectively, compared to 6-OHDA. All fractions significantly ($p < 0.05$) decreased the mitochondrial membrane integrity of healthy mitochondria to cell density by 0.59 and 0.88 for *C. edulis* and *D. stramonium*, respectively, compared to the 6-OHDA. *In silico* analysis revealed that norephedrine and noradrenaline exhibited high binding affinities for both D1 and D2 receptors, with the binding free energy of -4.34 and -6.73 kJ/mol for D1, and -5.91 and -7.43 kJ/mol for D2, respectively.

Both plant extracts and their fractions maintained cell viability, provided cytoprotection, reduced ROS and caspase 3/7 activity, and preserved mitochondrial integrity. These findings suggest that C*. edulis* and *D. stramonium* extracts could provide protection against cellular damage caused by Parkinson's disease, indicating potential for future research into their therapeutic applications. Further studies should explore the mechanisms and efficacy of these extracts *in vivo*.

Acknowledgments

I would like to express my heartfelt gratitude to those who have supported me throughout my dissertation journey:

First, a huge thank you to my supervisor, Prof. Vanessa Steenkamp. Your wisdom, patience, and belief in my potential have meant the world to me. You've guided me through the ups and downs of this journey, and I couldn't have asked for a better mentor.

To my co-supervisor, Mr Daniel de Beer, thank you for your insight and for always challenging me to think deeper. Your feedback pushed me to refine my work and made this project so much stronger.

To my parents, words can't express how grateful I am for your endless love and support. Thank you for being my rock, cheering me on every step of the way, and for all the sacrifices you've made to help me reach my dreams.

To my friends, thank you for lifting my spirits, reminding me to take breaks, and being there when I needed to vent or celebrate. You've made this journey so much lighter and filled with laughter.

Lastly, thank you to the National Research Foundation for funding. Your financial support allowed me to dedicate myself to this research, and I'm so appreciative for the opportunity.

Thank you all for being a part of this journey.

List of abbreviations

Symbols and numerical indicators

α-SN	Alpha-synuclein
˚C	Degrees Celsius
e^+	Electron
µg	Microgram
µL	Microliter
µM	Micromolar
%	Percentage
2D	2-Dimentional
3-MT	3-Methoxytyramine
6-OHDA	6-Hydroxydopamine
v/v	Volume per volume
w/v	Weight per volume

Abbreviations/Acronyms

Ac-DEVD-AMC	N-Acetyl-Asp-Glu-Val-Asp-7-amido-4-Methylcoumarin, Caspase-3 Substrate (Fluorogenic)
ACh	Acetylcholine
ACN	Acetonitrile
ADP	Adenosine diphosphate
ANOVA	Analysis of variance
Apaf-1	Apoptotic protease activating factor 1
ATCC	American Tissue Culture Collection
ATP	Adenosine triphosphate
Bax	Bcl-2 associated X protein
BBB	Blood brain barrier
Bcl-2	B-cell lymphoma protein 2

CAT	Catalase
C I	Complex I
C II	Complex II
C III	Complex III
C IV	Complex IV
Ca^{2+}	Calcium
CHAPS	3-[(3-cholamidopropyl) dimethylammonio]propane-1-sulfonate
CNS	Central nervous system
CO_2	Carbon dioxide
COMT	Catechol-*O*-methyltransferase
CoQ	Coenzyme Q
Cyt c	Cytochrome c
DA	Dopamine
DART-TOF-MS	Direct analysis in real time- time of flight-mass spectrometry
DAT	Dopamine transporter
DCM	Dichloromethane
dH_2O	Deionised water
DLP-1	Dynamin-like protein 1
DMSO	Dimethyl sulfoxide
DNA	Deoxyribonucleic acid
DMEM	Dulbecco's Modified Eagle's Medium
DOPA	3,4-Dihydroxyphenylalanine
DOPAC	3,4-Dihydroxyphenylacetic acid
DPPH	2,2-Diphenyl-1-picrylhydrazyl
EDTA	Ethylenediaminetetraacetic acid
ETC	Electron transport chain
EtoAc	Ethyl acetate
ESI	Electrospray ionisation

FAD	Oxidised flavin adenine dinucleotide
$FADH_2$	Reduced flavin adenine dinucleotide
FCS	Foetal calf serum
FI	Fluorescence intensity
FITC	Fluorescein isothiocyanate
g	Gram(s)
g	Relative centrifugal force
GSH	Glutathione
GTPase	Guanosine triphosphatase
h	Hour(s)
H^+	Hydrogen ion/ Proton
H_2DCF-DA	Dihydrodichlorofluorescein diacetate
H_2O	Water
H_2O_2	Hydrogen peroxide
HBSS	Hank's Balanced Salt Solution
HEPES	2-[4-(2-hydroxyethyl)piperazin-1-yl]ethane sulfonic acid
HVA	Homovanillic acid
IC_{50}	Half maximal inhibitory concentration
IL-1β	Interleukin-1β
IL-8	Interleukin-8
kDa	Kilodaltons
L	Liter
L-dopa	Levodopa
LBs	Lewy bodies
LC-MS	Liquid chromatography–mass spectrometry
LRRK-2	Leucine-rich repeat kinase

MAO (A or B)	Monoamine oxidase (A or B)
MAOI	Monoamine oxidase inhibitor/s
MDPV	3,4-Methylenedioxypyrovalerone
MeOH	Methanol
mg	Milligram
min	Minute(s)
mL	Milliliter
mM	Millimolar
MLKL	Mixed lineage kinase domain-like protein
MMP	Mitochondrial membrane potential
MPP^+	N-methyl-4-phenyl pyridine
MPT	Mitochondrial permeability transition
MPTP	1-Methyl-4-phenyl-1,2,3,6-tetrahydropyridine
MTBE	Methyl tert-butyl ether
MtDNA	Mitochondrial deoxyribonucleic acid
MTT	3-(4,5-dimethylthiazol-2-yl)-2,5-diphenyl tetrazolium bromide
nM	Nanomolar
NAD^+	Nicotinamide adenine dinucleotide
NADH	Reduced nicotinamide adenine dinucleotide
O_2^-	Oxide anion
O_2	Dioxygen
OS	Oxidative stress
PARP	Poly (ADP-ribose) polymerase
PBS	Phosphate-buffered saline
PC12	Rat pheochromocytoma
PD	Parkinson’s disease
Pink-1	Phosphatase and tensin homolog induced kinase-1
PMSF	Phenylmethylsulphonyl fluoride
RA	Retinoic acid

RFU	Relative fluorescence unit
RIPK	Receptor-interacting protein kinases
RNA	Ribonucleic acid
ROS	Reactive oxygen species
SANBI	South African National Biodiversity Institute
SEM	Standard error of the mean
SN	Substantia nigra
SNpc	Substantia nigra pars compacta
SOD	Superoxide dismutase
SPE	Solid phase extraction
SRB	Sulforhodamine B
TCA	Trichloroacetic acid
TH	Tyrosine hydroxylase
TNF- α	Tumour necrosis factor alpha
TRIS	Trisaminomethane
TrypLE	Trypsin-like enzymes
UPLC-Q-TOF-MS	Ultra-performance liquid chromatography-quadrupole time-of-flight mass spectrometry
VMAT-2	Vesicular monoamine transporter 2
WHO	World Health Organization

List of Figures

List of Tables

Table of Contents

Chapter 1: Introduction

Neurodegenerative diseases are neurological conditions that lead to targeted impairment and sustained degradation of connections between neurons in the central nervous system (CNS).[1] These diseases can impact various aspects, including motor function, cognitive abilities, speech, and respiratory capacity.[1] Examples of neurodegenerative diseases include Alzheimer's disease, Parkinson's disease (PD), spinocerebellar ataxia, and frontotemporal dementia.[2] In 2019, more than 50 million individuals were diagnosed with a neurological disorder globally, a figure that is projected to rise to 152 million by 2060.[2] Globally, these neurological diseases exhibit an incidence of 0.15% in individuals aged between 40 to 59 years, 1.52% in those aged 60 to 79 years, and 1.90% in individuals over 80 years.[3] The prevalence of neurological disorders in Europe is 1.6% for males and 1% for women aged 65 to 69, increasing to ~12.6% for those aged 85 to 89.[4]

Age is the primary risk factor for the development of neurodegenerative diseases, which include PD.[5] Genetic and environmental factors also play a significant role in facilitating the onset of these disorders. Hereditary gene mutations, where faulty genes are passed from parents to offspring, are implicated in various neurological conditions.[6] Additionally, prolonged exposure to specific chemicals and toxins, such as 1-methyl-4-phenyl-1,2,3,6-tetrahydropyridine (MPTP) and rotenone, have been associated with the development of PD.[6]

Neurodegenerative disorders are primarily classified by their characteristic signs and symptoms, including memory loss, tremors and muscle rigidity.[6] Diagnosing these disorders is challenging and often requires pathological examination for confirmation, with disease variability only verifiable at autopsy. Efforts are underway to develop reliable molecular markers for monitoring disease progression in clinical trials.[7]

The World Health Organization (WHO) has warned that unless urgent measures are taken worldwide, the neurological burden will become a critical and unsustainable public health risk.[8] Although efficient treatments are sorely needed, such will only become attainable when the fundamental causes and processes of these neurological diseases are completely understood.

1.1 Parkinson's disease

1.1.1 Prevalence of Parkinson's disease

Parkinson's disease is the second most common neurological disorder globally, affecting approximately 1% of people over 60 and over 4% by age 85.[9] Physical impairment and morbidity due to PD progress more rapidly than those caused by other neurodegenerative disorders. Over the past 25 years, the global prevalence of PD has doubled, with estimates from 2019 indicating that more than 8.5 million people were affected by the condition.[9] Although incidence rates have risen significantly over the past 20 years, the underlying causes remain largely unknown.[10]

Parkinson's disease was initially believed to be solely caused by environmental factors. However, recent studies indicate that a complex interaction between genetics and environmental factors contributes to disease progression. As a result, PD is recognised as a complex neurodegenerative condition resulting in a range of clinical manifestations.[11]

The symptoms of PD include tremors, difficulties with balance, bradykinesia (slowness of movement), and stiffness.[12,13] The emergence of these motor symptoms is generally connected to the gradual degeneration of dopaminergic neurons, specifically in the substantia nigra pars compacta (SNpc). This neuronal degeneration leads to dopamine (DA) deficiency in the striatum, a deep brain region involved in promoting voluntary movement.[14] As a result, the basal ganglia, a collection of subcortical nuclei crucial for movement regulation, becomes impaired. This dysfunction of the basal ganglia is the primary cause of movement disorders and impaired speech.[14,15] In addition to motor symptoms, PD is coupled with various non-motor symptoms, some of which can manifest many years before motor impairment.[11] These include constipation, sensory impairment, insomnia, and different neuropsychiatric symptoms. Despite this, motor symptoms remain the primary clinical diagnostic criterion for PD.[16]

1.1.2 Types of Parkinson's disease

1.1.2.1 *Sporadic Parkinson's disease*

Sporadic PD is the most common form of PD, occurring randomly in the population without a clear hereditary or genetic cause. It is believed to result from a complex interaction of environmental factors, aging, and genetic susceptibility rather than a single identifiable gene mutation.[17] Environmental pollutants, including pesticides like paraquat and toxins such as rotenone and MPTP, have been linked to sporadic PD. 1-Methyl-4-phenyl-1,2,3,6-tetrahydropyridine, in particular, targets and degrades the nigrostriatal pathway, closely mimicking the clinical features of idiopathic parkinsonism.[17-19] In addition to exposure to these neurotoxic substances, other factors such as living in rural areas, consuming groundwater, and working in professions like mining and farming, where exposure to toxic chemicals is more common, have been associated with a higher incidence of PD in individuals without a familial history of the disease.[20,21] Age is also a major risk factor for the development of sporadic PD, with the condition often linked to mitochondrial dysfunction, neuroinflammation, and oxidative stress (OS).[22] Most cases of PD are idiopathic, affecting individuals primarily between the ages of 55 and 65, with rare occurrences before 50.[23,24]

1.1.2.2 Familial Parkinson's disease

Familial Parkinson's disease is an inherited form of PD caused by defective genes passed from parents to their offspring.[22] Only 10–15% of cases are familial and attributed to Mendelian inheritance. Mutations in five genes are associated with familial PD: α-synuclein (α-SN), DJ-1, leucine-rich repeat kinase 2 (LRRK2), phosphatase and tensin homolog-induced kinase-1 (PINK1), and parkin.[22] The pathological hallmark common to both idiopathic and dominantly inherited PD is the formation of Lewy bodies (LBs), eosinophilic intracellular protein clusters composed of fibrillar filaments.[25] In familial PD, gene mutations lead to an early onset of symptoms and α-SN accumulation, which disrupts mitochondrial function. This mitochondrial dysfunction contributes to neurodegeneration in PD, hence research efforts focused on targeting mitochondrial function as a therapeutic approach.[26]

1.1.3 Biochemical markers of Parkinson's disease

1.1.3.1 α-Synuclein

Alpha-synuclein is a protein found throughout the body, with particularly high concentrations in the brain, and is thought to play a critical role in the development of PD.[17] This highly conserved protein plays an important role in regulating DA levels and facilitating vesicular neurotransmission.[27] A key characteristic of α-SN is its tendency to aggregate and interact with DA, forming oligomers that eventually transition into amyloid fibrils, which are deposited in LBs.[28] These aggregates are linked to various toxic processes, including mitochondrial dysfunction, impaired autophagy, and membrane damage. Faulty protein aggregation is thought to contribute to cell damage and the eventual death of neurons.[27]

1.1.3.2 Leucine-rich repeat kinase 2

Leucine-rich repeat kinase 2 (LRRK2) is a large multidomain protein with two key enzymatic functions: guanosine triphosphatase (GTPase) and kinase activity.[17] It plays an important role in regulating cytoskeletal vesicular transport, autophagy, and protein interactions.[27] The LRRK2's kinase-dependent interaction with dynamin-like protein 1 (DLP1), a known mitochondrial fission factor, promotes DLP1 translocation to the mitochondria, leading to mitochondrial fission, which is essential for the generation of new mitochondria.[27] Mitochondrial fission also plays a role in cellular quality control by aiding the elimination of impaired mitochondria.[29] Overexpression of LRRK2 enhances DLP1 recruitment to mitochondria, causing mitochondrial fragmentation, increased phosphorylation, and higher ROS production.[30] These abnormalities could potentially be addressed by inhibiting DLP1, suggesting that the LRRK2/DLP1 pathway regulates mitochondrial fission and clearance.[30]

1.1.3.3 Parkin

Parkin, an E3 ubiquitin ligase, plays a crucial role in PD pathogenesis by promoting mitochondrial biosynthesis, mitochondrial deoxyribonucleic acid (mtDNA) replication, and gene transcription, all of which are essential for sustaining mitochondrial respiration and function.[17] Through the ubiquitin-proteasome system, parkin tags damaged or dysfunctional proteins with ubiquitin, marking them for degradation.[17] It also maintains mitochondrial integrity by clearing defective mitochondria that can no longer function properly.[27] Mutations in parkin hinder its ability to remove faulty mitochondria, resulting in the accumulation of ROS. Additionally, reduced parkin

function may promote the formation of cytotoxic protein aggregates, further advancing PD progression.[17]

1.1.3.4 Phosphatase and tensin homolog induced kinase-1

Phosphatase and tensin homolog-induced kinase 1 (PINK1) is a kinase that activates parkin during the autophagic removal of damaged mitochondria, helping to protect neurons from excessive ROS production.[29] The PINK1 also supports mitochondrial stability by producing a mitochondrial protein involved in proteasome-induced apoptosis.[31,32] However, mutations in PINK1 impair mitophagy, the process responsible for selectively clearing defective mitochondria. This leads to the accumulation of damaged mitochondria, making neurons more vulnerable to cellular stress and oxidative damage, which may increase the risk of developing PD.[33,34]

1.1.3.5 DJ-1

DJ-1 is a very small, dense protein found on the outer membrane of mitochondria in neuronal cells.[29] It plays a crucial role in mitigating OS toxicity, regulating protein synthesis at the transcriptional level, and functioning as a molecular chaperone.[29] DJ-1 helps neutralise free radicals through self-oxidation, enhances mitochondrial function, and promotes the synthesis of glutathione (GSH). It also regulates neurotransmitter signalling, which increases DA production, transport, and receptor activity.[35] As a chaperone, DJ-1 assists in proper protein folding, refolds misfolded proteins, transports specific proteins to proteasomes, and contributes to ribonucleic acid (RNA) formation and regulation.[35] Mutations in the DJ-1 gene reduces its ability to protect cells from OS-induced damage and impair its chaperone function, resulting in the toxic buildup of misfolded proteins, and ultimately cell death.[36] When DJ-1's protective functions are compromised, oxidative damage can destroy neuronal cells, contributing to neurodegeneration.[37,38]

1.1.4 Neuropathological hallmarks of Parkinson's disease

Several cellular pathways contribute to the pathophysiology of PD, with α-SN accumulation playing a central role in disease advancement. Key processes involved include faulty folding of proteins and accumulation, disruptions in neuronal transmission, inflammation of neurons, and mitochondrial dysfunction (**Figure 1**).[39] These mechanisms ultimately result in the degeneration of nigrostriatal dopaminergic neurons and the accumulation of protein clusters in the cytoplasm, known as LBs. The degeneration of neurons that produce DA, depletes DA levels in the striatum,

disrupting the equilibrium between facilitatory and inhibitory signals in the basal ganglia, which triggers motor symptoms such as bradykinesia.[40]

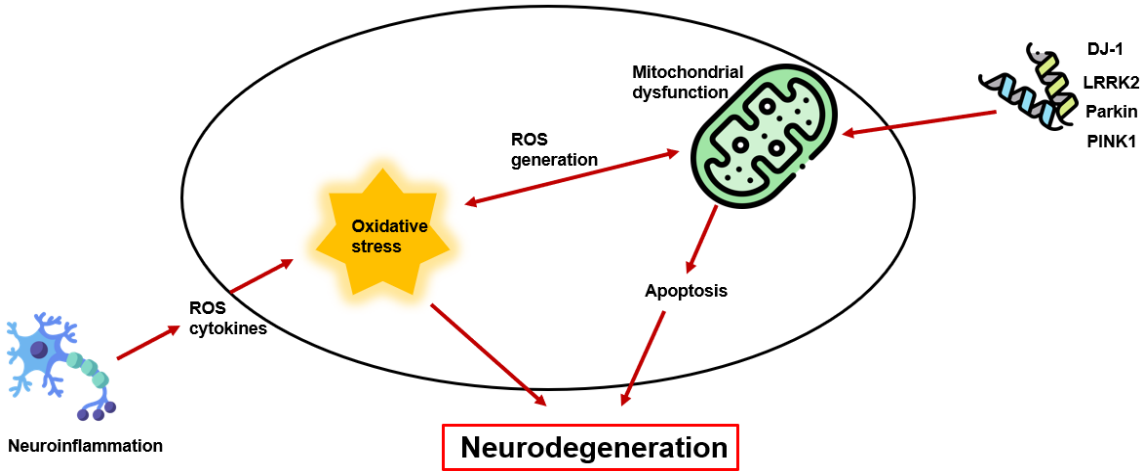

Figure 1. The cellular hallmarks of Parkinson's disease. (Reproduced with permission[41]) ROS: reactive oxygen species.

1.1.4.1 Oxidative stress

Oxidative stress is a harmful cellular state caused by excessive ROS production or accumulation, coupled with a weakened antioxidant defence system.[42] Key ROS molecules, such as hydrogen peroxide (H_2O_2) and superoxide (O_2^-), are central to this process. Microglia are the main source of ROS in the CNS, which are generated through cytoplasmic peroxides and mitochondrial oxidation reactions.[43] Complexes I and III of the mitochondrial electron transport chain are the primary sources of O_2^-, which can be converted to H_2O_2 and subsequently broken down by GSH peroxidases and catalase (CAT).[42]

The human body naturally generates ROS in amounts sufficient for key physiological functions, including immune system development, growth factor activation, and response to inflammation.[44,45] Reactive oxygen species also contribute to apoptosis and cell formation regulation.[44] However, an imbalance between ROS production and removal can be harmful, leading to neuronal damage and cell death, which contributes to the onset of neurodegenerative diseases.[46] Excessive ROS production can impair protein function, disrupt intracellular signalling, and induce cell death. Additionally, ROS can activate pro-inflammatory pathways, creating a hostile environment for neurons already at risk.[42]

Oxidative stress plays a crucial role in the pathophysiology of PD and can be induced by multiple factors, such as genetic mutations, mitochondrial dysfunction, DA autoxidation, iron accumulation, and neuroinflammation. These factors collectively lead to excessive ROS production, as depicted in **Figure 2**.[47] This overproduction of ROS significantly impacts cellular components like proteins, lipids, and deoxyribonucleic acid (DNA), making cells vulnerable to damage and initiating programmed cell death pathways.[48] This process is especially problematic when antioxidant defence is insufficient, a condition that worsens with age.[48]

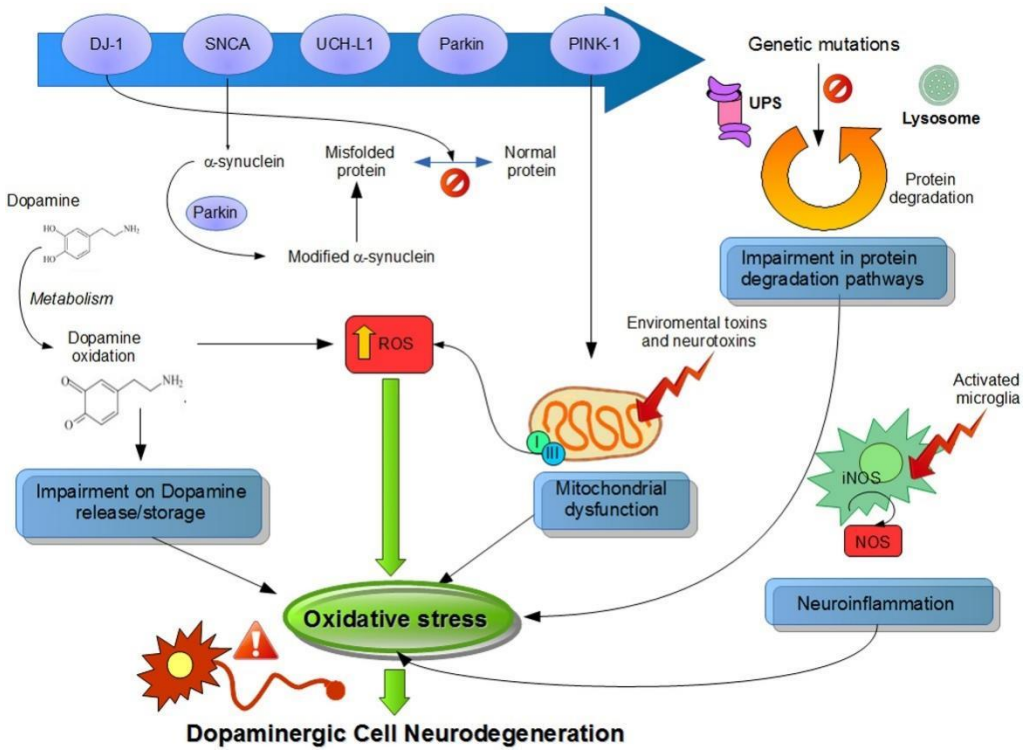

Figure 2. Processes that cause the formation of excessive reactive oxygen species, leading to oxidative stress in Parkinson's disease. (Reproduced with permission[49]) ROS: reactive oxygen species; PINK-1: phosphatase and tensin homolog-induced kinase 1; SNCA: alpha synuclein; UCH-L1: ubiquitin carboxyl-terminal hydrolase L1; NOS: nitric oxide synthase.

Dopamine, a key neurotransmitter required for coordinating movement by regulating synaptic transmission between neurons, is produced by dopaminergic neurons. In PD, patients experience movement disorders primarily due to DA deficiency.[50] Neuronal degeneration in PD results from both neuroinflammation and OS.[29] The SN, with high oxygen demand, but limited antioxidant enzymes like CAT and superoxide dismutase (SOD), renders dopaminergic neurons

particularly vulnerable to OS.[42] In the cytoplasm, DA can undergo autoxidation, forming quinones that further degrade into ROS.[51] Additionally, monoamine oxidases (MAO) generate ROS, particularly H_2O_2, as a byproduct of DA metabolism. Any factor that raises cytoplasmic DA levels can increase DA autoxidation and ROS production, contributing to PD development.[29]

1.1.4.2 Mitochondrial dysfunction

Mitochondria play a crucial role in various biological functions, including energy production through adenosine triphosphate (ATP) synthesis, maintaining cellular calcium ion homeostasis, lipid synthesis, iron-sulphur cluster formation, fatty acid degradation, and regulation of the apoptotic process.[52] The most important function of mitochondria is to convert nutrients and oxygen into ATP; in fact, mitochondria provide more than 90% of the ATP required by cells. Neurons exhibit extensive metabolic rates; therefore, they rely greatly on mitochondria to generate ATP, which results in the production of O_2^- and H_2O_2 free radicals.[53]

The mitochondrial membrane potential (MMP), generated by proton pumps in the electron transport chain (ETC), serves as a vital indicator of mitochondrial function, reflecting the electron transport and oxidative phosphorylation processes essential for ATP synthesis.[54,55] The MMP and ATP levels in the cell are relatively constant during normal physiological activity. As mentioned earlier, the MMP plays an important role in maintaining mitochondrial stability by selectively eliminating defective mitochondria and ensuring the transfer of ions and proteins necessary for proper mitochondrial activity.[54] Prolonged decreases or increases in MMP levels can result in a loss of cell viability, which contributes to the manifestation of a variety of diseases.[56]

The mitochondrial ETC is located in the inner cell membrane of the mitochondria (**Figure 3**) and consists of six components, namely complex I (C I), complex II (C II), coenzyme Q (CoQ) complex III (C III), cytochrome c (Cyt c) and complex IV (C IV).[52] These complexes stimulate the transformation of the reduction analogues from high-energy compounds that arise from the Krebs cycle reactions to oxygen and ultimately create an electrochemical gradient that crosses through the inner membranes of the mitochondria and drives the synthesis of ATP via ATP synthase.[56] Electrons produced by the reduction of nicotinamide adenine dinucleotide (NADH) to NAD^+ or flavin adenine dinucleotide ($FADH_2$) to FAD via C I and C II are transported via CoQ, C III, Cyt c, and C IV, which employs an electron to convert O_2 to H_2O (**Figure 3**). Complexes I, II, and IV pump protons into the inter-membrane space as electrons are transferred from the mitochondrial

matrix. This generates a concentration gradient of H^+ ions, which ATP-synthase uses to convert ADP into ATP.[53]

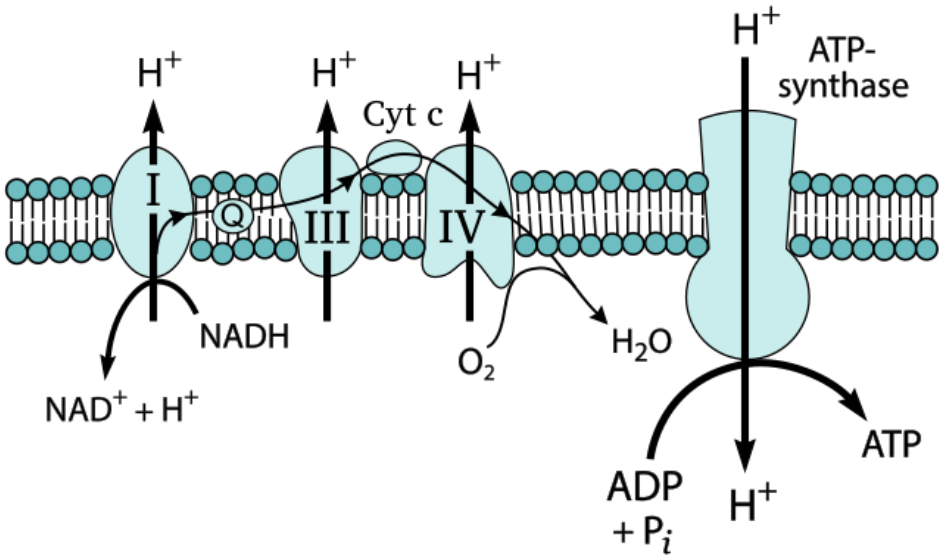

Figure 3. Depiction of the electron transport chain in the mitochondria, which is involved in oxidative phosphorylation. (Figure obtained from Research Commons) ADP: adenosine diphosphate, ATP: adenosine triphosphate, C I: Complex I, C II: Complex II, C III: Complex III, C IV: Complex IV; CoQ: coenzyme Q; Cyt c: cytochrome c; e^-: electrons; FAD: oxidised flavin adenine dinucleotide; $FADH_2$: reduced flavin adenine dinucleotide; H^+: protons; H_2O: water; NADH: reduced nicotinamide adenine dinucleotide; NAD^+: oxidised nicotinamide adenine dinucleotide; O_2: dioxygen.

Several gene mutations, including α-SN, LRRK2, parkin and PINK1, have been linked to mitochondrial dysfunction and are the primary cause of familial PD (**Figure 4**).[57] In mitochondrial dysfunction, C I activity in SN neurons is inhibited by α-SN accumulation or exposure to toxins (such as rotenone). Inhibition of C I disrupt the ETC function, thereby disrupting calcium homeostasis and ATP production, as well as inducing OS.[54] Changes in these genes can also lead to faulty mitophagy (the elimination of defective mitochondria via autophagy), resulting in the accumulation of defective mitochondria in neurons.[58] The interaction between these impaired functions leads to mitochondrial dysfunction, which ultimately results in neurodegeneration.[59]

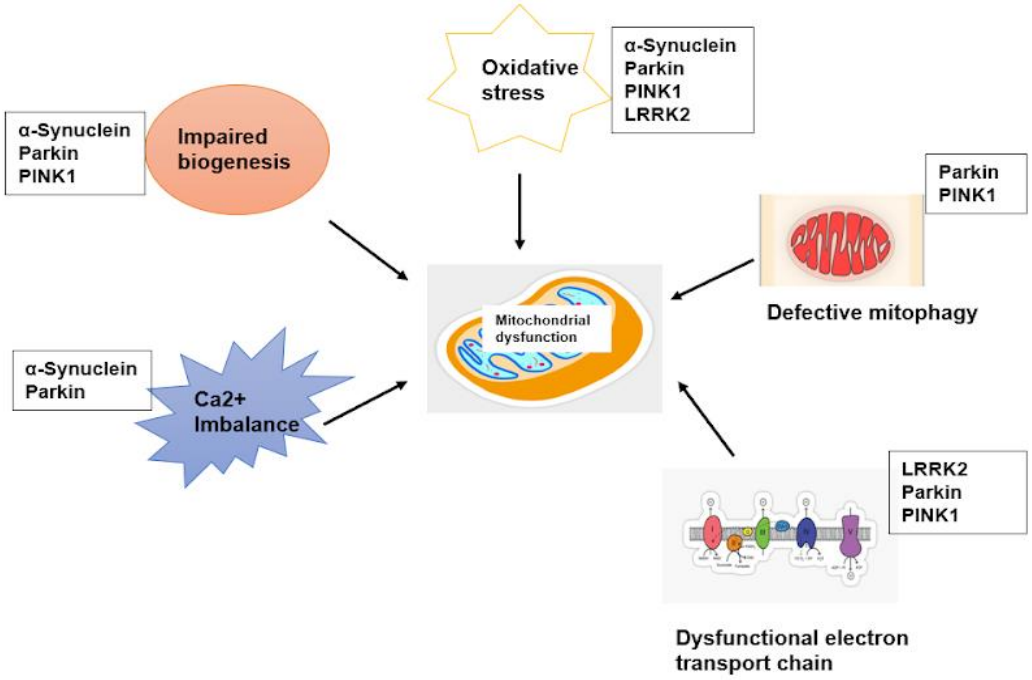

Figure 4. Depiction of the mechanisms which underlie mitochondrial dysfunction in Parkinson's disease; oxidative stress, defective mitophagy, impaired electron transport chain activity, calcium imbalance, and impaired biogenesis. (Figure redrawn with permission[59]) Ca^{2+}: calcium; PINK 1: PTEN-induced kinase 1; LRRK2: leucine-rich repeat kinase.

Natural antioxidants have been suggested as potential therapies to prevent age-related neurological disorders.[60] The human body produces antioxidants to defend against OS.[61] Both synthetic and natural antioxidants work to neutralise free radicals, repair ROS-induced damage, enhance immune function, and reduce the risk of degenerative diseases.[61] Thus, maintaining an optimal balance between ROS and antioxidants in mitochondria is essential for the proper functioning of cells, tissues, and organs.[62]

As PD is a complicated condition where mitochondrial damage and OS play a significant role in nigrostriatal dopaminergic neurodegeneration, antioxidants that inhibit both mechanisms are potential agents for the treatment of PD.[62] Phenols and flavonoids are among the most prevalent antioxidants and have indicated promising neuroprotective effects towards DA oxidation damage in various PD models.[63,64] Phenolic compounds help prevent the metabolism of hydroperoxides into free radicals and removes reactive lipid species, while flavonoids act as free radical scavengers, have anti-inflammatory properties, and immunomodulating activities.[63]

To support the rationale for using natural antioxidants in PD, clinical trials and *in vitro* studies have explored their role in reducing OS and neurodegeneration. For example, a clinical trial on CoQ_{10}, a potent antioxidant, was reported to slow down the progression of PD symptoms, demonstrating its therapeutic potential.[65] *In vitro* studies on *Ginkgo biloba* have revealed its antioxidant properties, and in animal models, extracts were found to protect dopaminergic neurons by reducing OS and preserving mitochondrial function.[66]

1.1.4.3 Cell death

Neuronal death occurs during the regular proliferation of neuronal cells and as a result of various pathological conditions such as acute injury, haemorrhage, pathogens, or genetic abnormalities. Neuronal death occurs primarily through two fundamental processes: apoptosis and necrosis.[67] In many neurodegenerative diseases, including PD, apoptosis is the primary pathway to neuronal death, making these pathways attractive potential treatment targets.[68]

1.1.4.3.1 Apoptosis

Apoptosis is a highly conserved biochemical process that has remained largely unchanged throughout evolution.[69] It consists of a sequence of energy-dependent events and is characterised by anatomical and physiological changes such as cell shrinkage, membrane-forming protrusions, segregation, chromatin condensation, and fragmentation of DNA.[67] Unlike necrosis, apoptosis preserves membrane integrity, preventing the expulsion of cell elements into the extracellular environment. Instead, dying cells form apoptotic bodies, which are recognised by neighbouring cells and phagocytosed without triggering a response to inflammation.[70] Apoptosis is biochemically defined by higher rates of protein breakdown and enhanced activity of caspase.[71]

Apoptosis is regulated by various initiator and executioner caspases and occurs via two primary pathways: the intrinsic and extrinsic pathways, subject to where the cell death signal originates (**Figure 5**).[72] In the extrinsic pathway, apoptosis is induced by the stimulation of trimeric receptors on the cell surface known as 'death receptors' (e.g., Fas receptor).[72] When ligands (e.g., Fas ligand) bind to the receptors, they form a death-receptor complex that activates pro-caspase-8, cleaving it into caspase-8.[62,73] Caspase-8, in turn, stimulates executioner caspases -3, -6, and -7, which break down substrates like poly (ADP-ribose) polymerase (PARP), plasma membrane

cytoskeletal proteins, and nuclear proteins, leading to structural and biochemical modifications associated with apoptosis.[62,73,74]

The intrinsic pathway is triggered by cellular stress, such as DNA damage, increased ROS production, or exposure to neurotoxins (**Figure 5**).[75] Neurotoxin accumulation in the mitochondria of dopaminergic neurons inhibits C I, resulting in reduced ATP production and increased ROS production.[76] This impairs MMP, causing a loss of MMP and the opening of the mitochondrial permeability transition (MPT) pore.[62] When the MPT pore opens, Cyt c is expelled and integrates with apoptotic protease-activating factor-1 (Apaf-1) and caspase-9 to form an apoptosome.[77] This energy-dependent process then recruits executioner caspases, initiating the apoptotic cascade (**Figure 5**).[62]

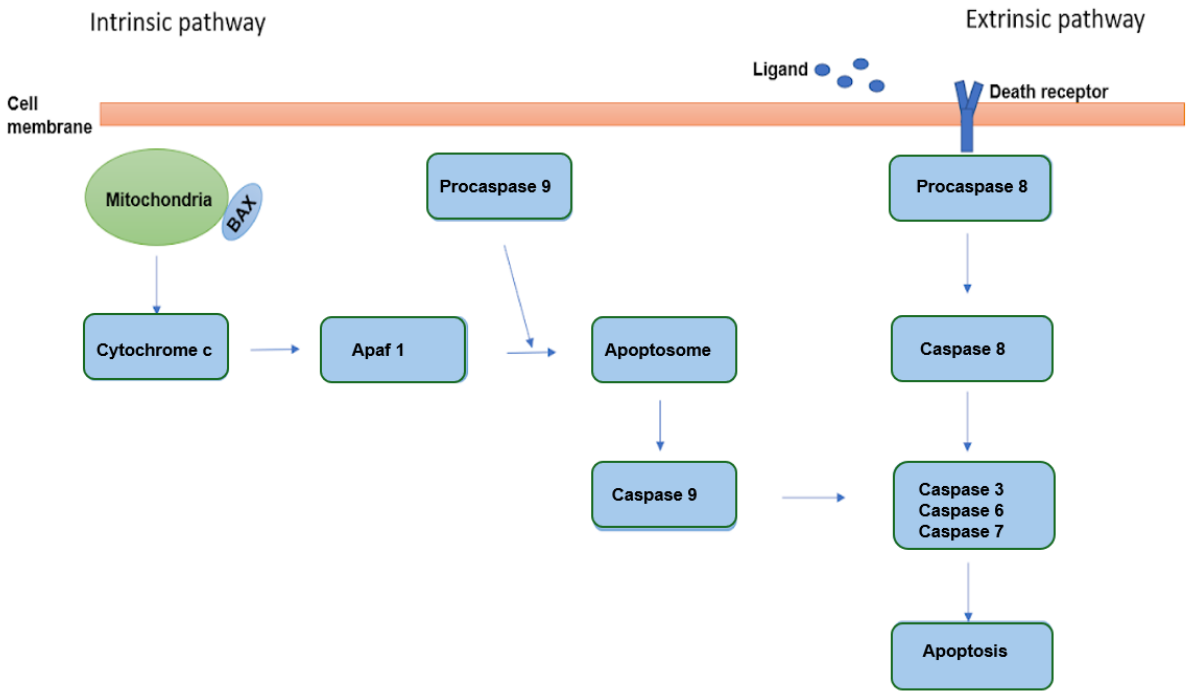

Figure 5. Diagram indicating the intrinsic and extrinsic apoptotic pathways of cell death. (Reproduced with permission[67]) BAX: Bcl-2 associated X protein; Apaf 1: apoptotic protease activating factor 1.

1.1.4.3.2 Necrosis

Necrosis is an irreversible type of cell death caused by severe cellular stress such as injury, infection, or oxidative damage.[78,79] Necrosis, in contrast to apoptosis, does not follow a systematic mechanism for cellular disintegration; rather, it entails organelle expansion, plasma membrane rupture, and cellular lysis, resulting in the release of the intracellular contents into adjacent tissue and inciting an unwanted inflammatory response **(Figure 6)**.[80] The subsequent

inflammatory cascade not only causes harm to local cells, but it can also increase stress signals across the tissue, exacerbating the injury, contributing to disease progression.[80]

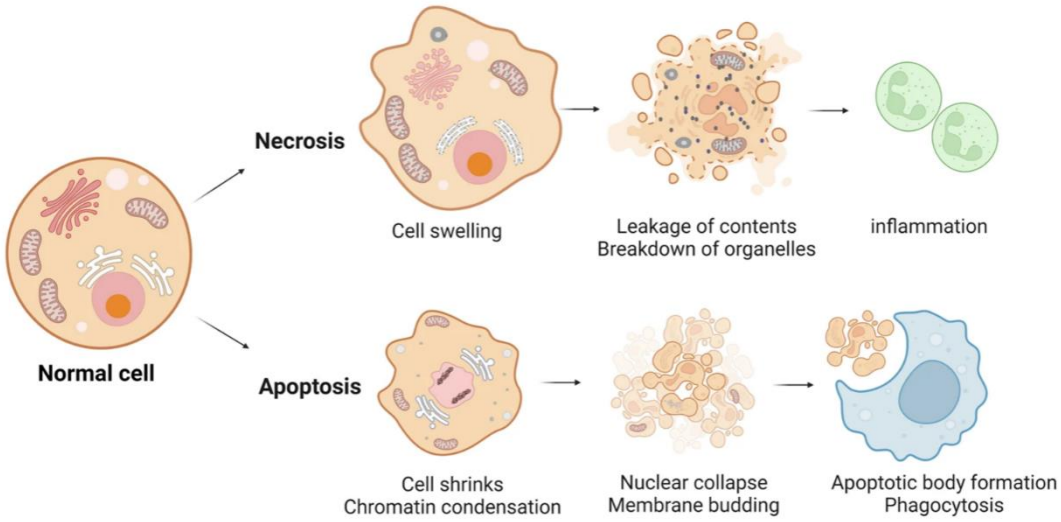

.

Figure 6. Morphological patterns of cell death via necrosis and apoptosis. (Reproduced with permission[81])

Necroptosis, also known as programmed necrosis, is a controlled type of cell death where apoptosis is suppressed, and necrotic pathways are stimulated by apoptotic signals such as Fas and TNF-α.[82,83] Unlike traditional necrosis, necroptosis is a regulated process involving receptor-interacting protein kinases (RIPK1 and RIPK3) and mixed lineage kinase domain-like protein (MLKL).[84] When death receptors such as TNF-α or Fas are activated, RIPK1 and RIPK3 produce an aggregate, the necrosome, which triggers necroptosis.[85] This necrosome formation causes RIPK3 to phosphorylate MLKL, which then assembles and integrates in the cell membrane, destroying its integrity and resulting in cellular rupture.[86] This rupture causes cellular contents to "leak" into the surrounding environment, triggering a localised inflammatory response.[87] Elevated inflammatory markers have been detected in the brains of individuals with neurodegenerative disorders, such as PD, suggesting that inflammatory cell death, potentially through mechanisms like necroptosis, may contribute to the neuronal damage linked to the disease.[22,88]

1.1.5 Current treatments for Parkinson's disease

At present, there is no cure for PD.[89,90] Current pharmaceutical treatments aim to alleviate symptoms by targeting motor coordination, autonomic functions, memory, and other neurological processes in the brain rather than providing a cure.[91] Treatment plans for PD are highly individualised, tailored to each patient's specific needs and circumstances.[92] Medications such as DA agonists, MAO inhibitors (MAOIs), DA precursors (e.g., levodopa), and anticholinergics are commonly used to manage the motor symptoms of PD (**Figure 7**).[93]

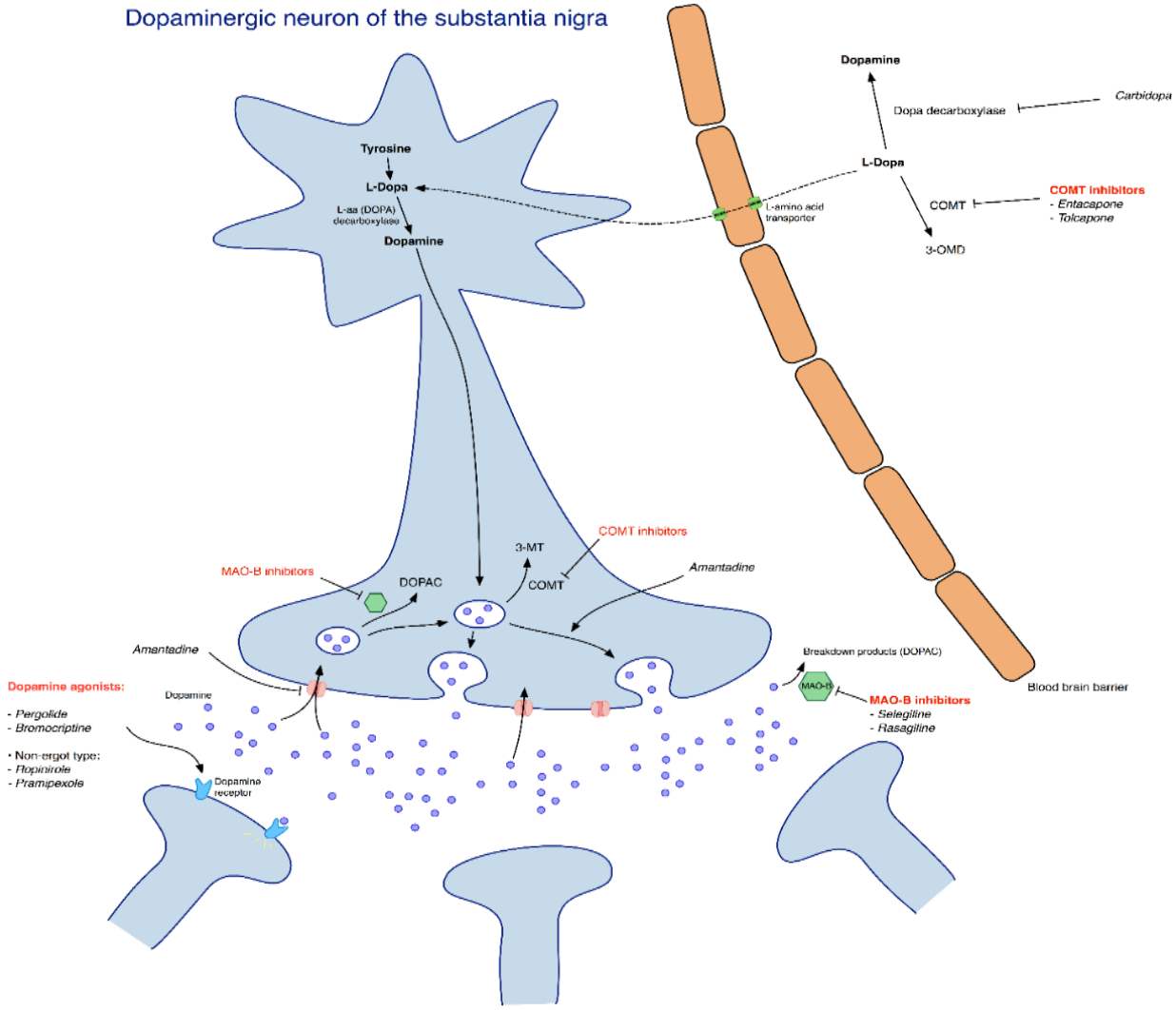

Figure 7. Current treatments of Parkinson's disease. (Figure obtained from Research Commons) 3-MT: 3-methoxytyramine, 3-OMD: 3-O-methyldopa, COMT: catechol-O-methyltransferase, DOPAC: 3,4-dihydroxyphenylacetic acid, L-dopa: levodopa, MAO: monoamine oxidase.

1.1.5.1 Conventional therapy

As discussed in **Section 1.1.1** (page 2), the primary cause of motor impairment in PD is the loss of dopaminergic neurons in the SNpc, leading to decreased DA activity in the striatum. Current approved treatments aim to increase DA levels in the striatum to alleviate motor symptoms.[94] However, these therapies provide only temporary relief, as their effectiveness decreases with the progression of dopaminergic neurodegeneration.[94] The conventional therapies outlined below emphasise the biological processes that regulate DA levels to help manage PD symptoms.[94]

1.1.5.1.1 Levodopa

More than sixty years after its discovery, levodopa (L-dopa) remains the primary medication for treating PD, largely due to its higher compliance rate compared to other PD drugs.[92] Levodopa, a DA precursor, is absorbed in the intestines, crosses the blood brain barrier (BBB) through amino acid transport, and is converted into DA within the CNS, thereby increasing DA levels in the SN (**Figure 7)**.[92,95]

The effectiveness of L-dopa diminishes as the disease progresses, because the bioavailability of L-dopa in the brain decreases due to the loss of dopaminergic neurons and receptors.[90,96,97] Therefore, it is frequently co-administered with peripheral DA decarboxylase inhibitors (such as benserazide or carbidopa), which prevent the metabolism of L-dopa to DA outside the brain, enhancing its CNS absorption and reducing peripheral side effects.[90,98]

Levodopa therapy can lead to side effects, including motor fluctuations, hallucinations, orthostatic hypotension, dyskinesia, and "wearing-off" effects, where PD symptoms reappear as the drug's effects wane.[92] These motor fluctuations are common due to L-dopa's short half-life; consequently, it is often combined with other medications, such as DA agonists, to achieve an "L-dopa-sparing effect" and prolong its duration of action.[99]

1.1.5.1.2 Dopamine receptor agonists

In patients younger than 50 years, DA agonists are often used as the first-line treatment to delay the initiation of L-dopa therapy and reduce the risk of L-dopa-induced dyskinesia.[94] These agonists are effective as monotherapy for mild to moderate PD.[91] They provide temporary relief

from PD symptoms by increasing DA production, mimicking DA's function, and reducing its oxidative breakdown (**Figure 7**).[40,100]

Dopamine receptor agonists stimulate striatal DA receptors directly, without the need for chemical modification as required for L-dopa.[101] Additionally, they have a longer duration of action than L-dopa and have do not compete with plasma amino acids for absorption or transportation to the brain.[102] Potential side effects of DA agonists may include cognitive abnormalities, orthostatic hypotension, and motor dysfunction, such as dyskinesia.[99]

1.1.5.1.3 Catechol-*O*-methyltransferase inhibitors

Catechol-*O*-methyltransferase (COMT) is an enzyme that metabolises DA into 3-methoxytyramine (3-MT), which thereafter undergoes oxidation by MAO B to generate inactive metabolites (**Figure 7)**.[94] In the absence of COMT inhibitors, a much smaller amount of L-dopa reaches the CNS because it is metabolised into 3-*O*-methyldopa in the intestine through COMT activity.[94] The accumulation of 3-*O*-methyldopa, a metabolite of L-dopa, can increase the toxic effects associated with long-term L-dopa treatment.[102]

Catechol-*O*-methyltransferase inhibitors allow more L-dopa to enter the CNS, enhancing its bioavailability and extending its elimination half-life. Medications like entacapone and tolcapone are used to manage the "wearing-off" effects experienced by patients on L-dopa. However, these medications may cause side effects, including severe diarrhoea, dyskinesia, and, in the case of tolcapone, liver damage, requiring close patient monitoring.[99]

1.1.5.1.4 Monoamine oxidase inhibitors

Monoamine oxidase B is an enzyme that breaks down DA to produce 3,4-dihydroxyphenylacetic acid (DOPAC), which is then converted into HVA by COMT (**Figure 7**).[103] These drugs are responsible for increasing the concentration of free DA in the synaptic cleft by preventing its degradation by MAO, thus extending the duration of action of L-dopa.[92,104] Rasagiline and selegiline are examples of drugs in this class. Rasagiline is the more potent of the two drugs and has been shown to be effective in treating the "wearing off" effects caused by prolonged L-dopa therapy.[92] However, MAO B inhibitors are not typically the first-line treatment for PD due to several dietary restrictions, potential side effects, and safety concerns, as well as their propensity to cause drug-to-drug and drug-food interactions.[102,105]

1.1.5.1.5 Other drugs

Acetylcholine (ACh) is a neurotransmitter involved in both brain and body functions, including muscle contractions.[106] In PD, DA deficiency impairs the inhibition of ACh release by muscarinic auto receptors, leading to an excessive release of ACh.[106] This overproduction disrupts the transmission of signals from the motor control centres of the cerebral cortex by affecting the nerve endings of the striatal indirect pathway neurons.[102] Excess ACh in the brain can cause CNS depression, speech disorders, seizures, impaired mobility, and respiratory difficulties.[106] As a result, anticholinergic medications like benztropine and trihexyphenidyl are effective in reducing mobility issues in patients with early-stage PD or those resistant to conventional Parkinson's treatments.[93] While these medications do not directly affect dopaminergic signalling, they modify ACh activity, which plays a role in movement regulation, helping to alleviate tremors and dystonia.[94] However, anticholinergics must be used cautiously due to side effects such as urinary retention, dry mouth, memory loss, and vision problems.[99]

1.1.5.2 Challenges with current pharmacological treatments

To control motor symptoms, patients often require increased doses, additional therapies, or adjustments to their treatment plan.[5] Choosing the right combination of drugs and personalised dosages is crucial for effective PD management. However, even with these adjustments, patients frequently experience ongoing motor and neurological issues. Due to the significant side effects associated with conventional PD medications, which primarily alleviate symptoms without targeting the underlying DA depletion in the SN, there is a pressing need for innovative therapeutic approaches with improved safety profiles.[92]

Although PD remains incurable, current research is dedicated to discovering improved treatments with fewer side effects. Traditional medicinal herbs and their bioactive phytochemicals are emerging as a promising path for developing safer, more effective therapies.[102] Rather than targeting a single pathway, plant-based therapeutic compounds are gaining attention for their ability to address multiple pathogenic mechanisms, making them particularly relevant for tackling the complexities of neurodegenerative diseases.[107]

1.1.6 Medicinal plant therapy

Plants have long played a vital role in healing human injuries and illnesses.[108] The increasing recognition of natural products has amplified the demand for medicinal plants in both developed

and developing nations.[108] Herbal medicine remains integral to both traditional and modern medical practices.[108] Plants produce a wide variety of secondary metabolites, which are essential sources for numerous pharmacological drugs.[108] Many studies underscore the diverse therapeutic and pharmacological benefits of medicinal plants.[109-111]

Therapeutics derived from plants originally took the form of basic pharmaceuticals such as powders, teas, vaporisers, and other natural remedies.[112,113] Since the early 1900s, when morphine was first extracted from opium, the isolation and extraction of active compounds from plants for medicinal purposes became increasingly important.[114] Along with morphine, other drugs like codeine, digoxin, and quinine were also derived from herbal remedies, many of which remain in widespread use today.[115,116] In recent years, drug development strategies have focused on standardising herbal remedies, identifying analytical marker compounds, and expanding research across a variety of topics and methodologies.[117] The two plants explored in this study for their *in vitro* effects on PD are discussed below.

1.1.6.1 Catha edulis

Catha edulis Forsk., commonly known as Khat (**Figure 8**), is a small, evergreen, flowering shrub belonging to the Celastraceae family.[118] Native to Africa and Yemen, this psychostimulant plant thrives in regions such as Ethiopia and other neighbouring African countries, including South Africa.[119]

Khat chewing has been associated with improved social interaction, enhanced individual performance, and increased work productivity.[120] It is also traditionally used for self-medication, particularly for treating obesity and depression. Medicinally, Khat chewing has been used to treat asthma, reduce appetite, and combat fatigue. However, heavy use is linked to increased rates of psychosis and depression.[120] Chronic consumption of *C. edulis* can lead to dependency, liver toxicity, sexual dysfunction, cardiovascular issues, and psychosis, among other side effects.[120] Despite these toxic effects, reports suggest that they also have therapeutic potential, such as antimicrobial effects, antidepressant-like effects, and possible applications in regeneration of neuronal tissues.[119] Khat has gained global popularity.[118,120] Regular users of the herb report feelings of comfort, euphoria, heightened mental alertness, and an overall sense of enjoyment.[120]

The primary active compounds in *C. edulis* are cathine, norephedrine, and cathinone, which are responsible for its toxicological and medicinal effects.[121] These compounds share structural similarities with amphetamine and noradrenaline, and the ß-keto analogue of amphetamine may

lead to dependence through its psychostimulatory effects on the nervous system.[121] Fresh Khat leaves are estimated to contain 8 mg of norephedrine, 36 mg of cathinone, and 120 mg of cathine per 100 g of leaves.[120]

Figure 8. *Catha edulis* pant: A) tree, B) flowers, and C) leaves.[122]

1.1.6.2 Datura stramonium

Datura stramonium L., commonly known as Jimsonweed (**Figure 9**), is an annual plant belonging to the Solanaceae family.[123] *Datura stramonium* is commonly used in Africa to treat injuries, swelling, fever, and respiratory ailments.[124] The plant's dried leaves, roots, or flowers are commonly smoked to relieve asthma and cough. Infusions of the leaves are used to alleviate insomnia, relax bronchial muscles in asthma, and treat conditions like diarrhoea and peptic ulcers.[108,125] The leaves are applied as an ointment for swelling, wounds, and burns.[126]

This herbaceous shrub has been extensively studied for its production of tropane alkaloids, atropine and scopolamine, which contain a methylated nitrogen molecule (N-CH_3) and serve as the source of anticholinergic compounds.[108,123] While highly toxic, especially in its seeds and leaves, controlled doses of *D. stramonium* are used for therapeutic purposes.[119,123,127]

Phytochemical analysis of *D. stramonium* has revealed the presence of carbohydrates, tannins, saponins, flavonoids, alkaloids, phenols, and glycosides.[108] Atropine and scopolamine, the main pharmacologically active compounds, are CNS depressants that act as competitive antagonists of muscarinic cholinergic receptors. Scopolamine, which affects the CNS and digestive system, is also used to manage PD symptoms.[70]

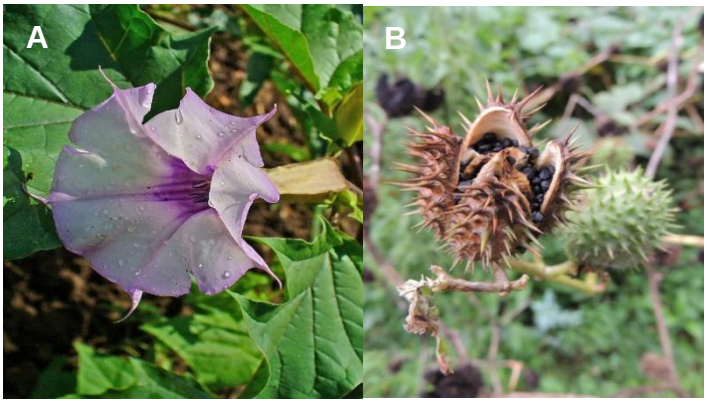

Figure 9. *Datura stramonium* plant: A) leaves and flower, and B) seedpods.[128]

1.2 *In vitro* experimental models for Parkinson's disease

Over the years, several preclinical models have been developed ranging from cell lines to animal models to study the aetiology and pathogenesis of various diseases in humans.[16] *In vitro* models, such as basic cell cultures, offer a controlled environment ideal for investigating specific pathogenic pathways and identifying the genes and proteins involved.[16] Several *in vitro* models of PD use neurotoxins to mimic important disease characteristics.[16,19]

A human neuroblastoma cell line (SH-SY5Y) and a rat pheochromocytoma cell line (PC12) are among the most frequently used due to their neuronal features.[129] Upon development, these cell lines produce and release catecholamines while also developing neuron-like structures such as neurites. They are useful models for PD research because they are easier to maintain than primary neurons.[130,131] SH-SY5Y cells, specifically, resemble immature catecholaminergic neurons, with neurite structures and neuronal marker expression In their undifferentiated state.[132] Even so, they are a good model for investigating PD-related characteristics like mitochondrial dysfunction, OS, and dopaminergic signalling.[133]

Neurotoxins such as 6-OHDA, MPTP, rotenone, and paraquat are commonly used in cellular models to create PD-like pathology, with each mimicking distinct hallmarks of the disease's pathogenesis.[132] For example, 6-OHDA produces OS and preferentially damages dopaminergic neurons, which closely resembles the neuronal loss seen in PD.[134] MPTP, conversely, passes through the BBB and impairs mitochondrial activity, resulting in LB formation also observed in PD patients.[135] Rotenone similarly disrupts mitochondrial function and induces α-SN aggregation, both of which are key contributors to neurodegeneration in PD.[136]

Paraquat, a known inducer of OS, has variable effects on motor function.[137] Together, these neurotoxins provide valuable insights into the mechanisms of PD and aid in evaluating potential therapeutic strategies.

SH-SY5Y cells and 6-OHDA were selected for their proven use in mimicking PD. SH-SY5Y cells have human-derived dopaminergic properties, are easy to differentiate, and are widely used in PD studies, which makes them more reliable than other cellular models such as PC12. 6-Hydroxydopamine, with its ability to precisely target dopaminergic neurons and induce OS, provides a focused approach to studying PD pathology. Together, these models provide important insights into PD processes and treatment possibilities.

1.2.1 Human neuroblastoma cells

The SK-N-SH cell line, which resembles undeveloped responsive neuroblasts, is the source of SH-SY5Y cells. Since the loss of dopaminergic neurons is a hallmark of PD, the SH-SY5Y cells are best suited for *in vitro* PD research.[112,138] They exhibit nerve cell-like processes and express key components of the DA uptake system, such as the DA transporter (DAT), a protein found exclusively in dopaminergic neurons of the CNS, which maintains DA balance through specific uptake, and vesicular monoamine transporter (VMAT), which facilitates DA storage.[134,138] Additionally, SH-SY5Y cells can produce DA due to the expression of DA-β-hydroxylase and tyrosine hydroxylase, enzymes involved in neurotransmitter synthesis.[138]

A drawback is that the SH-SY5Y cells represent immature neurons and hence treatment with retinoic acid (RA), is required to differentiate these cells to obtain a more distinct dopaminergic neuronal phenotype.[133] However, these differentiation-inducing agents may induce tolerance, making it difficult to assess cytotoxicity or cytoprotection in the differentiated cells.[138] Therefore, undifferentiated SH-SY5Y cells are used in the experimental research on PD, as they represent a suitable model for studying cytotoxicity and cytoprotection. However, the cells require treatment with compounds such as 6-OHDA, MPTP, paraquat, and rotenone to stimulate neuronal damage, thereby mimicking the degeneration of dopaminergic neurons in patients with PD.

The toxin of choice to induce neuronal damage in this study was 6-OHDA.[139-141] It is well-established that 6-OHDA contributes to the generation of H_2O_2 and other ROS, which can damage the cellular structure as well as the function of the SN.[134] The harmful effects of 6-OHDA are also linked to DNA damage, lipid oxidation, depletion of naturally occurring GSH, and

neuronal degeneration.[142,143] As shown in **Figure 10**, 6-OHDA is structurally similar to DA, but is hydroxylated, allowing it to specifically target and destroy dopaminergic/ catecholaminergic neurons due to its high affinity for the DA transporter.[144,145]

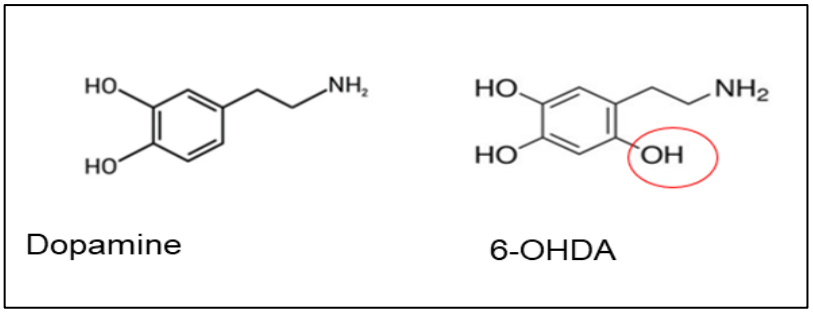

Figure 10. Chemical structures of dopamine and 6-hydroxydopamine (6-OHDA), indicating the structural similarity. (Figure obtained from Research Commons)

The mechanism of action of 6-OHDA to simulate neurodegeneration involves its selective toxicity toward dopaminergic neurons. This neurotoxin enters the cells via the DA transporter, where it accumulates and undergoes non-enzymatic auto-oxidation, thus increasing the formation of free radicals such as O_2^- or OH (**Figure 11**).[146] Increased production of free radicals damages nucleic acids and proteins in neurons and disrupts mitochondrial functions by inhibiting the function of C I and IV which disrupts the downstream processes, resulting in decreased ATP production, which then induces apoptosis of the dysfunctional neurons.[134]

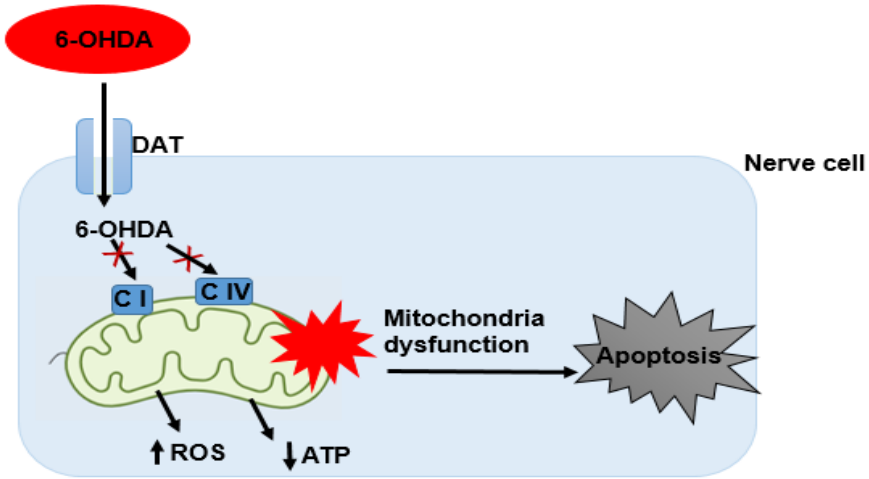

Figure 11. Mechanism of action of 6-hydroxydopamine in nerve cells. (Reproduced with permission[144])
6-OHDA: 6-hydroxydopamine, ATP: adenosine triphosphate, C I: complex I, DAT: dopamine transporter, ROS: reactive oxygen species.

1.3 *In silico* docking

In silico docking, also known as molecular docking, is a computerised technique for simulating the interaction of a ligand with a target protein, determining binding affinity and ideal orientations within the receptor binding site.[147,148] This approach provides accurate understanding of interactions between molecules, allowing researchers to assess the efficacy and selectivity of compounds. In the context of PD, *in silico* docking is useful for identifying and improving drugs that target critical receptors, such as D1 and D2 receptors, which play an important role in the irregularities in motor function associated with PD.[149]

In silico docking simulates the binding of ligands to these receptors, allowing researchers to estimate the affinity the proposed ligands have for the selected targets. This speeds up the drug development process by selecting potential candidates for *in vitro* and *in vivo* testing, minimising the requirement for extensive experimental screening.[150] Furthermore, it lays the foundation for the development of accurate and efficient therapeutics by providing extensive knowledge into the molecular processes that regulate receptor modulation. This method is very useful in designing targeted treatments that can potentially enhance PD outcomes.[151]

1.4 Aim and objectives

The aim of the study was to determine the effect of the crude extract and fractions of *Catha edulis* and *Datura stramonium*, on 6-OHDA-induced cytotoxicity in the SH-SY5Y human neuroblastoma cell line, which serves as a model of PD.

The objectives of the study were to:

- Conduct phytochemical screening to confirm the presence of chemotaxonomic markers of *C. edulis* and *D. stramonium*, using ultra-performance liquid chromatography-mass spectrometry.
- Assess inherent cytotoxicity of fractions and crude extract on SH-SY5Y neuroblastoma cell density using the SRB assay.
- Assess the effect of 6-OHDA on SH-SY5Y neuroblastoma cell density using the sulforhodamine B (SRB) assay.
- Determine the cytoprotective ability of crude extracts and fractions on 6-OHDA-induced cytotoxicity in SH-SY5Y cells using SRB assay.

- Determine the IC_{50} of pure compounds (atropine and scopolamine) and their cytoprotective ability on 6-OHDA-induced cytotoxicity in SH-SY5Y cells using the SRB assay.
- Assess cellular morphology using phase contrast microscopy.
- Assess the neuroprotective mechanism of action of *C. edulis* and *D. stramonium* extracts and fractions in the SH-SY5Y neuroblastoma PD model by determining the following parameters:
    - intracellular ROS generation using the 2',7'-dichlorodihydrofluorescein diacetate (H_2DCFDA) assay.
    - anti-apoptotic properties using the Ac-DEVD-AMC cleavage assay.
    - mitochondrial membrane integrity using the mitochondrial staining assay.
- Conduct *in silico* docking analysis of *C. edulis* and *D. stramonium* chemotaxonomic markers to assess binding affinities with D1 and D2 receptors.

Chapter 2: Materials and methods

Approval to conduct this study was obtained from the Research Ethics Committee of the Faculty of Health Sciences, University of Pretoria (Appendix I). All reagents used, as well as the preparation thereof are listed in Appendix II.

2.1 Plant material

Catha edulis (PM0001, leaves) and *Datura stramonium (*P12600, Leaf/root mixture) was transferred from the Council for Scientific and Industrial Research (CSIR) to the Natural Compound Library at the Department of Chemistry, University of Pretoria. The dried plant material was stored in Ziploc bags at room temperature in the dark.

2.2 Preparation of plant extracts

Extraction was undertaken in sintered glass funnels fitted with stopcocks and labelled with the sample code. Pre-ground dried plant material (7.0 to 7.3 g) was added to a glass flask. Thereafter, 50 mL dichloromethane (DCM): methanol (MeOH), at a ratio of 1:1 was added to the funnels, which were partially submerged in an ultrasonic bath (containing water at room temperature) for 1 h. The water temperature was maintained below 25°C to ensure the DCM did not evaporate. After the first extraction, the solvent mixture was filtered using a Whatman qualitative filter paper (Grade 1, 150 mm; Sigma Aldrich, St Louis, USA) into round-bottom flasks and stored at room temperature in the dark. The marc was extracted a second time with 100% MeOH (50 mL) and the procedure repeated.

The DCM:MeOH and MeOH extracts were combined in round bottom flasks and dried under reduced pressure using a rotational evaporator (Buchi Rotavapor R-300, with a Buchi B-300 Heating Bath and a Buchi V-300 Vacuum Pump; Labotec, Midrand, South Africa). After drying, the extracts were reconstituted in MeOH, transferred into pre-weighed 10 mL glass polytops, and dried at 35°C for 6 h using a Genevac® EZ-2 Plus Mk III centrifugal evaporator (United Scientific, Ipswich, United Kingdom).

After drying, a portion of the crude extract was transferred into pre-weighed 10 mL plastic tubes for fractionation. The crude extract was reconstituted in a 6:3:1 mixture of HPLC-grade (>98%) MeOH: ethyl acetate (EtOAc): methyl tert-butyl ether (MTBE), the amount which was determined

by the Hamilton® Microlab® STARLETTM M automated liquid handler (Hamilton Robotics, Inc; Nevada, United States of America) and vortex-mixed until solubilised.

The solubilised crude extract was decanted onto dental cotton wool inserted into 10 mL glass polytops and dried via centrifugal reduced pressure. Once dried, the crude extract-saturated cotton wool was inserted into empty 6 cc polypropylene Strata® (Phenomenex®) solid-phase extraction (SPE) cartridges containing a single frit (Separations, Phenomenex; Torrance, California, USA) and stored at 4°C till use.

Fractionation was carried out using a Gilson® GX-241 ASPEC® liquid handler (Gilson Scientific via LASEC SA (Pty) Ltd, Gilson Inc.; Middleton, Wisconsin, USA) and C8 HyperSep® 2 g/6 mL cartridge (Anatech Instruments (Pty) Ltd, ThermoFisher Scientific Inc.; Waltham, USA). The absorbent of the cartridge was activated with 100% MeOH (11 mL), thereafter with MeOH: H_2O (5:95) using a Gilson® Verity® 4060 solvent pump (Gilson Scientific via LASEC (Pty) Ltd, Gilson Inc.; Middleton, Wisconsin, USA). The cotton wool-loaded cartridges were fitted onto C8 HyperSep® cartridges and fractionated at a flow rate of 10 mL/min with a washout step for the injector between each solvent system. Fractions were labelled with the suffix F1 to F7 to indicate the gradient solvent system used. An aqueous solvent system was used for F1 to F6 with an increasing gradient of MeOH, after which F7 was created using MeOH: acetonitrile (ACN) [1:1, v/v] (**Table 1**). After elution of the fraction using pressurised air, each fraction was stored in a barcoded plastic tube at -40°C until use.

Table 1. The proportion of solvent used per volume during fractionation.

Fraction	Solvent (% by volume)		
	MeOH	**H_2O**	**ACN**
F1	5	95	0
F2	20	80	0
F3	40	60	0
F4	80	20	0
F5	90	10	0
F6	100	0	0
F7	50	0	50

ACN: acetonitrile, H_2O: water, MeOH: methanol

Once fractionation was completed, the fractions were pipetted into a 96 deep-well plate (BioPointe Scientific Inc. via Separations (Pty.) Ltd., BioPointe Scientific Inc.; Claremont, California, USA), and mapped into a spreadsheet via the MicroLab® system. The deep-well plates were then dried under centrifugal reduced pressure for 14 h using the Genevac® HT-6 Series 3i centrifugal evaporator (United Scientific, SP Scientific; Ipswich, UK). Once dry, the tubes were placed into polyurethane bags and stored at 4°C for future use. The dried samples in the deep-well plate were reconstituted in biological-grade dimethyl sulfoxide (DMSO) to achieve a final concentration of 5 mg/mL. The reconstituted samples were then transferred to FluidX® 1.0 mL EXT Co-Mold Jacket tubes arranged in a pre-packed 96-position rack (FluidX Ltd., Cheshire, UK), facilitated by the MicroLab® system. Aliquots (40 µL) were pipetted into a deep-well plate and heat-sealed with an aluminium heat sealer using the BIOBASE® PS-2 Semi-automated plate sealer (BIOBASE Group; Shandong, China). Plates were stored at -80°C to ensure no phytochemical degradation occurred. The samples in the FluidX® tubes are stored in a Hamilton® Verso® Q20 -80°C freezer (Hamilton Company via Separations (Pty) Ltd, Hamilton Storage GmbH, Switzerland) in the Department of Chemistry.

2.2.1 Ultra-performance liquid chromatography-mass spectrometry

2.2.1.1 Sample preparation

Dried stock extracts and primary fractions, used in the preparation of the bioassay library samples, were used to prepare the samples for analysis. The crude extract as well as each fraction was reconstituted in water: MeOH [1:1, v/v] (ROMIL® SpS-grade Methanol 215) solvent system. The samples were filtered through 0.22 µm nylon syringe filters (Agela® Technologies). Stock sample solutions were diluted to a concentration of 5 000 ppm.

The samples were analysed using an ultra-performance liquid chromatography quadrupole time-of-flight mass spectrometry (UPLC-Q-TOF-MS) in both the positive and negative ionisation modes. For elution of the samples, a generic methanol/water-based solvent system was used (**Table 2**). The mobile phase flow rate was set to 0.3 mL/min. Leucine enkephalin (m/z ESI+ = 556.2771; m/z ESI- = 554.2615) was used as an internal accurate mass reference and introduced in-source every 20 s.

Table 2. The in-house gradient solvent system used for for ultra-performance liquid chromatography-quadrupole time-of-flight mass spectrometry analysis.

Time (min)	Percent dH_2O + 0.1% Formic Acid (v/v)	Percent MeOH + 0.1% Formic Acid (v/v)
0.00	97	3
1.00	97	3
14.00	0	100
17.00	0	100
17.50	97	3
20.00	97	3

dH_2O: deionised water, MeOH: methanol, min: minutes, v/v: volume/volume

High resolution mass spectrometry data was acquired using a Waters Acquity UPLC system coupled to a Waters LCT Premier TOF MS and Phenomenex Kinetex C8 column (1.7 µm, 50 × 2.1 mm). The samples were prepared as per **Section 2.2** (page 25) and placed into glass vials. The run time was 20 min, and the photodiode array (PDA) detector linked to the system was used to extract the chromatogram at an absorbance of eLambda 800 nm.

2.3 Cell culture and maintenance

The SH-SY5Y neuroblastoma cell line (ATCC CRL-2266) was grown in-house at the Department of Pharmacology (University of Pretoria). The cells were cultured in T_{25} cm^2 flasks in a 1:1 mixture of Ham's F12 medium and Dulbecco's modified Eagle's medium (DMEM) (Sigma Aldrich, St Louis, USA). The medium was supplemented with 10% foetal calf serum (FCS) (Sigma-Aldrich, St Louis, USA), and 1% penicillin-streptomycin. The cells were incubated in an HF 212 UV incubator (Heal Force®, Shanghai, China) at 37°C in a 5% CO_2 humidified atmosphere. The medium was changed twice a week, and cells were split when a ~80% confluency was reached. Confluent cells were washed with 1 mL medium free of FCS, and enzymatically detached by adding 3 mL trypsin-like enzymes (TrypLE) solution for 4 min. Cells were harvested using centrifugation (5 min, 200 *g*), and the pellet was re-suspended in 1 mL culture medium.

2.3.1 Cell viability

Viability of SH-SY5Y cells was determined using the trypan blue assay.[152] This assay is based on the principle that the dye (trypan blue) is excluded from live, intact cell membranes while incorporated into dead cell membranes. The cell counting solution was prepared by adding 20 µL of the cell suspension to an Eppendorf tube (Sigma-Aldrich, St Louis, USA) containing 180 µL of 0.1% (w/v) trypan blue (Sigma-Aldrich, St Louis, USA). An aliquot of 20 µL of cell counting solution was added to a haemocytometer and the number of viable cells were counted using a microscope (Reichert-Jung, MicroStar110 Illuminator Model 1130B, New York Microscope Company, USA). The number of viable cells in suspension were calculated using the formula:

$$Viable\ cells\ \left(\frac{cells}{mL}\right) = \frac{Desired\ seeding\ density\ (\frac{cells}{mL})}{Total\ viable\ cell\ count\ \div 5} \times 10^5$$

The cells in suspension were diluted with complete growth media, to attain the desired seeding density per well. The following formula was used to calculate the volume of the original cell suspension to be added to the complete growth media:

$$Volume\ of\ cell\ suspension\ required = \frac{Desired\ seeding\ density\ (\frac{cells}{mL})}{Viable\ cells\ (\frac{cells}{mL})} \times Desired\ volume\ (mL)$$

2.4 The effect of 6-hydroxydopamine, crude extract, and fractions on cell density

Cells were seeded at a density of 10 000 cells per well (100 µL, 1 x 10^4 cells/mL) in a 96-well plate and incubated overnight for cellular attachment. Cells were exposed to either 100 µL medium (negative control), 0.5% DMSO (vehicle control), 1% saponin (positive control; Sigma Aldrich, St Louis, USA), 6-OHDA (5 – 150 µM, in-well concentrations), crude extracts (1, 3.1, and 10 µg/mL, in-well concentrations), or fractionated plant extracts (F1 to F7; 1, 3.1, and 10 µg/mL, in-well concentrations) in FCS-free medium for 48 h. Blanks consisting of 5% FCS-supplemented medium were used as sterility and background noise control.

The SRB assay was used to determine cytotoxicity as described by Vichai, *et al.*,[153] with adjustment to the volumes. Following exposure, the cells were fixed by adding 50 µL of a 50% (v/v) trichloroacetic acid (TCA) solution (Sigma-Aldrich, St Louis, USA) to each well. The plates were incubated at 4°C overnight. After 24 h, each well was washed using low-pressure running water, followed by drying wells in an oven at 40°C for approximately 1 h. Thereafter, 100 µL of a

0.057% (w/v) SRB stain (Sigma-Aldrich, St Louis, USA) in 1% acetic acid was added to all wells, and the plate was incubated in the dark for 30 min at 25°C. Excess SRB stain was removed by washing the cells with 150 µL acetic acid, and this wash step was repeated until all unbound stain was removed. Thereafter, the plate was dried in the oven for approximately 30 min. The bound dye was solubilised by adding 200 µL of tris aminomethane (TRIS) buffer (10 mM; pH 10.5) to the wells, after which the plate was covered with foil and placed on an orbital plate shaker (Gemmy Industrial Corporation, Taipei, Taiwan) for 1 h. The plate was then placed in the Synergy 2 HTX Multi-Mode plate reader (BioTek, Highland Park, USA), and the absorbance was read at 510 nm with a reference wavelength of 630 nm. Cell density was calculated using the following equation:

$$Cell\ density\ (\%) = \frac{Average\ absorbance(fractions)}{Average\ absorbance\ (NC)}\ x\ 100$$

2.5 The cytoprotective ability of the crude extracts and fractions

Cells were seeded as per **Section 2.4** (page 29), after which they were treated with 50 µL 6-OHDA (IC_{50} = 72.83 µM) for 2 h. Saponin (1%) was used as positive control. After exposure, cells were treated with 50 µL crude extracts or fractions (F1 to F7) at in-well concentrations of 1, 3.1, and 10 µg/mL for 48 h. The SRB assay, as described in **Section 2.4** (page 29), was used to assess cytoprotective ability, which was measured by the difference in cell density of the treated wells compared to the positive control (6-OHDA).

2.6 The effect of pure compounds on SH-SY5Y cell density

The pure compounds (atropine and scopolamine) were purchased from Thermo Fisher Scientific (Waltham, USA). For atropine a stock solution (1 mM) was prepared by dissolving 5.6 mg in 8 mL DMSO. For scopolamine a stock solution (1 mM) was prepared by dissolving 3.51 mg in 8 mL DMSO. All stock standards were stored as 150 µL aliquots at -80°C.

Cells were seeded as per **Section 2.4** (page 29). After incubation cells were exposed to either 100 µL medium (negative control), 0.5% DMSO (vehicle control), 1% saponin (positive control) (Sigma Aldrich, St Louis, USA), or pure compounds (5 - 200 µM in-well concentrations) in FCS-free medium for 48 h. Blanks consisting of 5% FCS-supplemented medium were used as sterility and background controls. The SRB assay, as described in **Section 2.4** (page 29), was used to assess the IC_{50} concentration of the pure compounds.

2.7 The cytoprotective ability of pure compounds

Cells were seeded as per **Section 2.4** (page 29), after which they were treated with 50 µL 6-OHDA (IC_{50} was predetermined as 72.83 µM) for 2 h. Saponin (1%) was used as positive control. After exposure, cells were treated with 50 µL atropine or scopolamine (49.48 and 48.26 µM in-well concentrations) for 48 h. The SRB assay, as described in **Section 2.4** (page 29), was used to assess cytoprotective ability. The latter was measured as the difference in cell density compared to the positive control (6-OHDA).

2.8 Cellular morphology

Cell morphology was assessed using phase contrast microscopy. An optical mechanism serves as the basis for the method, which translates variations in light phase and amplitude changes that manifest as variations in image contrast.[154] Cells were seeded into 94-well plates and incubated for 24 h for attachment. Cells were exposed to 6-OHDA (50 µL, 72.83 µM in-well concentration) for 2 h. After the incubation period cells were treated with 50 µL of either *C. edulis* (F 1) or *D. stramonium* (F 4) at concentrations of 1, 3.1, and 10 µg/mL. The treated cells were incubated for 48 h after which morphology was assessed microscopically (Zeiss Axiovert CFL40 microscope, Carl Zeiss AG, Oberkochem, Germany). Photomicrographs were captured at 40x magnification, of three representative images per treated well.

2.9 Intracellular reactive oxygen species generation

The enzymatic cleavage of 2',7'-dichlorodihydrofluorescein diacetate (H_2DCFDA) to the highly fluorescent dichlorofluorescein diacetate was used to determine the intracellular ROS concentration.[155-157] Cells were seeded and exposed as per **Sections 2.4** and **2.5** (page 29 and 30, respectively). Potassium persulfate (1 mM in-well concentration) was used as the positive control. After 48 h treatment, the medium was replaced with 100 µL H_2DCFDA (10 µM in PBS) followed by 2 h incubation at 37ºC. The fluorescence intensity was measured at an excitation wavelength of 480 nm and an emission wavelength of 590 nm (Synergy II, Biotek Instruments, Inc, Winooski, USA). Fluorescence intensity was blank-adjusted and normalised according to the SRB assay described by Vichai *et al*.[153] The ROS concentration was determined using the formula:

$$Intracellular\ ROS\ concentration\ (\%\ of\ negative\ control) = \frac{FIs}{FIc} \times 100$$

With FI_s being the normalised fluorescence intensity of the blank-adjusted sample and FI_c being the normalised average of the blank-adjusted negative control.

The 3.1 µg/mL concentration was used in all subsequent mechanistic assays, as there was no consistent trend in identifying specific fractions that effectively reduced intracellular ROS generation and improved cytoprotection.

2.8 Apoptosis

The Ac-DEVD-AMC cleavage assay as described by Cordier *et al.*,[158] was used to determine caspase-3/7 activity. The cleavage of Ac-DEVD-AMC results in a strong fluorescent product.[159] Cells were seeded and exposed as described in **Sections 2.4** and **2.5** (page 29 and 30, respectively), for 48 h. Cisplatin (29.85 µM in-well concentration) served as the positive control. After the 48 h incubation period, the medium was replaced with 25 µL of cold lysis buffer (10 mM HEPES, 2 mM CHAPS, 5 mM EDTA, 0.5 mM PMSF, 4.3 mM β-mercaptoethanol) and incubated for 15 min on ice. Thereafter, 100 µL of substrate buffer (10 µM Ac-DEVD-AMC, 10 mM HEPES, 5 mM EDTA, 0.5 mM PMSF, 4.3 mM β-mercaptoethanol) was added, and the plate incubated for 4 h at 37ºC. The fluorescent intensity (FI) was measured at an excitation of 355 nm and emission of 460 nm using the Synergy II plate reader, which was adjusted by subtracting the blank value with normalisation relative to caspase 3/7 activity and cell density relative to the negative control as per the equation:

$$Caspase-3/7\ activity\ (Fold-change\ relative\ to\ negative\ control) = \frac{FI\ sample}{FI\ of\ average\ negative\ control}$$

2.9 Mitochondrial integrity

Mitochondrial integrity was assessed using the cytopainter mitochondrial staining kit (ab112145, Abcam, UK). All procedures were performed according to the manufacturer's instructions to ensure reliable and accurate results. In this assay, a red tracking dye permeates live cells and produces fluorescence, allowing for the assessment of mitochondrial health.[160] Cells were seeded and exposed as per **Sections 2.4** and **2.5** (page 29 and 30, respectively). Potassium persulfate was used as positive control (1 mM in-well concentration). After exposure, the media was removed and replaced with 100 µL of a 0.3 times dilution of the cytopainter red (6 µL of 500x dye to a total of 10 mL FCS-free media) (Abcam via Biocom Africa, Pretoria, South Africa). The plate was then incubated for 30 min in a humidified incubator at 37ºC. After incubation, the dye was replaced with 100 µL FCS-free media. Fluorescence was read using aFLUOstar optima plate reader (BMG Labtech, Offenurg, Germany) set at an excitation and emission wavelength

of 544 nm and 620 nm, respectively. The relative fluorescence unit (RFU) was compared to the negative control and normalised by the cell density. Results are expressed as a ratio of the mitochondria to cell density compared to the negative control, similar to the SRB assay.

2.10 *In silico* docking

2.10.1 Protein preparation

Protein preparation was performed using the Protein Preparation Wizard in Maestro. During this process, water molecules were removed, bond orders were assigned, and hydrogen atoms were added to the chemical structures of the marker phytochemicals detected in *C. edulis* and *D. stramonium.* Additionally, bonds to metals were deleted, and formal charges on the metals and neighbouring atoms were adjusted within a specified range. Thereafter the protonation state for the residues in the chemical structures were adjusted to reflect physiological conditions and minimise potential errors in structures. The chemical structure was then refined with a restrained minimisation to reduce steric clashes and optimise geometry while maintaining the overall conformation. Lastly, potential binding sites were identified using a grid-based cavity prediction algorithm, with the OPLS-2005 force field applied for energy minimisation.

2.10.2 Ligand preparation

Ligand preparation was initiated by constructing the 2-dimensional (2D) structure of each compound detected in *C. edulis* and *D. stramonium* using SMILES conversion on Chem Draw Ultra 10.0. The 2D structures were then converted to a 3-dimensional (3D) structure using the same software. The software's SMILES conversion feature ensured the correct initial molecular structure, including proper chirality. The aim was to generate a low-energy 3D structure for each input, which accurately reflected the proposed molecular geometry.

Further ligand refinement was conducted using the LigPrep module in Maestro. In this step, chirality was preserved from the 3D structure, and the original ionisation states of the ligands were maintained. Tautomers were generated during this process, replacing any existing conformers to ensure that different possible forms of the ligand were considered. The conformational space was explored using the Monte Carlo method, a robust algorithm for finding the global minimum by testing a wide range of possible conformations. The search involved exploring all rotatable single bonds to account for the flexibility of the ligand. This process identified the global energy minimum multiple times, confirming the most stable ligand

conformations.

Finally, the OPLS_2005 force field was applied during the energy minimisation step, ensuring accurate structural refinement based on the least square minimisation approach. This methodology ensured that the ligand was prepared with the lowest energy, best conformer, and appropriate molecular properties for subsequent molecular docking or simulation studies.

2.10.3 Active site determination

Using the Glide docking model, grids were generated to evaluate the binding interactions between the ligand and the protein's active sites. These grids were created using the Receptor Grid Generation module in Glide, following standard procedures to define the receptor's active site. The generation of grids involves mapping the electrostatic and geometric properties of the receptor to provide an accurate docking environment. The grid defined the shape and electrostatics of the receptor, allowing for the precise placement of ligands within the protein's active site. Additionally, constraints were incorporated into the grid files, ensuring that certain critical interactions (such as hydrogen bonds with specific residues) were included during docking. Multiple fields were used to represent the receptor's properties, progressively enhancing the accuracy of ligand scoring. This included factors like steric and electrostatic complementarity, which are essential for determining the favourable binding poses of the ligand. This comprehensive approach allowed the Glide model to predict optimal ligand-receptor interactions, providing insights into binding strength and mode, and supporting drug discovery by identifying potential therapeutic targets.

2.10.4 Molecular docking

A ligand molecule was selected so that it could be excluded from the grid generation with the van der Waals radius scaling set to 1.00. The ligand was docked using the docking functionality in extra precision (XP) mode. The most feasible orientation of the ligands in the binding pocket was predicted, and the strength of the interaction in that orientation was quantified from a scoring function.

2.10.5 Targets for docking

Structure-based analysis is the process where the protein structure of a target (enzyme, receptor etc) is used to identify interactions with ligands.[161] Whilst there are many targets encoded into the human genome, enzymes and g-coupled protein receptors are the most targeted, with 47% and 30% of known drugs acting on these targets respectively.[162] Structure-based analysis is the technique that identifies interactions between ligands and a target's protein structure, such as a receptor.[163] In this study molecular docking was used to investigate how chemotaxonomic markers detected in *C. edulis* and *D. stramonium* will interact with D1 and D2 receptors. This computational approach predicts binding affinity and receptor specificity, providing potential efficacy and mechanisms of chemotaxonomic markers compounds.

Molecular docking is particularly valuable in PD research, as it facilitates the exploration of strategies to counteract dopaminergic neurodegeneration and DA deficiency, which underlie the motor impairments characteristic of PD.[164] The D1 and D2 receptors were selected as targets because of their role in controlling motor function.[149,163]

2.11 Data analysis and statistics

Raw data was captured using Microsoft Excel (Microsoft Office Suite) and statistical analyses were performed using GraphPad Prism 8.0.2 (GraphPad Software, San Diego, California, USA). At least three biological and technical repeats were performed ($n \geq 9$). All data was expressed as the mean ± standard error of the mean (SEM). Changes in protein content was calculated using the Kruskal-Wallis analysis of variance test with Dunn's multiple comparison post-test. For cytotoxicity studies, the logarithm of the concentration of the crude extracts/fractions/isolated compounds was plotted against the response (reduction in cell density – compared to the positive control of 6-OHDA). Outliers were identified and removed using GraphPad Robust regression and the outlier removal (ROUT) method. The indicator of significance was $p \leq 0.05$.

Chapter 3: Results and discussion

3.1 Phytochemistry

The phytochemical profiles of *C. edulis* and *D. stramonium* encompass a diverse array of secondary metabolites, including alkaloids, flavonoids, and phenolic compounds, which underpin their pharmacological and therapeutic properties.[165,166] *Catha edulis* is characterised by its phenylpropylamino alkaloids, including cathine and cathinone, which act as CNS stimulants.[121] *Datura stramonium* is distinguished by its tropane alkaloids, including atropine, hyoscyamine, and scopolamine, which exhibit potent anticholinergic activity and have been extensively studied for their neuropharmacological importance.[108]

These compounds, also referred to as chemotaxonomic biomarkers are essential for targeted analytical identification (**Table 3)**. Advanced techniques such as liquid chromatography-mass spectrometry (LC-MS) allow for accurate detection and quantification of these chemotaxonomic biomarkers, providing essential information about their biosynthetic processes and pharmacologic mechanisms.

In the chromatogram of *Catha edulis,* distinct peaks were observed for cathine and cathinone, despite their high similarity and near indistinguishability (**Figure 12**). Peaks A and B likely correspond to closely eluting molecules, potentially identified as cathine and/or norephedrine (**Table 4**). Compound A was detected only in the crude extract and fraction 2, whereas compound B was present in the crude extract and all fractions, with protonated peaks at 151.10 Da. Similarly, Dhabbah *et al*., reported peaks for cathine in *C. edulis* leaves at 152.11 Da using direct analysis in real-time (DART) TOF MS. Field *et al*., further identified GC/MS peaks for cathine in methanolic extracts of *C. edulis* at 151 Da, corroborating these findings.[167,168]

The absence of cathinone in the *C. edulis* extract is attributed to its instability, as it is highly prone to oxidation during drying or processing of the plant material.[169] In the study by Pendl *et al.*, where LC-MS was used to analyse cathine and cathinone in *C. edulis* plant, a reduction in cathinone content was noted and ascribed to oxidative decomposition.[170,171] This decomposition leads to the formation of a “dimer” compound, 3,6-dimethyl-2,5-diphenylpyridine.[169]

Table 3. Chemotaxonomic markers of *Catha edulis* and *Datura stramonium* utilised in targeted liquid chromatography-mass spectrometry analysis.

Compound	Neutral monoisotopic mass (Da)	Chemical formula	Chemical structure
Catha edulis			
Cathinone	149.0841	$C_9H_{11}NO$	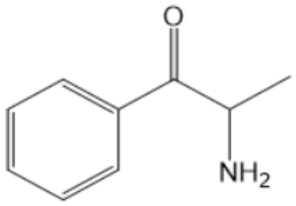
Cathine	151.0997	$C_9H_{13}NO$	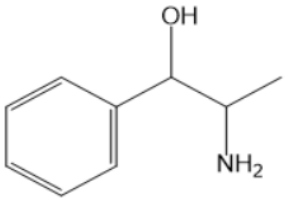
Norephedrine	151.0997	$C_9H_{13}NO$	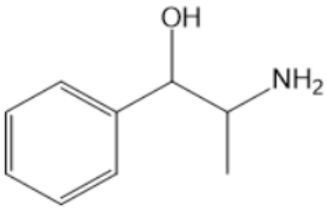
Datura stramonium			
Atropine	289.1678	$C_{17}H_{23}NO_3$	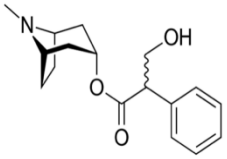
Scopolamine	303.1470	$C_{17}H_{21}NO_4$	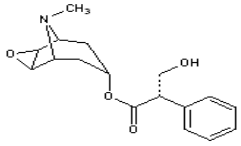
Hyoscyamine	289.1679	$C_{17}H_{23}NO_3$	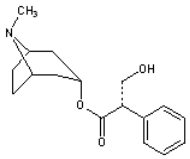

Da: Daltons

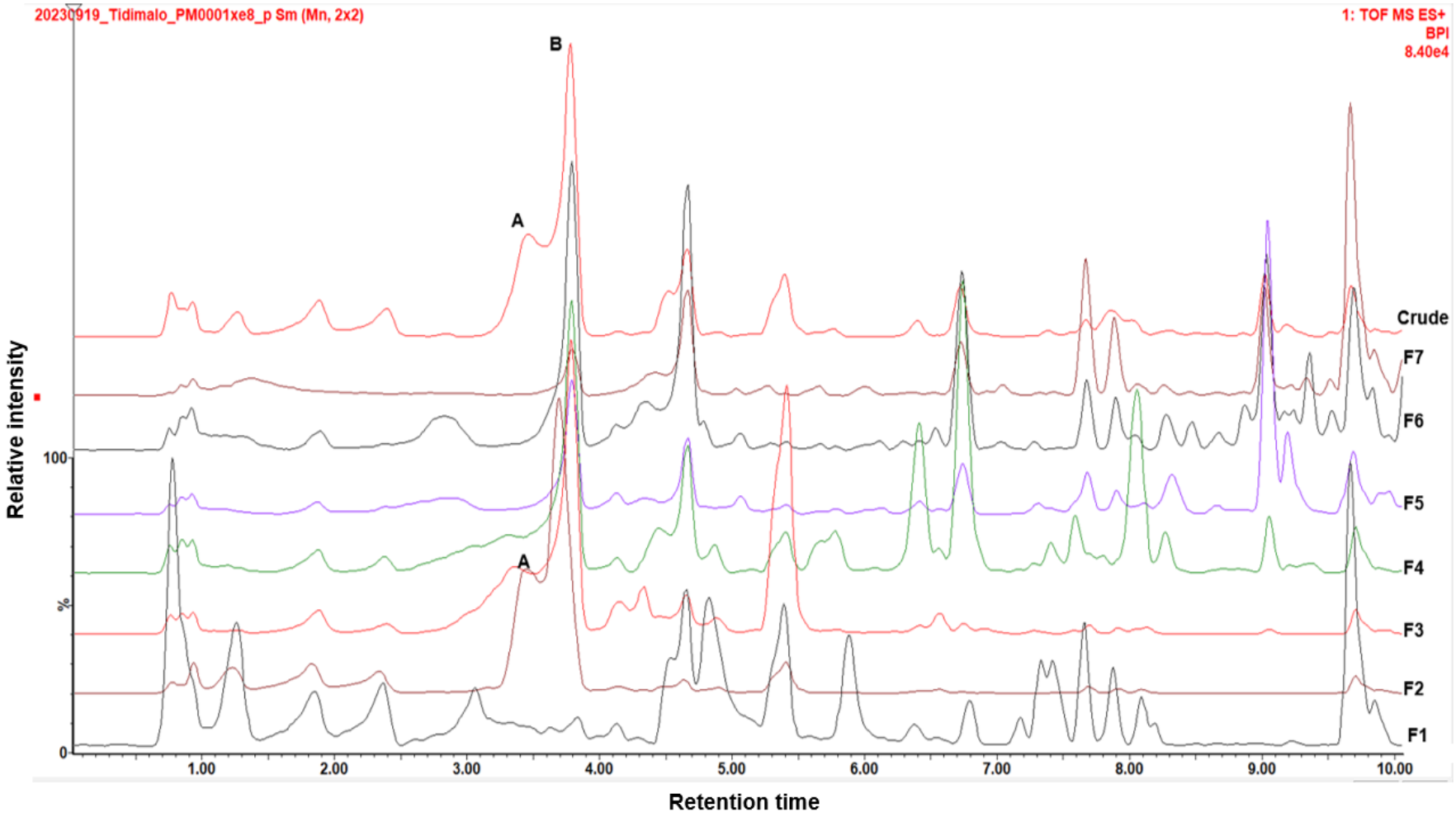

Figure 12. Chromatograms of *Catha edulis* crude extract and fractions 1 - 7 analysed in the positive electrospray ionisation mode. Peaks: A and B: cathine or norephedrine.

Table 4. Compounds detected in the crude extract and fractions of *Catha edulis* using ultra-performance liquid chromatography-mass spectrometry.

Peak retention time (min)	Identified compound	m/z Ion	Neutral mass (Da)	Theoretical mass (Da)	Mass difference (ppm)	λ_{max} (nm)
A 3.461	Cathine or Norephedrine	152.1084 $[M+H]^+$	151.1011	151.0997	9.27	295
B 3.791	Cathine or Norephedrine	152.1084 $[M+H]^+$	151.1011	151.0997	9.27	295

min: minutes, Da: Daltons, ppm: parts per million, nm: nanometer.

Only cathine and its isomer norephedrine were provisionally detected from among the compounds listed in **Table 3** (Page 38). Both are metabolites of S-(-)-cathinone, and their relative abundances are influenced by environmental conditions at the time of harvest, including temperature, humidity, soil composition, and light exposure.[169] Despite sharing the same chemical structure and accurate mass, cathine and norephedrine are stereoisomers, differing subtly in their 3D structures.[172] These structural differences are reflected in their closely related retention times and accurate masses, as shown in **Table 4**.

The chemotaxonomic markers: hyoscyamine (A), noradrenaline (B), and atropine (C) were identified in *D. stramonium* (**Figure 13**). However, the peak for atropine (C) was not easily distinguishable due to co-elution with hyoscyamine. The co-elution is likely a result of their nearly identical molecular weights and similar chemical structures as stereoisomers, making their chromatographic separation challenging.[173]

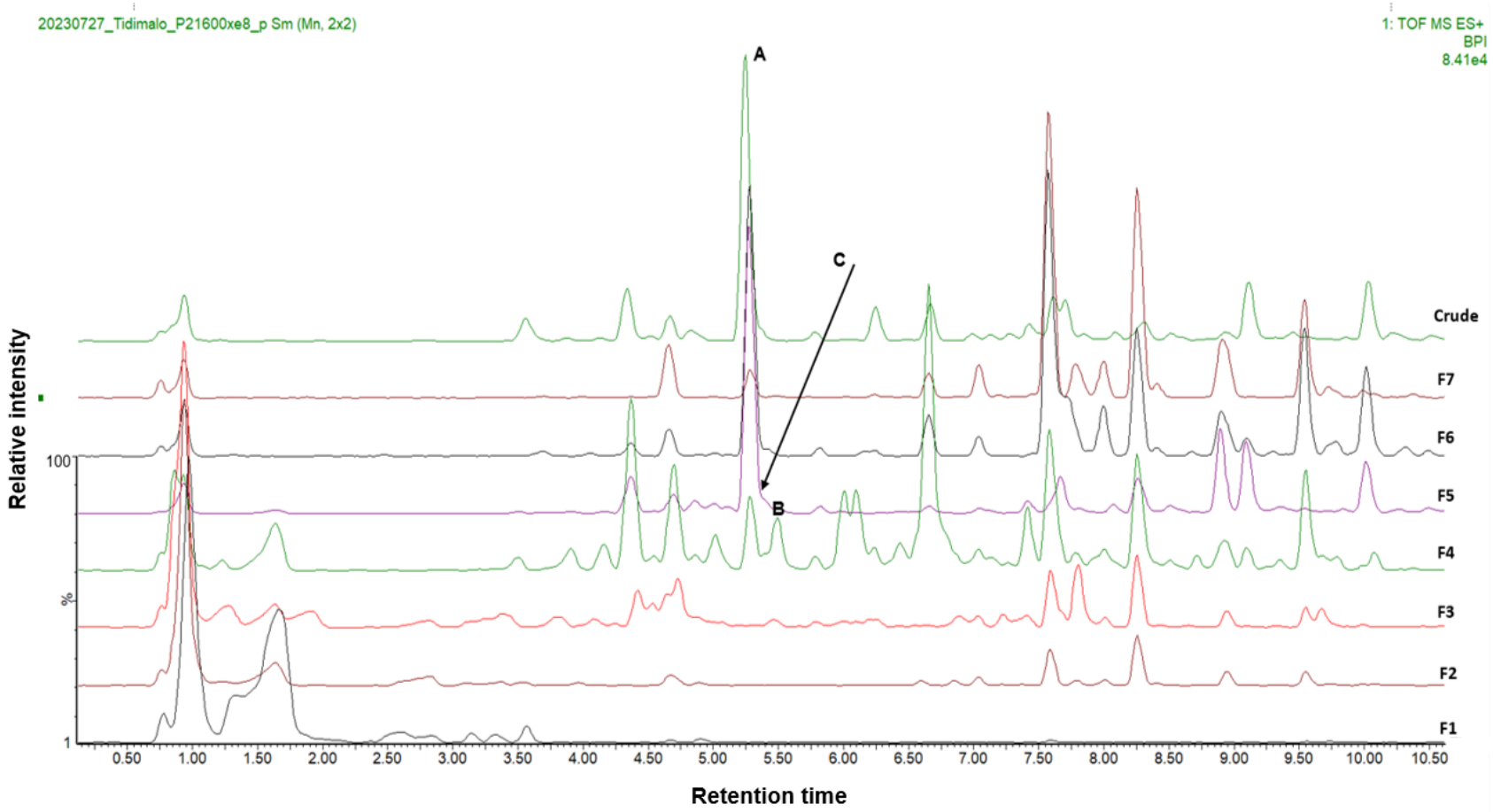

Figure 13. Chromatograms of *Datura stramonium* crude extract and fractions 1 - 7 analysed in the positive electrospray ionisation mode Peaks: A: Hyoscyamine, B: Noradrenaline, C: Atropine.

In the crude extract, all three compounds appeared as overlapping and broad peaks, reflecting the presence of a complex mixture of secondary metabolites. This co-elution resulted in reduced resolution of individual compound peaks. Fractionation, however, improved separation, with the resulting fractions exhibiting distinct intensities and well-defined peak profiles (**Figure 13**).

Hyoscyamine (A) and atropine (C) were more prominent in the crude extract, as well as in fractions 5 and 6. This finding is consistent with that of Yadav *et al*., who only detected atropine and hyoscyamine, of the known chemotaxonomic markers of *D. stramonium,* using GC-MS analysis.[174] Noradrenaline (B) was most prominent in fraction 4, indicating successful polarity-based separation. Notably, the compounds of interest were absent in fractions 1–3, most likely because they were not extracted or were present at concentrations below the detection threshold.

Interestingly, scopolamine, one of the chemotaxonomic markers of *D. stramonium*, was not detected in the extract, likely due to its very low concentration. This finding is in agreement with Miraldi *et al*., who reported that atropine (0.134 µg/mg) was present at higher concentrations than scopolamine (0.044 µg/mg) in trichloromethane leaf extracts of *D. stramonium* when quantified using GC-MS.[175] In contrast, Jakabova *et al*., found higher scopolamine (131.66 µg/mg) content compared to atropine (4.25 µg/mg) in methanolic flower extracts of *D. stramonium* flowers using LC-MS.[176] These contrasting results suggest that scopolamine levels may vary significantly depending on the part of plant analysed, with lower levels in leaves and higher levels in flowers.

It is well established that phytochemical content can differ depending on the specific plant part, soil conditions, and the time of year the plant is collected.[176] Additionally, alkaloid concentrations are known to vary across different plant tissues, further contributing to the observed differences in scopolamine levels.[176]

Table 5. Compounds detected in the crude extract and fractions of *Datura stramonium* using ultra-performance liquid chromatography-mass spectrometry.

Peak retention time (min)	Identified compound	m/z Ion	Neutral mass (Da)	Theoretical mass (Da)	Mass difference (ppm)	λ_{max} (nm)
A 5.286	Hyoscyamine	290.175 $[M+H]^+$	289.168	289.1676	-0.735	295
B 5.491	Noradrenaline	290.175 $[M+H]^+$	169.074	169.0739	-0.215	295
C 5.437	Atropine	290.175 $[M+H]^+$	289.168	289.1677	-0.139	295

min: minutes, Da: Daltons, ppm: parts per million, nm: nanometer.

Hyoscyamine and atropine, both tropane alkaloids, exhibited similar retention times (**Table 5**) due to their structural similarities, while noradrenaline, a hydrophilic phenylpropylamino alkaloid, eluted earlier, consistent with its polarity. These results demonstrate the efficiency of the fractionation process in isolating bioactive compounds while highlighting potential challenges in separating structurally similar alkaloids under the chromatographic conditions employed.

3.2 Cytotoxicity of the crude extract and fractions

The crude extract and fractions 1, 2, 4, 6 of *C. edulis* exhibited minimal albeit concentration-dependent cytotoxicity in the SH-SY5Y cells, with higher concentrations producing slight reductions in cell viability (**Figure 14A**). At lower concentrations (1 µg/mL), these fractions increased cell density by ~10%, likely due to a hormetic effect (a biphasic response where low doses stimulate beneficial outcomes), whereas at higher concentrations cytotoxicity was evident. In contrast, fractions 3 and 5 did not induce concentration-dependent cytotoxicity, nor was there a significant reduction in cell viability noted for most of the tested concentrations. However, at 10 µg/mL, the crude extract and fraction 6 significantly reduced cell density by 17.9% ($p < 0.001$) and 12.34% ($p < 0.0001$), respectively. Among the tested samples, the *C. edulis* crude extract demonstrated the highest cytotoxicity, significantly decreasing cell density by approximately 17.9% ($p < 0.0001$) at 10 µg/mL.

The minimal cytotoxicity noted for *C. edulis* is consistent with previous findings.[177] In a study, where SH-SY5Y cells were also used for cytotoxicity determination, a dose-dependent effect, with significant cytotoxicity was only noted at higher concentrations for synthetic cathinone.[177] Valente *et al*., also demonstrated a dose-dependent response, showing that synthetic cathinones, such as 3,4-methylenedioxypyrovalerone (MDPV), induced minimal cell death at lower concentrations (0.1 mM), while higher concentrations (10 mM) resulted in greater cell death in SH-SY5Y cells.[178] From these results, it can be deduced that cathinones, including those naturally present in *C. edulis*, are less toxic at lower doses, further supporting the minimal cytotoxicity observed in the current study.

Catha edulis also contains a complex mixture of compounds, including alkaloids, flavonoids, and other phytochemicals, which may contribute to its reduced cytotoxicity. It is possible that these compounds interact in a way that mitigates the potential cytotoxic effects.[165]

Fractions 1, 4, and 5 of *D. stramonium* displayed concentration-dependent cytotoxicity in SH-SY5Y cells (Figure 14B). Fraction 1 reduced cell density by 11.43%, 16.47%, and 22.41% ($p < 0.05$) as concentrations increased from 1, 3.1, to 10 µg/mL, respectively, compared to the negative control. Fraction 4 reduced cell density by 11.37% at 10 µg/mL, while fraction 5 reduced cell density by 8.39% and 4.84% at lower concentrations (1 and 3.1 µg/mL). Interestingly, at the highest concentration (10 µg/mL), fraction 5 slightly increased cell density by 3.07%.

The crude extract and fractions 2 and 3 did not exhibit concentration-dependent cytotoxic effects, with all concentrations showing minimal cytotoxicity. Fraction 2 reduced cell density by 6.38%, 4.46%, and 8.81% at 1, 3.1, and 10 µg/mL, respectively. For fraction 6, the lowest concentration showed minimal cytotoxicity, reducing cell density by 4%, while higher concentrations reduced it by 11.4% and 9.63%, respectively. Fraction 7 showed minimal cytotoxicity at 1 and 10 µg/mL, while the 3.1 µg/mL concentration slightly increased cell density.

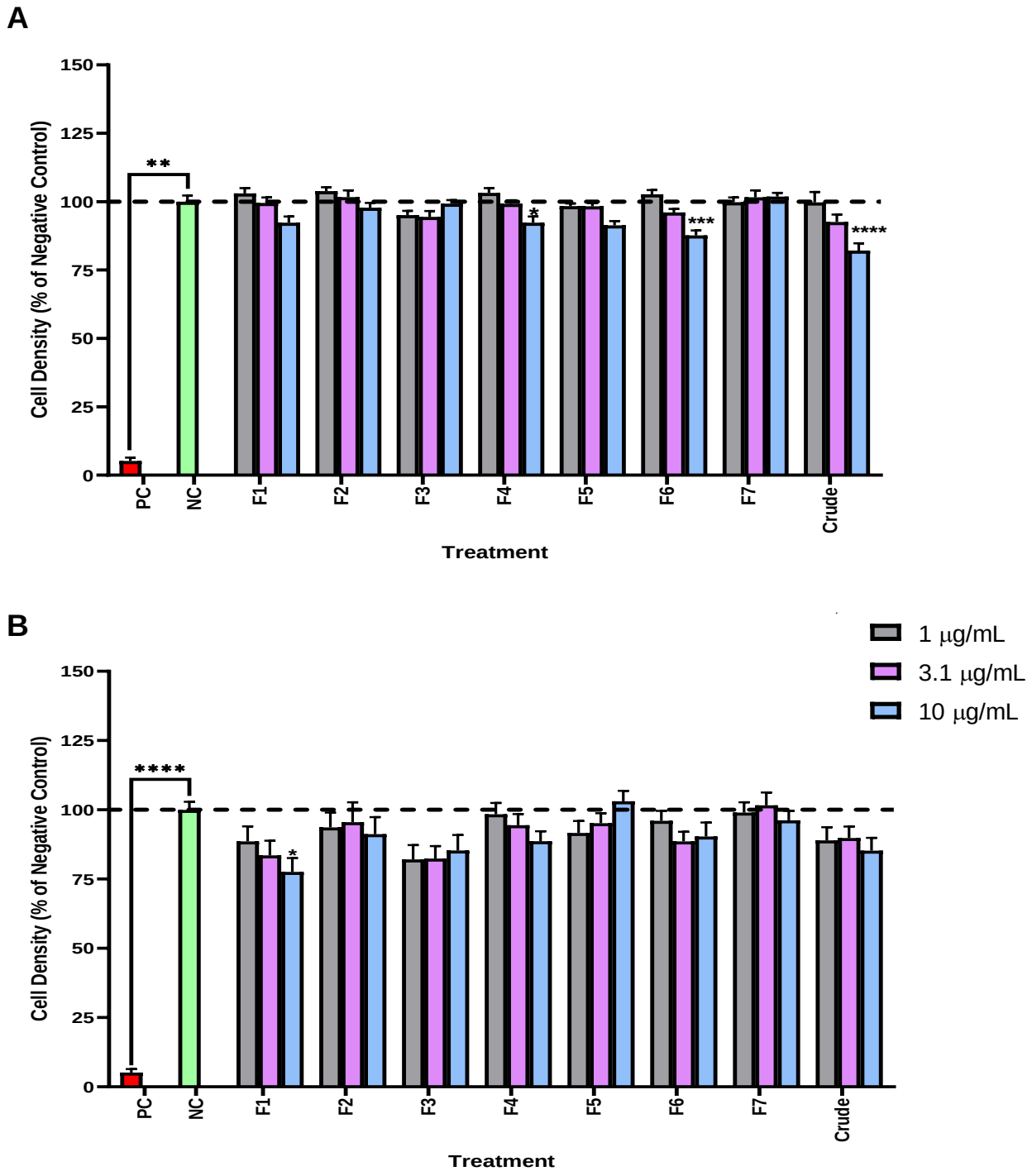

Figure 14. The cytotoxic effect of *Catha edulis* (A) and *Datura stramonium* (B) crude extract and fractions on the SH-SY5Y cells. Values are shown as means ± SEM of three biological and technical repeats (n=9). Significance was determined relative to the negative control; * $p < 0.05$, ** $p < 0.01$, *** $p < 0.001$, **** $p < 0.0001$. NC: negative control (FCS-free media) and PC: positive control (1% saponin).

The minimal cytotoxicity observed for *D. stramonium* extract could be attributed to the concentrations that were tested being below the potential cytotoxic threshold. In a previous study it was reported the methanol extract's IC_{50} was 39.48 µg/mL, suggesting that concentrations below this value are unlikely to cause significant cytotoxicity.[179] Supporting this, studies on other Solanaceae plants with similar alkaloid profiles, such as *Datura inoxia* and *Hyoscyamus niger*, have demonstrated comparable results. *Datura inoxia* methanol extract exhibited concentration-dependent cytotoxicity, reducing cell viability to below 50% at concentrations above 25 µg/mL, with an IC_{50} of 66.53 µg/mL in PC12 cells. However, at lower concentrations (3.125–12.5 µg/mL), cell viability was ≥ 90%.[180]

Similarly, *Hyoscyamus niger* demonstrated neuroprotective effects in rotenone-induced rat models by restoring antioxidant enzyme activity; SOD and CAT and increasing GSH levels.[181] These findings suggest that *D. stramonium*, like other Solanaceae plants, may exert minimal cytotoxicity at lower concentrations, possibly due to its alkaloid composition and associated antioxidant properties.

3.3 Cytotoxicity of 6-hydroxydopamine

6-Hydroxydopamine exerted a concentration-dependent effect on cell viability, with an IC_{50} of 72.83 µM (**Figure 15)**. No further cytotoxicity was observed at higher concentrations, as the cell density plateaued. This could be ascribed to a saturation effect, where a threshold concentration maximises cell death or the presence of cellular resistance mechanisms that prevent additional cytotoxicity. The results are corroborated by Luo *et al*., where the authors reported that treatment with 6-OHDA (75 µM) significantly reduced the cell viability of SH-SY5Y cells to approximately 60% after 24 h of treatment using the 3-(4,5-dimethylthiazol-2-yl)-2,5-diphenyl tetrazolium bromide (MTT) assay.[182]

Wei *et al*. found that the IC_{50} of 6-OHDA in SH-SY5Y cells was 100 µM after 24 h of treatment (MTT assay).[183] A dose-dependent effect of 6-OHDA with an IC_{50} of 150 µM after 24 h of incubation has also been reported (MTT assay).[184] The higher IC_{50} values may be attributed to varying experimental parameters, including the assay used; MTT versus SRB, cell line variability, and incubation times.[185]

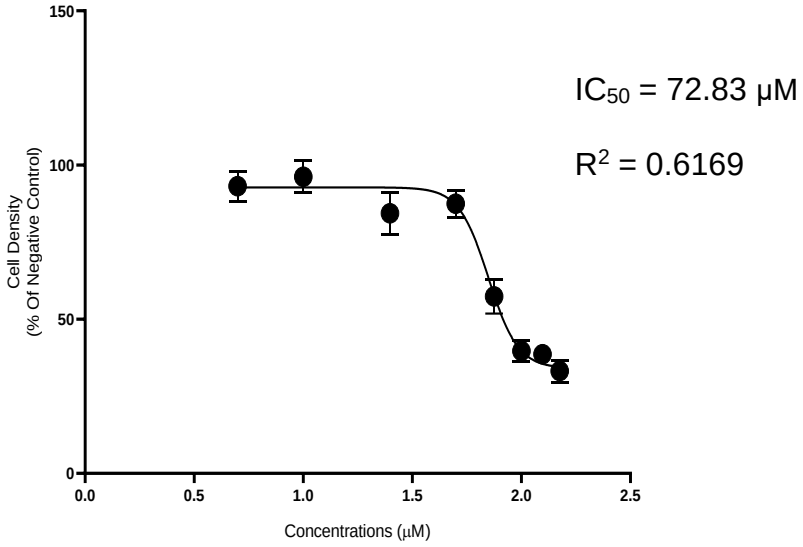

Figure 15. SH-SY5Y cell viability after 6-hydroxydopamine treatment. Values are shown as means ± SEM of three biological and technical repeats (n=9). IC_{50}: half-maximal inhibitory concentration; R^2: coefficient of determination.

The state of cell differentiation is also of importance, as it leads to the up-regulation of enzymes and transporters such as tyrosine hydroxylase and DAT. Lopes *et al.* differentiated SH-SY5Y cells using RA and 1% FBS over ten days and observed increased vulnerability to 6-OHDA-induced cytotoxicity.[144,186] Despite these variations, the current results offer valuable insights into the cytotoxic effects of 6-OHDA on SH-SY5Y cells. It was therefore decided to determine the activity of the plant extracts relative to the IC_{50} concentration of 6-OHDA (72.83 μM).

3.4 Cytoprotection of the crude extract and fractions

In the PD model, 6-OHDA acts as an OS inducer, playing a crucial role in the pathogenesis of PD. It has been demonstrated that 6-OHDA-induced cytotoxicity in SH-SY5Y cells is dependent on both the concentration and exposure time. In a previous study, a reduction in cell viability of 35% was noted after treatment with 100 μM 6-OHDA for 24 h.[187] In the present study, treatment with 6-OHDA alone resulted in a significant ($p < 0.0001$) decrease in cell density by ~ 81.38% relative to the negative control (**Figure 16**).

Dose-dependent cytoprotection was observed when cells were treated with *C. edulis* fractions 1, 2, and 6 (**Figure 16A**). For fraction 1, cell density increased significantly by 11.3% ($p < 0.0001$), 9.91% ($p < 0.001$) and 9%, at respective concentrations compared to the 6-OHDA control. Fraction 2 increased cell density by 11.85% ($p < 0.0001$), 5.12% and 0.44% at concentrations of 1, 3.1, and 10 µg/mL, respectively, compared to 6-OHDA. Fraction 6 significantly increased cell density at all three concentrations tested.

Fraction 3 showed the same increase in cell density at both 1 and 10 µg/mL concentrations, with significant increases of 9.77% ($p < 0.001$) and 9.7% ($p < 0.001$), respectively, compared to 6-OHDA. Fraction 5 exhibited a similar trend. Fraction 4 displayed the highest cytoprotection at 3.1 µg/mL, with a significant increase in cell density of 13.37% ($p < 0.0001$). At all concentrations tested, the crude extract and fraction 7 demonstrated similar results, with increases in cell density of 5.89% ($p < 0.05$) and 6.87% ($p < 0.01$), respectively. Among all the fractions, fraction 1 displayed the highest cytoprotection.

Although *C. edulis* extract exhibited cytoprotection, the level was generally low, which may be ascribed to the presence of the alkaloid, cathine.[188] Cathine, although primarily known for its stimulating properties, may have mild cytotoxic effects that could counteract the plant's protective action. Cathine has structural resemblance to other psychoactive drugs such as amphetamine, which has been reported to interfere with various cellular processes, including cell signalling.[189] The observed cytoprotection may therefore reflect a balance between the beneficial properties of *C. edulis*' phenolics and flavonoids, which are potent antioxidants, and the potential toxicity of its alkaloid content.

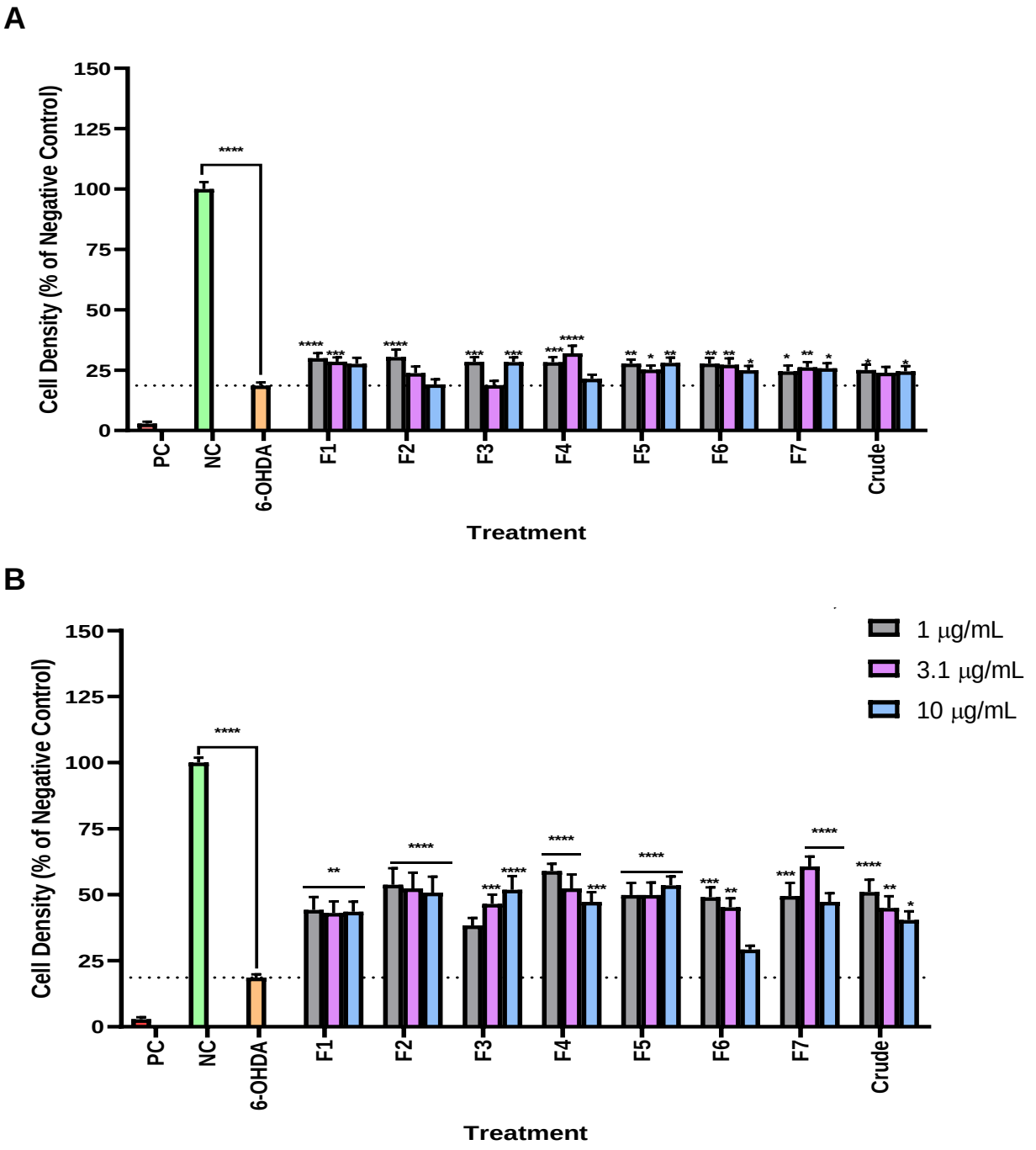

Figure 16. Cytoprotective effect of *Catha edulis* (A) and *Datura stramonium* (B) crude extracts and fractions against 6-hydroxydopamine-induced neurotoxicity in SH-SY5Y cells after 48 h exposure. Values are presented as means ± SEM of three biological and technical repeats (n=9). Significance relative to 6-OHDA; * $p < 0.05$, ** $p < 0.01$, *** $p < 0.001$, **** $p < 0.0001$. 6-OHDA: 6-hydroxydopamine (72.83 µM), NC: negative control, and PC: positive control (1% saponin).

Datura stramonium crude extract and fractions increased cell density across various concentrations when compared to the 6-OHDA control (**Figure 16B**). The crude extract and fractions 3, 4, and 6 demonstrated a dose-dependent response. In fraction 3, as the concentration increased the cell densities also increased significantly ($p < 0.001$).

Fraction 4 increased cell density by 40.32% ($p < 0.0001$), 33.80% ($p < 0.0001$), and 28.71% ($p < 0.001$), at 1, 3.1, and 10 µg/mL, respectively compared to 6-OHDA. A similar trend was noted for the crude extract and fraction 6. The lower cytoprotection observed at higher concentrations could be due to the complex interactions between different compounds found in the plant extracts, potentially reducing the overall protective effect.

Fractions 1, 2, and 5 showed consistent cytoprotection across all concentrations, increasing cell density by an average of 25.02% ($p < 0.01$), 33.70% ($p < 0.0001$), and 32.51% ($p < 0.0001$), respectively. Fraction 7 demonstrated the highest cytoprotection at 3.1 µg/mL, with a significant ($p < 0.0001$) increase in cell density by 42.12%. In contrast, fraction 6 exhibited the lowest cytoprotection at 10 µg/mL, increasing cell density by 10.62% compared to the 6-OHDA control. This reduced cytoprotection could be due to an additive cytotoxic effect between phytochemicals and 6-OHDA. Despite these variations, fraction 4 displayed the highest average cytoprotection overall, with an increase in cell density by 34.28%.

Datura stramonium extracts demonstrated greater cytoprotection at lower concentrations, indicating that intrinsic cytotoxicity may limit their beneficial effects at higher doses. This aligns with the known CNS depressant effects of tropane alkaloids, such as atropine and hyoscyamine, which are neuroprotective at low doses but can cause adverse effects, including sedation and confusion, at higher doses due to their anticholinergic properties.[190] Although there are no studies that have specifically evaluated the neuroprotective effects of *D. stramonium* extracts on 6-OHDA-induced SH-SY5Y cells, findings from research on *Datura inoxia* offer relevant insights. In that study, lower concentrations of the extract enhanced cell survival in glutamate-induced toxicity, increasing cell density to 77%, compared to approximately 49% viability in the glutamate control group.[180] These results suggest that *Datura* species, including *D. stramonium*, may exhibit similar neuroprotective effects at lower concentrations, supporting their potential for therapeutic applications in neurodegenerative conditions.

The cytotoxic activity and cytoprotection of *C. edulis* and *D. stramonium* crude extracts and fractions on cell density in 6-OHDA-naïve and 6-OHDA-exposed cells after 48 h of treatment is summarised in **Table 6.**

To further support the cytoprotective results, a qualitative analysis was conducted to observe cell morphology. Under normal cell culture conditions (negative control), SH-SY5Y cells exhibited a healthy morphology with increased density, growing as monolayers characterised by flattened morphology and elongated neurites (**Figure 17A**). However, treatment with 6-OHDA resulted in morphological changes; causing the cells to become rounded, lose density, and exhibit impaired neurite formation (**Figure 17B**). These morphological changes are consistent with apoptosis, likely due to the increased caspase-3 activity and elevated Cyt c levels triggered by 6-OHDA-mediated cell damage.[191]

Mitochondria play a crucial role in apoptosis, and in response to various stressors, proteins such as Cyt c are released into the cytosol, triggering the apoptotic caspase cascade.[192] Lazaro *et al*. demonstrated that in 6-OHDA-treated SH-SY5Y cells, Cyt c is released through the MPT pore, resulting in mitochondrial damage.[193] Similarly, Latchoumycandane *et al*., observed that rat dopaminergic neurons exposed to 100 µM 6-OHDA for 3 and 6 h experienced an 80% to 200% increase in cytosolic Cyt c levels, indicating mitochondrial dysfunction linked to 6-OHDA-induced cell death.[191]

Additionally, Moosavi *et al*., reported that 6-OHDA treatment in SH-SY5Y cells led to cell body shrinkage, a reduction in the number of living cells, and increased cell debris after 24 h.[194] These findings suggest that 6-OHDA-mediated cell death involves a combination of necrosis and apoptosis.[185]

Table 6. The effect of the crude extract and fractions of *Catha edulis* and *Datura stramonium* on cell density in 6-hydroxydopamine-naïve (cytotoxicity) and 6-hydroxydopamine-exposed (cytoprotection) cells after 48 h treatment. Statistical significance was determined relative to the negative (for naïve cells) or 6-OHDA (for exposed cells) treated cells (controls).

			Cell density (% relative to negative control) ± SEM							
Plant	**Concentration (µg/mL)**	**Cytotoxcity/ cytoprotection**	**F1**	**F2**	**F3**	**F4**	**F5**	**F6**	**F7**	**Crude**
Catha edulis	1	Cytotoxicity	103.03 ± 1.95	103.84 ± 1.46	95.1 ± 1.54	103.24 ± 1.73	98.37 ± 0.97	102.67 ± 1.58	99.81 ± 1.71	99.74 ± 3.77
		Cytoprotection	29.92 ± 2.13	30.47 ± 3.05	28.4 ± 1.94	28.24 ± 2.14	27.69 ± 1.74	27.21 ± 2.44	24.48 ± 2.46	25.09 ± 2.12
	3.1	Cytotoxicity	99.52 ± 2.01	101.67 ± 2.46	94.43 ± 2.16	99.21 ± 1.30	98.29 ± 1.20	96.05 ± 1.30	101.57 ± 2.52	92.60 ± 2.71
		Cytoprotection	28.53 ± 1.80	23.74 ± 2.75	18.82 ± 1.71	31.99 ± 3.10	25.19 ± 1.74	27.22 ± 2.64	26.20 ± 2.13	23.91 ± 2.45
	10	Cytotoxicity	92.31 ± 2.26	97.80 ± 1.74	99.25 ± 1.32	92.32 ± 2.24	91.37 ± 1.52	87.66 ± 1.84	101.87 ± 1.32	82.1 ± 2.66
		Cytoprotection	27.62 ± 2.52	19.06 ± 2.15	28.32 ± 1.96	21.45 ± 1.55	28.03 ± 2.21	24.98 ± 1.75	25.78 ± 2.09	24.53 ± 2.14
Datura stramonium	1	Cytotoxicity	88.57 ± 5.46	93.62 ± 5.38	82.07 ± 5.19	98.42 ± 4.04	91.61 ± 4.32	96.00 ± 3.64	99.01 ± 3.72	88.96 ± 4.73
		Cytoprotection	44.26 ± 4.86	53.76 ± 6.24	38.36 ± 2.87	58.94 ± 2.77	49.92 ± 4.51	49.05 ± 3.72	49.51 ± 4.97	51.06 ± 4.63
	3.1	Cytotoxicity	83.53 ± 5.32	95.54 ± 7.15	82.38 ± 4.54	94.41 ± 4.06	95.16 ± 3.57	88.60 ± 3.45	101.29 ± 4.66	89.78 ± 4.17
		Cytoprotection	43.12 ± 4.31	52.42 ± 5.95	46.51 ± 3.57	52.42 ± 5.21	49.92 ± 4.72	45.25 ± 3.39	60.74 ± 3.70	44.97 ± 4.43
	10	Cytotoxicity	77.59 ± 4.96	91.19 ± 6.17	85.31 ± 5.61	88.63 ± 8.63	103.06 ± 3.79	90.37 ± 5.03	96.22 ± 3.39	85.25 ± 4.62
		Cytoprotection	43.55 ± 3.85	50.79 ± 6.06	51.83 ± 5.23	47.33 ± 3.65	53.56 ± 3.30	29.24 ± 1.44	47.32 ± 3.27	40.41 ± 3.29

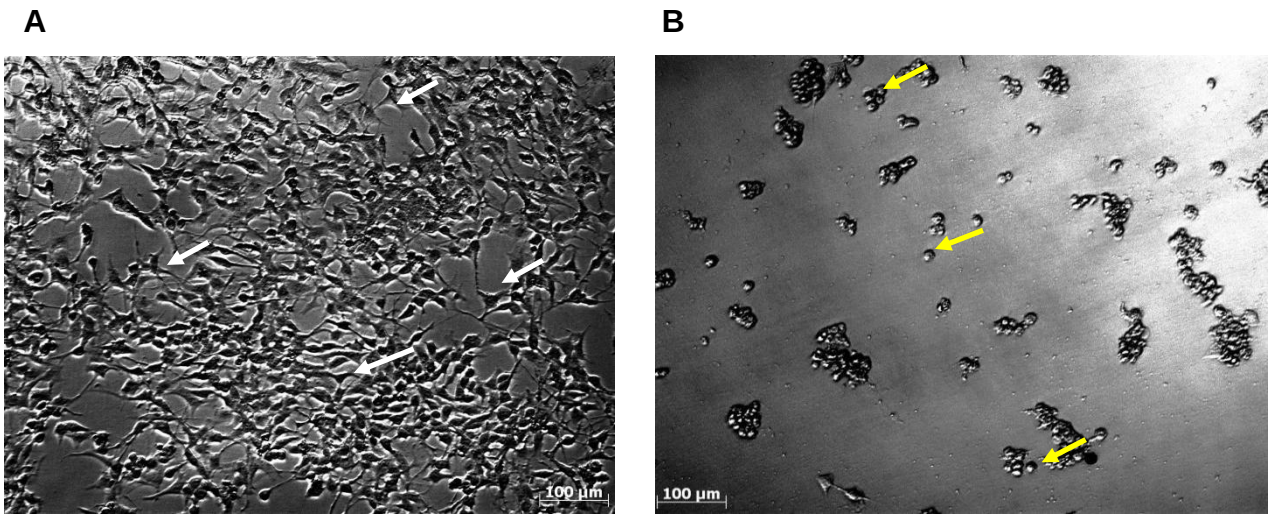

Figure 17. The effect of the negative control (media without foetal calf serum) and 6-hydroxydopamine on SH-SY5Y cellular morphology. Phase contrast microscopy at 40× magnification. The SH-SY5Y cells were treated with (A) media without foetal calf serum (negative control) and (B) the IC_{50} of 6-hydroxydopamine (72.83 µM). White arrows indicate elongated neurites, while yellow arrows indicate rounded cells (B). IC_{50}: half-maximal inhibitory concentration.

Fractions 1 and 7 of *C. edulis* and *D. stramonium* were selected for morphological analysis as they displayed the best cytoprotection at all concentrations tested (**Figure 18**). Cells treated with either *C. edulis* or *D. stramonium* showed similar morphology, with most cells retaining intact, long protruding neurites, which correlates with the cytoprotection results. *C. edulis* exhibited the highest cytoprotective activity at 3.1 µg/mL. In contrast, the lowest concentration (1 µg/mL) of *D. stramonium* showed better cytoprotective activity than 3.1 and 10 µg/mL.

Concentration	*Catha edulis*	*Datura stramonium*
1 µg/mL	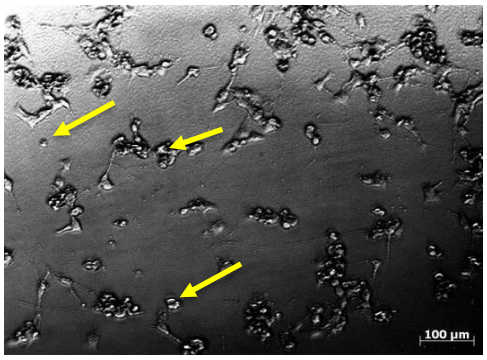	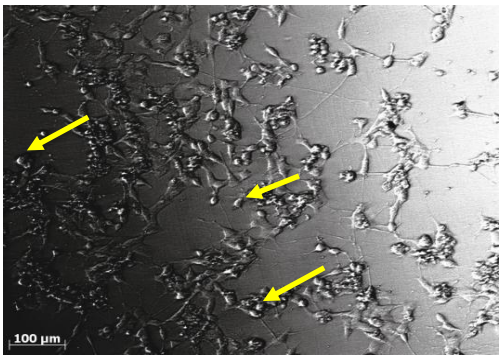
3.1 µg/mL	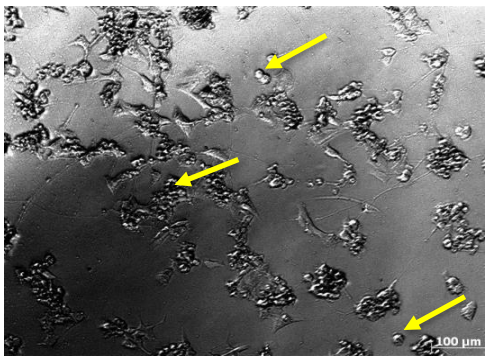	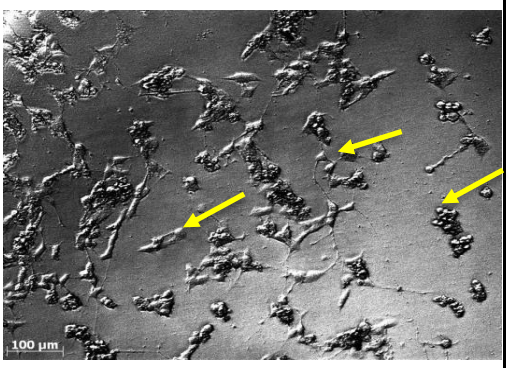
10 µg/mL	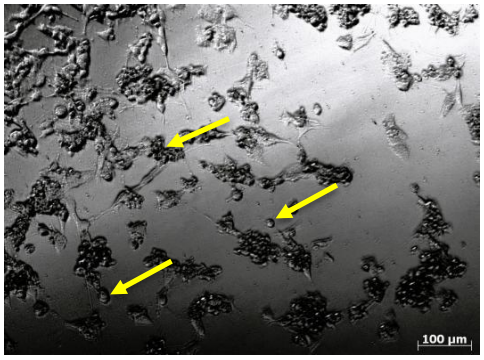	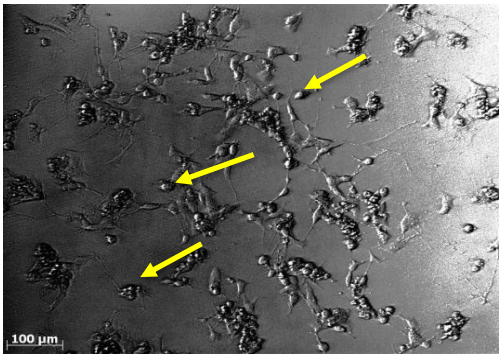

Figure 18. Photomicrographs indicating the effect of *Catha edulis* and *Datura stramonium* extracts (1, 3.1, and 10 µg/mL) on SH-SY5Y cell morphology when pre-treated with 6-hydroxydopamine and incubated for 48 h. Phase contrast microscopy at 40× magnification. Yellow arrows indicate apoptotic bodies. 6-OHDA: 6-hydroxydopamine.

The cell morphology observations support the cytoprotection results. However, cell morphology alone cannot distinguish between cell death by necrosis or apoptosis. Although the exact mechanism of cell death was unclear, both *C. edulis* and *D. stramonium* crude extracts and fractions, managed to increase cell viability, providing a foundation for future research. Preserving the survival of dopaminergic neurons in PD could alleviate the efficiency of currently available treatments.

3.5 Cytotoxicity and cytoprotection of the phytochemical markers

Atropine and scopolamine induced a concentration-dependent effect on cell viability (**Figure 19A and B**). The IC_{50} was determined as 49.48 µM in the current study, which is contrary to the IC_{50} of 1.74 µM obtained by Lochner *et al*.[195] A similar discrepancy was noted for the IC_{50} of scopolamine, 48.26 µM versus 2.09 µM.[195] The large difference in values is ascribed to differences in cell lines, as Lochner *et al.* utilised the human embryonic kidney (HEK293) cell line, which differs in sensitivity and response compared to SH-SY5Y cells used in this study.

Further discrepancies are evident in the IC_{50} values for scopolamine reported by Suthprasertporn *et al*.,[196] who reported an IC_{50} of 2 mM, compared to the IC_{50} of 48.26 µM determined in the current study. Differences across studies may be ascribed to the use of different cytotoxicity assays. For instance, the MTT assay measures metabolic activity, while the SRB assay assesses protein content, potentially leading to differing interpretations of cytotoxic effects.[197]

A

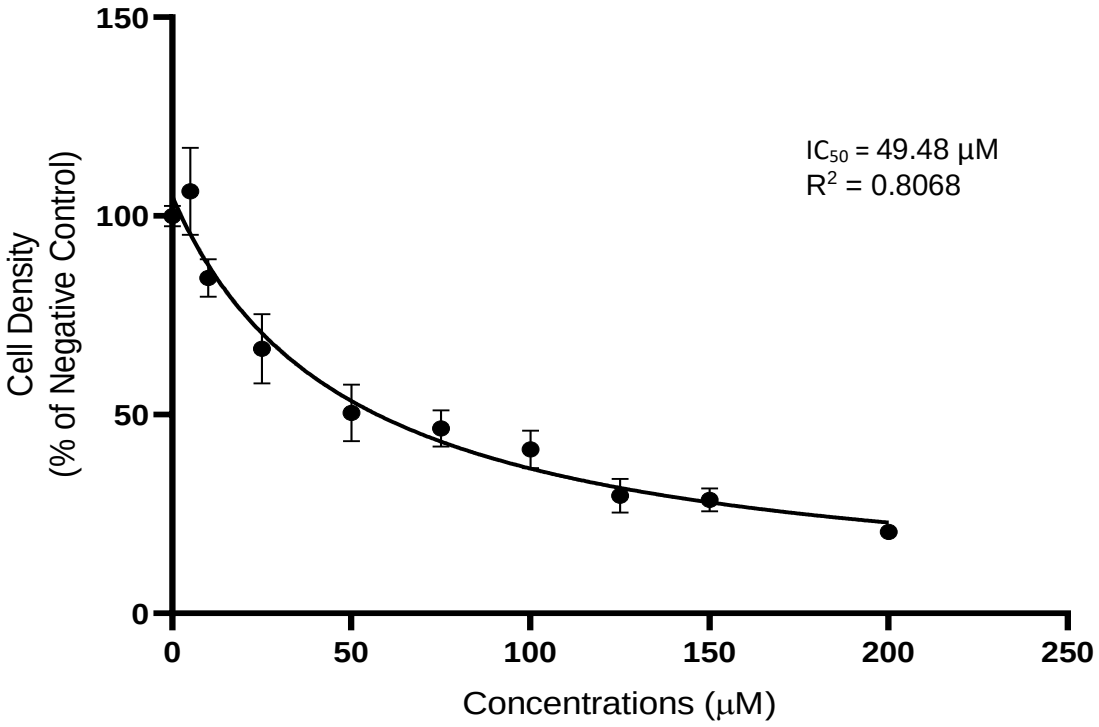

B

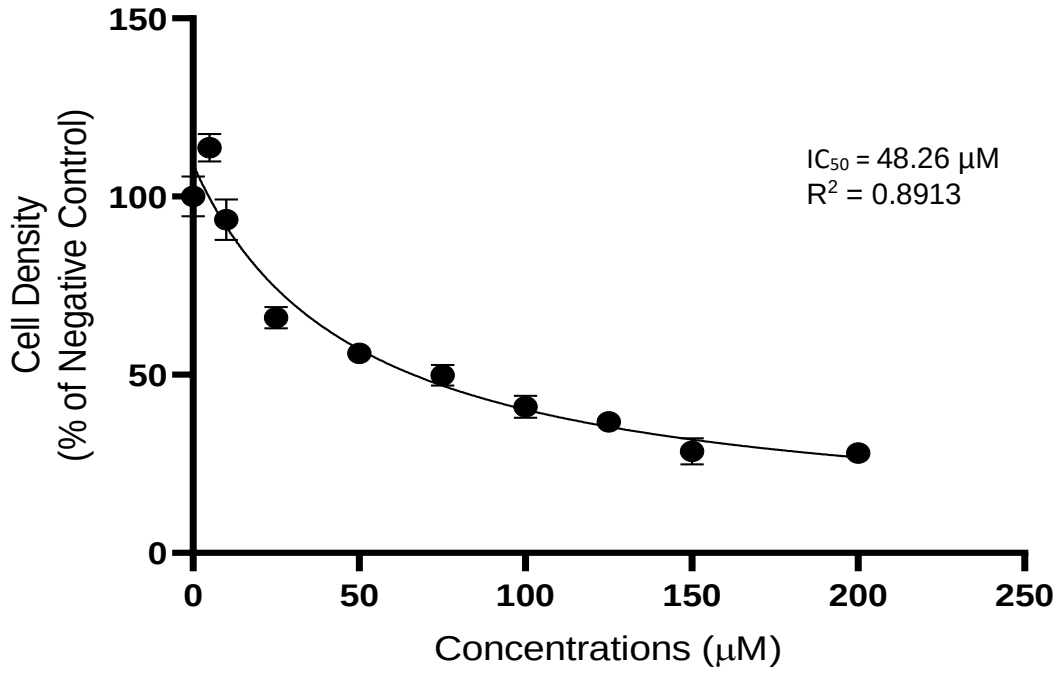

Figure 19. The effect of atropine (A) and scopolamine (B) on SH-SY5Y cell density. IC_{50}: half-maximal inhibitory concentration; R^2: coefficient of determination.

Treatment with 6-OHDA alone significantly ($p < 0.0001$) reduced cell density by 81.38% compared to the negative control (**Figure 20**). The observed cell loss is corroborated by the findings of a study where 6-OHDA treatment was shown to reduce cell density in neuronal cell lines as discussed in **Sections 3.3 and 3.4** (page 46 and 47).[198]

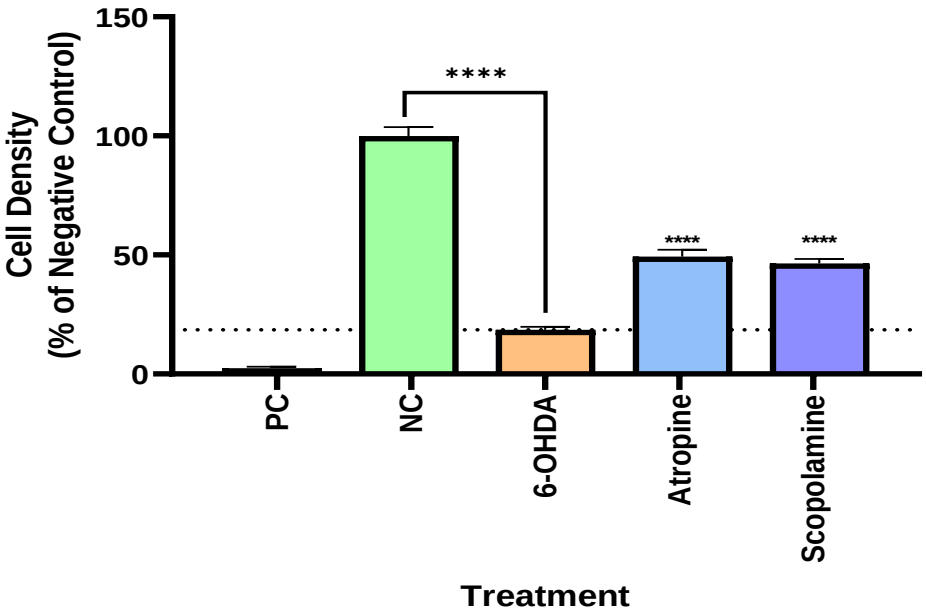

Figure 20. The cytoprotective activity of pure compounds (atropine and scopolamine) on 6-hydroxydopamine induced cytotoxicity in SH-SY5Y cells. Results are reported as mean ±SEM of three biological and technical repeats (n=9). Significance is expressed relative to 6-OHDA; **** $p < 0.0001$. 6-OHDA: 6-hydroxydopamine (72.83 µM), NC: negative control, and PC: positive control (1% saponin).

Atropine and scopolamine significantly ($p < 0.0001$) increased cell density by 30.69% and 27.88% compared to 6-OHDA, respectively (**Figure 20**). It is proposed that both compounds counteract the cytotoxic effects induced by 6-OHDA, likely through their activity as muscarinic receptor antagonists. Alkaloids, in general, are known to exhibit neuroprotective effects by reducing oxidative stress, alleviating neuroinflammation, inhibiting cholinesterases, and preventing apoptosis while modulating autophagy.[199]

In support of the cytoprotective results, cell morphology was visualised and captured (**Figure 21**). Treatment with atropine and scopolamine resulted in a mixed cellular response, with some cells maintaining their elongated morphology and intact neurites, while others exhibited a rounded shape. These observations are consistent with the cytoprotective effects demonstrated in the viability assays, where both compounds significantly preserved cell survival compared to

6-OHDA-treated cells (**Section 3.4;** page 53). The presence of intact cells with neurites indicates that atropine and scopolamine effectively mitigated the neurotoxic effects of 6-OHDA in a subset of the cell population. However, the appearance of some rounded cells may reflect incomplete protection or variability in the extent of cytoprotection across the culture, emphasising the partial but notable protective role of these compounds.

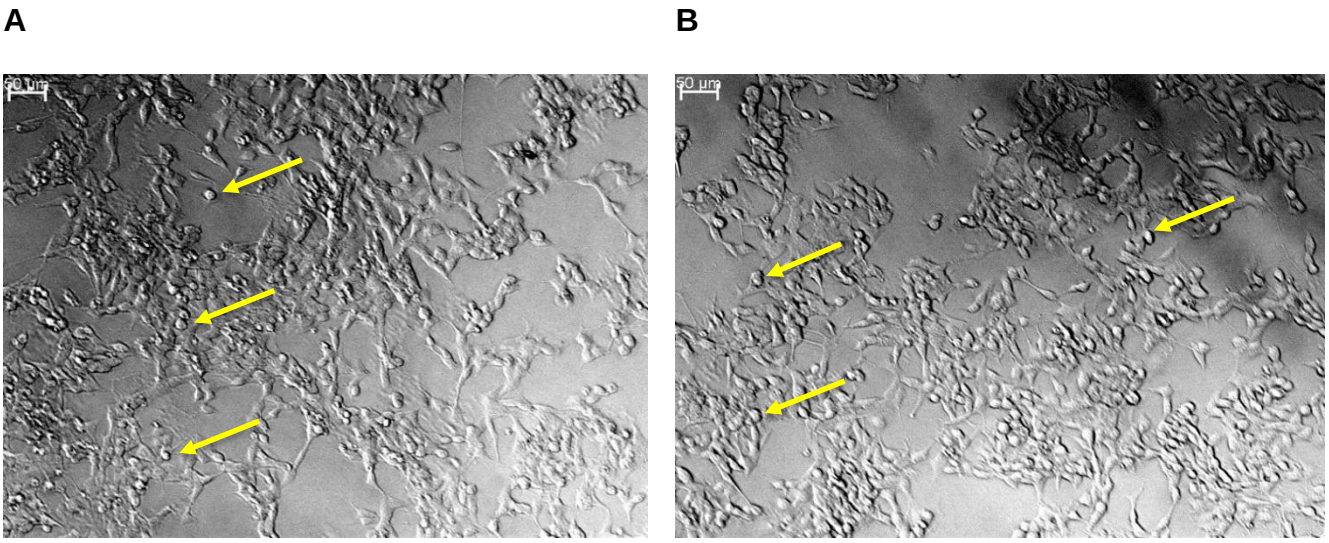

Figure 21. Photomicrographs indicating the effect of A) atropine (49.48 µM) and B) scopolamine (48.26 µM) on SH-SY5Y cell morphology, after pre-treatment with 6-hydroxydopamine, followed by exposure of the cells to the compound for 48 h. Phase contrast microscopy at 40× magnification. Yellow arrows indicate apoptotic bodies. 6-OHDA: 6-hydroxydopamine.

3.6 Intracellular reactive oxygen species generation

Treatment with 6-OHDA alone increased intracellular ROS generation by 2.82 ± 0.25-fold compared to the negative control (**Figure 22**). These findings are in agreement with those obtained in other studies, where 6-OHDA-induced oxidative stress was identified as a key contributor to neuronal damage through excessive ROS production.[182,200,201] Jaisin *et al*., observed a 1.55 ± 0.10-fold increase in ROS levels when SH-SY5Y cells were treated with 50 µM 6-OHDA for 24 h.[200] Similarly, Luo *et al*., found that treatment with 75 µM 6-OHDA led to a 2.5-fold increase in ROS compared to the controls.[182] Chen *et al*., reported a 2.3-fold increase in ROS formation after treating SH-SY5Y cells with 100 µM 6-OHDA for 1 h.[202] Ikeda *et al*., found that ROS levels increased 3.7-fold when SH-SY5Y cells were treated with 6-OHDA.[203]

The variation in ROS generation across studies can be attributed to different experimental conditions such as 6-OHDA concentration, exposure duration, and assay type.[182] Also, in this study, the fluorescence results were normalised to protein content to compensate for changes in

cell density caused by cell death (using the SRB assay), a factor that was not considered in the studies conducted by the other authors.

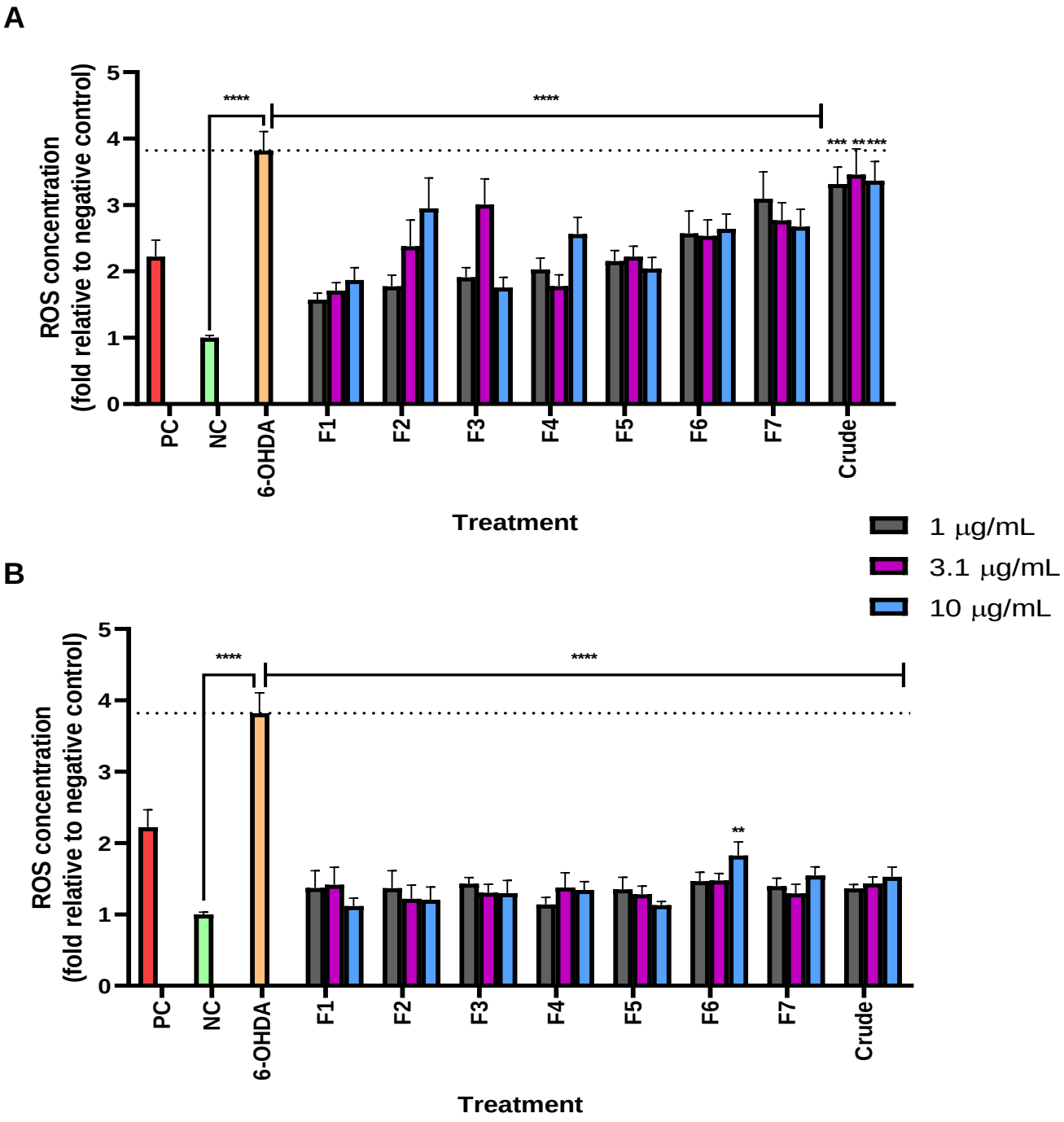

Figure 22. The effect of *Catha edulis* (A) and *Datura stramonium* (B) crude extract and fractions on 6-hydroxydopamine induced reactive oxygen species generation in SH-SY5Y cells. Results are reported as mean ± SEM of three biological and technical repeats (n=9). Significance is expressed relative to 6-OHDA; ** $p < 0.01$, *** $p < 0.001$, **** $p < 0.0001$. 6-OHDA: 6-hydroxydopamine (72.83 µM), ROS: reactive oxygen species, NC: negative control, and PC: positive control (500 µM potassium persulfate).

Catha edulis crude extract and fractions significantly ($p < 0.0001$) reduced 6-OHDA-induced ROS generation at all concentrations tested (**Figure 22A**). Fraction 7 showed a concentration-dependent decrease, significantly ($p < 0.0001$) reducing ROS by 0.73 ± 0.12-fold, 1.05 ± 0.02-fold, and 1.15 ± 0.01-fold at 1, 3.1, and 10 µg/mL, respectively

Fractions 1 and 2 also demonstrated concentration-dependent reductions, with a smaller increase in ROS observed at higher concentrations. Fraction 1 significantly ($p < 0.0001$) reduced ROS by 2.5 ± 0.19-fold, 2.11 ± 0.16-fold, and 1.95 ± 0.1-fold at 1, 3.1, and 10 µg/mL, respectively. Fraction 6 consistently reduced ROS across all concentrations tested.

The reduction in ROS levels noted in this study is most likely due to *Catha edulis's* antioxidant capabilities. *C. edulis* is reported to contain high concentrations of phenolics and flavonoids, which have strong free radical-scavenging properties.[181,204-206] Abdelwahab *et al*., reported a high phenolic and flavonoid content in *C. edulis*, whereas Vinokur *et al*., found that *C. edulis* leaves contained high concentrations of polyphenols and ascorbic acid, which will boost antioxidant potential.[207,208] *C. edulis* oil extract was shown to possess antioxidant activity (23.5-23.6 µg ascorbic acid equivalent (AAE/kg of dry matter) using the 2,2-diphenyl-1-picrylhydrazyl (DPPH) assay.[209]

Further evidence supporting these findings comes from research on other phenolic-rich plants. Noui *et al.* investigated *Ephedra alata*, a plant with a biochemical profile similar to *C. edulis,* as both contain, ephedrine.[210] *Ephedra alata* demonstrated antioxidant activity in the DPPH assay, with an IC_{50} value of 12.25 ± 1.09 µg/mL, and was also found to have a high total phenolic content of 358.06 ± 10.74 µg gallic acid equivalent (GAE)/mg. These findings emphasise the critical role of phenolic compounds in *C. edulis* in mitigating OS, a key contributor to cellular damage in PD. By lowering ROS levels, *C. edulis* demonstrates potential therapeutic benefits, as reflected in the cytoprotective effects discussed in **Section 3.4** (page 49).[200] This implies that the antioxidant properties of *C. edulis* could provide significant advantages in reducing OS linked to the disease.[211]

Datura stramonium crude extract and fractions also significantly reduced 6-OHDA-induced ROS generation at all concentrations tested (**Figure 22B**). Fractions 2, 3, and 5 exhibited concentration-dependent reductions in ROS, with increasing concentrations leading to further decreases in ROS generation. The crude extract and fraction 6 also showed a concentration-

dependent reduction in ROS, although higher concentrations, displayed a slight increase in ROS generation. These findings may be attributed to the phenolic and flavonoid content of *D. stramonium.* Al-Snafi *et al*. reported the presence of alkaloids, flavonoids, phenols, and glycosides in a methanol extract of *D. stramonium*.[109] Similarly, Matcha *et al*., reported that the methanol extract of *Datura metel* effectively inhibited DPPH radicals at concentrations of 5 and 10 µg/mL.[212] Furthermore, Roy *et al*. observed that the methanol extract of *Datura metel* seeds had a high phenolic acid content (268.6 µg GAE/mg of dried sample), indicative of its antioxidant capabilities.[213]

One of the compounds identified in *D. stramonium,* is noradrenaline, also known as norepinephrine. Norepinephrine is reported to protect neurons against OS induced in SH-SY5Y cells by increasing the supply of GSH from astrocytes via β3-adrenoceptor stimulation.[201] Glutathione is one of the most important antioxidants synthesised in cells and is known to neutralise free radicals, further supporting the ROS-reducing effects observed in *D. stramonium* extracts.[214]

Following these assays, the 3.1 µg/mL concentration for both plants was selected for further mechanistic assays due to the inconsistent dose-dependent responses and unclear results in the cytoprotection and intracellular ROS assays at lower and higher concentrations. The selection of this concentration, provides a balanced approach for subsequent investigations, avoiding the confounding effects seen at higher concentrations and allowing for clearer insights into the underlying mechanisms.

3.7 Apoptosis

6-Hydroxydopamine is known to induce apoptosis primarily by activating caspase-3.[200] The activation of caspase-3 in PD is strongly associated with neuronal death.[215-217] The release of Cyt c from mitochondria facilitates this process, further linking mitochondrial dysfunction to neurodegeneration.[191,218]

Cisplatin is known to induce apoptosis in neuronal cells,[219] and this was noted by the significant increase in caspase 3/7 activity (**Figure 23**). Similarly, treatment with 6-OHDA alone significantly ($p < 0.0001$) increased caspase 3/7 activity by 4.13 ± 0.07-fold compared to the negative control (**Figure 23**). This finding is supported by Jaisin *et al*., who reported a 2.0 ± 0.11-fold increase in caspase-3 activity in SH-SY5Y cells treated with 50 µM 6-OHDA.[200] Luo *et al*., observed that treatment with 75 µM 6-OHDA resulted in a significant increase in cell death with cleaved

caspase-3 protein levels being ~25-fold higher than the control group.[182] These results confirm that 6-OHDA induces caspase-3 activity.

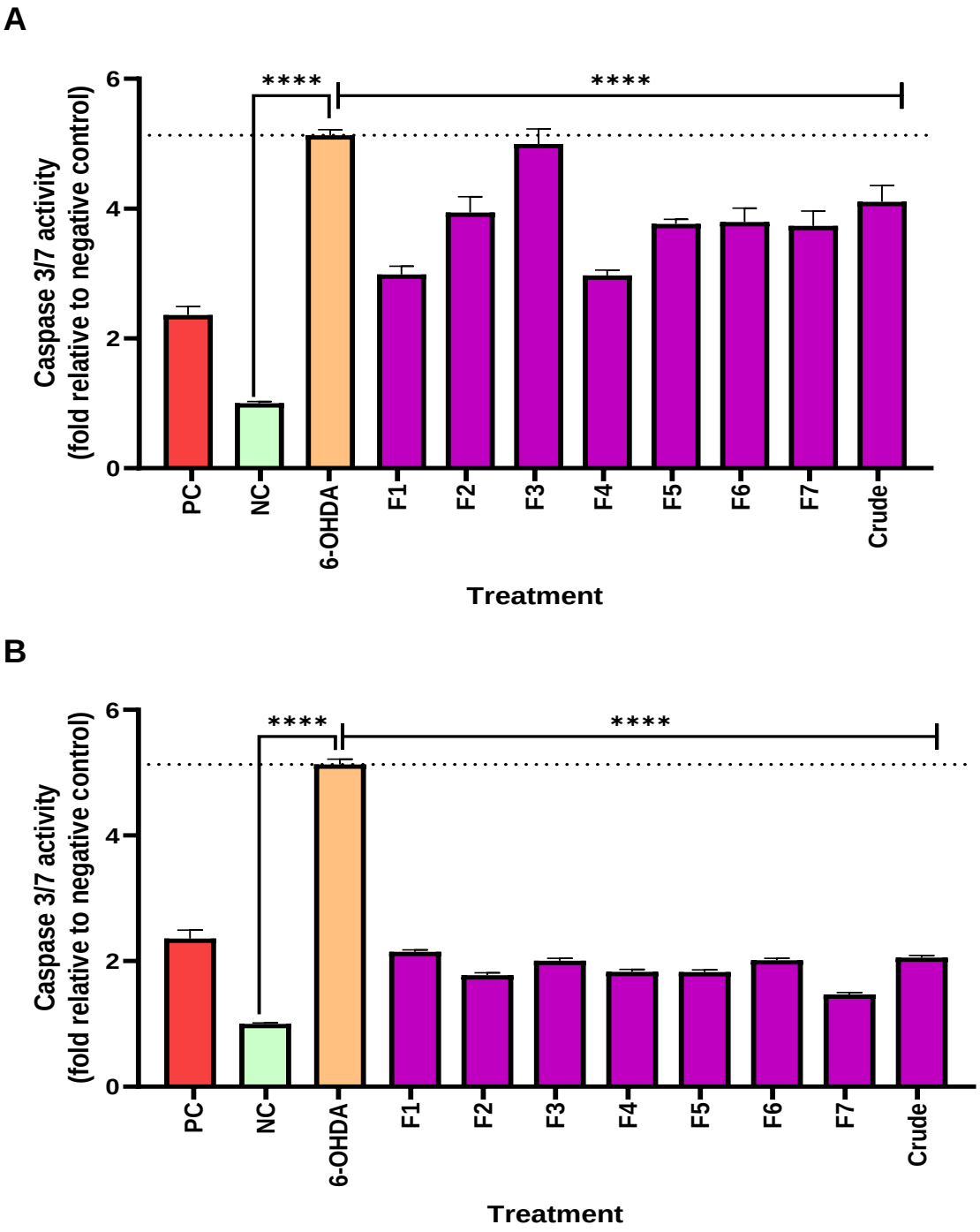

Figure 23. The effect of *Catha edulis* (A) and *Datura stramonium* (B) crude extract and fractions (3.1 µg/mL) on 6-hydroxydopamine induced caspase 3/7 activity. Results are reported as mean ± SEM of three biological and technical repeats (n=9). Significance is expressed relative to 6-OHDA; ****p < 0.0001. 6-OHDA: 6-hydroxydopamine (72.83 µM), NC: negative control, and PC: positive control (29.85 µM cisplatin).

Catha edulis crude extract and fractions also significantly ($p < 0.0001$) reduced caspase 3/7 activity (**Figure 23A**). Fractions 1 and 4 demonstrated the most pronounced effect. Fraction 4 exhibited the highest reduction in caspase 3/7 activity, decreasing it by 2.16 ± 0.01-fold compared to 6-OHDA, possibly indicating a unique phytochemical profile that enhances its anti-apoptotic properties. The variability in caspase 3/7 reduction may be attributed to differences in the phytochemical composition of the fractions, as *C. edulis* is rich in phenolic compounds, flavonoids, and alkaloids, all known for their antioxidant and anti-apoptotic properties.[207] The reduction in caspase 3/7 activity observed in this study is corroborated by other studies, where it is suggested that flavonoids inhibit caspase activation and protect against OS-related apoptosis.[220] In PD models, OS, triggered by agents like 6-OHDA, leads to increased ROS generation and activation of the apoptotic pathway, including the caspase cascade.[221] The reduction in ROS generation previously observed with *C. edulis* extracts likely contributes to the decreased caspase 3/7 activity, which is consistent with research demonstrating that alleviating OS can prevent apoptotic cell death.[222]

The crude extract and fractions of *D. stramonium* significantly ($p < 0.0001$) reduced caspase 3/7 activity (**Figure 23B**). The crude extract and fractions 1, 3, and 6 demonstrated virtually equivalent reductions in caspase 3/7 activity, indicating that the phytochemicals responsible for this inhibition are likely evenly distributed across the crude extract and these fractions. Notably, Fraction 7 showed the greatest reduction in caspase 3/7 activity, decreasing it by 3.66 ± 0.05-fold, suggesting a higher concentration of active compounds in this fraction.

The notable reduction in caspase 3/7 activity aligns with existing research highlighting the anti-apoptotic properties of the phytochemical compounds, such as alkaloids, flavonoids, and phenolics in *D. stramonium.*[166] *Datura stramonium* is known for its therapeutic and neuroprotective effects, which are attributed to its phenolic compounds and flavonoids.[108] These compounds possess the ability to scavenge free radicals, preserve cellular integrity, and mitigate OS and apoptosis, thereby enhancing their therapeutic potential.[223]

In a previous study it was demonstrated that *D. stramonium* leaf extract exhibited nephroprotective effects against methotrexate-induced nephrotoxicity by reducing OS-mediated inflammation and caspase 3 activity.[224] These findings suggest that *D. stramonium* provides

protection in various models through apoptosis modulation via similar mechanisms, underscoring its medicinal value.

The observed reduction in caspase 3/7 activity indicates that *C. edulis* and *D. stramonium* may hold therapeutic potential in safeguarding neuronal cells from OS-induced apoptosis, a key feature of PD. Both plant extracts appear to mitigate apoptosis by inhibiting caspase 3/7 activity, likely through their capacity to reduce OS and, consequently, the activation of apoptotic pathways associated with cellular damage. This underscores the promise of these plant extracts as neuroprotective agents.

3.8 Mitochondrial membrane integrity

Potassium persulfate, an oxidising agent, induces OS and generates ROS, disrupting MMP, impairing ATP production, and potentially opening the MPT pore. This mitochondrial damage is reflected by an increased ratio of damaged mitochondria to cell density (**Figure 24**). Similarly, 6-OHDA treatment increased fluorescence intensity, indicating significant mitochondrial damage, and reduced cell density. After normalising fluorescence to cell density, the 6-OHDA-treated group increased the ratio of healthy mitochondria to cell density by 0.50 ± 0.3 compared to the control, indicating increased mitochondrial damage per cell. This suggests increased mitochondrial damage per cell, likely due to mitochondrial stress or dysfunction induced by 6-OHDA. These findings align with existing literature. Silva *et al.* reported that treatment of SH-SY5Y cells with 100 µM 6-OHDA caused significant MMP depolarisation, increasing the monomer-to-aggregate ratio to 150% of the control.[187] Similarly, Shih *et al.* observed that 100 µM 6-OHDA treatment induced approximately 70% MMP depolarisation in SH-SY5Y cells.[225]

The self-oxidation of DA to 6-OHDA produces free radicals and unstable quinones, which trigger the oxidation of lipids and damage to the mitochondrial membrane. This damage ultimately leads to the disintegration of the MMP, which causes cell death.[134,198,226] There is a demonstrated correlation between MMP depolarisation and ROS production, as well as MMP depolarisation and neuronal death.[227-229]

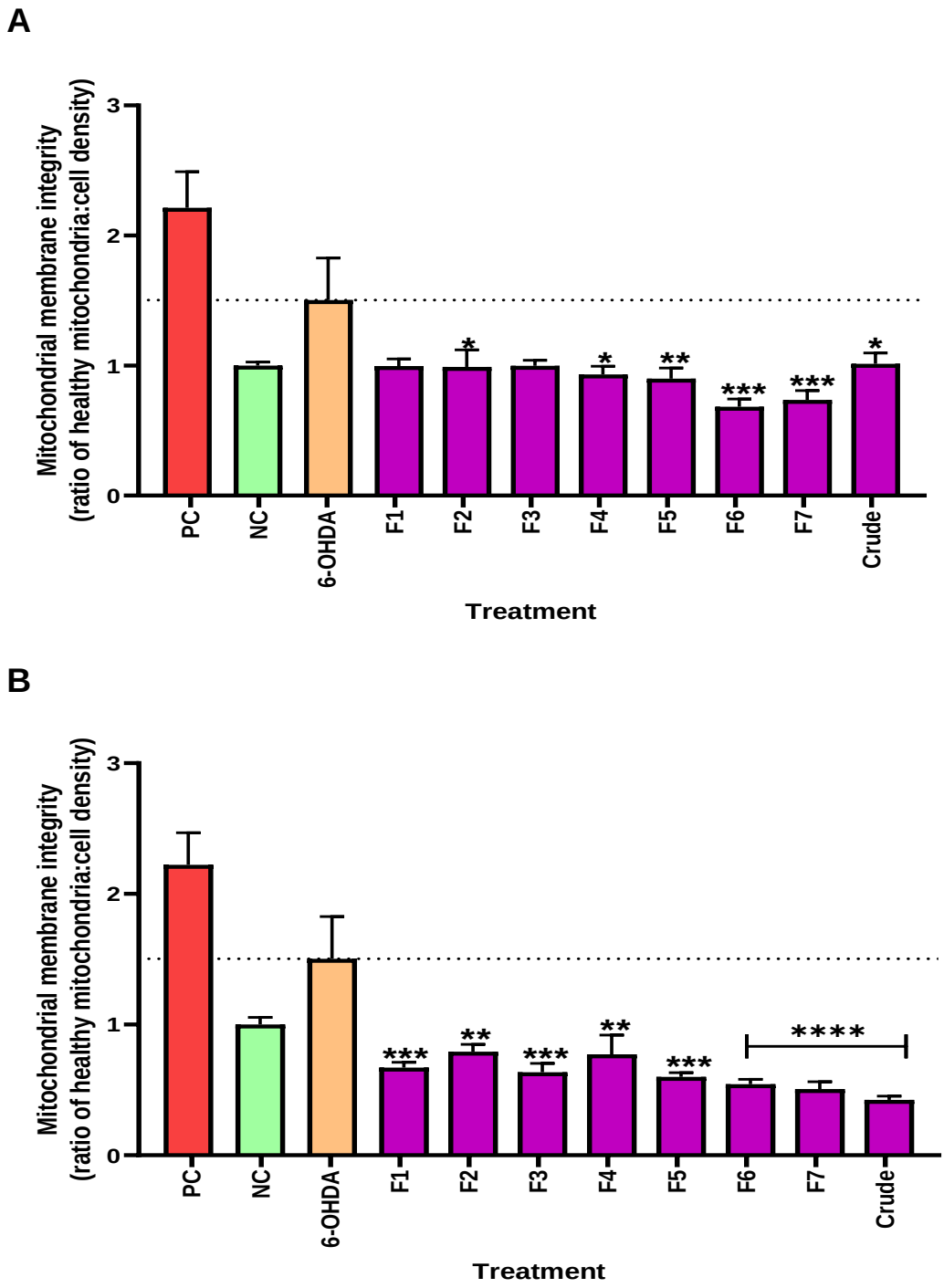

Figure 24. The effect of *Catha edulis* (A) and *Datura stramonium* (B) crude extract and fractions (3.1 µg/mL) on mitochondrial membrane integrity. Results were reported as mean ±SEM of three biological and technical repeats (n=9). Significance is expressed relative to 6-OHDA; * $p < 0.05$, ** $p < 0.01$, *** $p < 0.001$, **** $p < 0.0001$. 6-OHDA: 6-hydroxydopamine (72.83 µM), NC: negative control, and PC: positive control (1 mM potassium persulfate).

The crude extract and fractions of *C. edulis* demonstrated the ability to preserve mitochondrial integrity, as indicated by the significant reduction in the ratio of healthy mitochondria to cell density (**Figure 24A**). The crude extract and fractions 1 to 5 showed a relatively consistent protective effect, while fraction 6 demonstrated the most significant reduction in the ratio, decreasing by 0.82 ± 0.26 ($p < 0.001$) compared to 6-OHDA, suggesting a stronger ability to maintain mitochondrial integrity. This effect may be attributed to a higher concentration of protective bioactive compounds or a unique combination of phytochemicals.

Similarly, *D. stramonium* extracts and fractions also maintained mitochondrial integrity (**Figure 24B**), reducing the ratio of healthy mitochondria to cell density. Fractions 1, 3, and 5 displayed comparable and significant ($p < 0.001$) reductions in the ratio of healthy mitochondria to cell density, while the crude extract showed the most significant reduction in the ratio of healthy mitochondria to cell density, decreasing by 1.08 ± 0.29 ($p < 0.0001$) compared to 6-OHDA. This highlights the potential of *D. stramonium* to protect against mitochondrial disruption, likely mediated by its antioxidant properties

The mitochondrial integrity observed for *D. stramonium* in this study might be attributed to its antioxidant property, hence mitigating OS and preventing mitochondrial impairment. For instance, co-incubation of the methanol extract of *Hyoscyamus niger* with MPP^+, which is known to induce mitochondrial dysfunction, significantly reduced the generation of hydroxyl radicals.[181] This reduction in ROS may have contributed to preserving mitochondrial function. Additionally, given that *D. stramonium* contains phenolic and flavonoid compounds with significant antioxidant potential, it is likely that its protective effects are mediated through similar mechanisms, emphasising its role in reducing OS and preserving mitochondrial integrity.

The reduction in mitochondrial damage caused by *C. edulis* and *D. stramonium* fractions is of importance, as mitochondrial dysfunction is a key factor in cell death, particularly in PD.[53] By protecting mitochondria, *C. edulis* and *D. stramonium* fractions may help mitigate OS and apoptosis, as supported by the results where a reduction in ROS and caspase activity was noted. The rich phytochemical content of both plants, including alkaloids, flavonoids, and phenolics, likely contributes to this effect by scavenging ROS and preventing mitochondrial membrane collapse, supporting their role in enhancing mitochondrial stability under oxidative conditions.[230] These results align with literature on plant-derived compounds, such as flavonoids and phenolic

compounds, which are known for stabilising mitochondrial membranes and preventing dysfunction under oxidative conditions.[230]

The established link between mitochondrial dysfunction, OS, and apoptosis in PD suggests that *C. edulis* and *D. stramonium* crude extracts and fractions could be valuable for therapeutic interventions aimed at maintaining mitochondrial function and preventing cell death. Both *C. edulis* and *D. stramonium* extracts play a protective role in maintaining mitochondrial integrity, potentially mitigating the cellular damage induced by OS and apoptotic signalling pathways. This maintenance of mitochondrial health is essential, as it reduces the likelihood of cell death and helps maintain overall cellular function.

3.9 *In silico* docking

The free energies calculated from the docking studies revealed higher binding affinities of norephedrine than cathine for both D1 and D2 receptors (**Table 7**). The binding free energy values of norephedrine for D1 and D2 were -4.34 KJ/mol and -5.91 KJ/mol, respectively, whereas the values for cathine were -3.9 KJ/mol and -5.31 KJ/mol, for D1 and D2, respectively. Norephedrine has a higher binding affinity, especially for the D2 receptor, as indicated by its lower (more negative) binding free energy values. This is important because one of the main therapeutic approaches for PD symptoms is DA receptor antagonism. [231,232]

The docking poses and 2D ligand-protein interaction diagrams for each compound at the D1 and D2 receptors is depicted in **Table 7**. The results indicate that apomorphine, a known D1 receptor agonist,[233] primarily formed interactions via π-π stacking, hydrogen bonding, and a salt bridge. In contrast, cathine and norephedrine formed distinct binding interactions, with cathine forming a hydrogen bond and norephedrine forming a salt bridge to specific amino acid residues. Notably, both compounds shared only one common amino acid residue with apomorphine, suggesting a different binding orientation that may influence their functional efficacy at the D1 receptor.[234]

Similarly, in the D2 receptor, risperidone, a well-known antagonist,[235] predominantly formed interactions via π-π stacking, hydrogen bonding, and a salt bridge (**Table 7**). Norephedrine shared several amino acid residues with risperidone, suggesting similar binding modes and supporting its potential as a D2 receptor modulator. In contrast, cathine formed a hydrogen bond to a unique amino acid residue, indicating a slightly different binding configuration. This variation could impact cathine's binding efficiency and functional activity at the D2 receptor.[236]

Table 7. Binding affinity of compounds identified in *Catha edulis* for dopamine receptors (D1 and D2)

Dopamine receptor	Ligand	Ligand-interaction	Common residues	Other residues	Affinity (KJ/mol)
D1 Receptor	Apomorphine	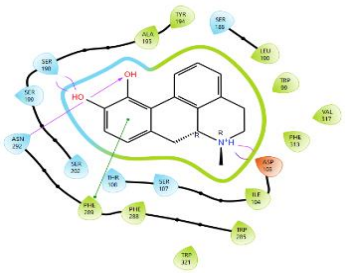	ASN292, ASP103, PHE289, and SER198	-	-
	Cathine	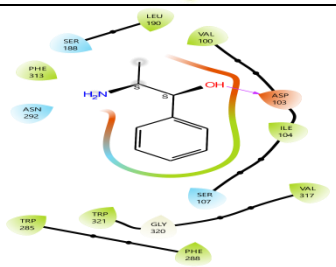	ASP103	-	-3.9
	Norephedrine	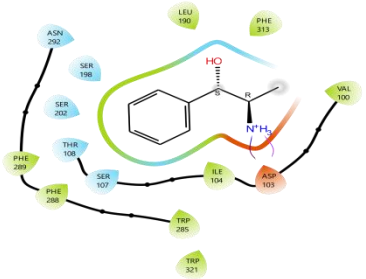	ASP103	-	-4.34
D2 receptor	Risperidone	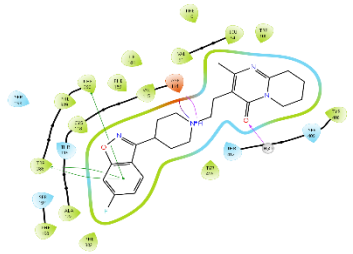	ASP114, H_2O, PHE390, and TRP386	-	-
	Cathine	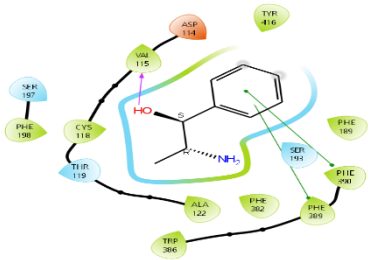	PHE390, and TRP386	VAL115	-5.31
	Norephedrine	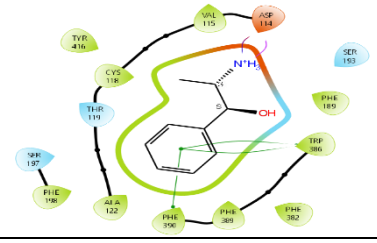	ASP114, PHE390, and TRP386	-	-5.91

Cathine and norephedrine interacted with dopaminergic modulators at activator sites, including apomorphine at the D1 receptor and risperidone at the D2 receptor. These interactions suggest their potential to influence receptor activity through distinct binding mechanisms. Given the critical role of D2 receptors in motor control pathways disrupted by DA deficiency in PD, norephedrine's strong binding to these receptors suggests it could mimic DA's effects or modulate receptor activity.[237] This potential to alleviate motor symptoms positions norephedrine as a compelling candidate for further research into treatments targeting dopaminergic pathways.[238] Notably, D2 agonists play a key role in relieving motor symptoms in PD by modulating the disrupted indirect pathway of the basal ganglia.[239] However, its promise as a treatment requires a cautious and thorough evaluation, particularly in understanding its specificity, efficacy, and safety in restoring dopaminergic signalling in PD patients.

The molecular docking assessment of compounds present in *D. stramonium* (atropine, hyoscyamine, and noradrenaline) within the D1 and D2 receptors showed notable differences in binding affinities (**Table 8**). The highest binding affinity to both receptors was shown by noradrenaline, which displayed free energy values of -6.73 KJ/mol for D1 and -7.43 KJ/mol for D2. In contrast, both atropine and hyoscyamine displayed lower affinities: atropine binds with a binding free energy of -4.55 KJ/mol for D1 and -4.31 KJ/mol for D2, and hyoscyamine with energy values of -5.54 KJ/mol for D1 and -4.34 KJ/mol for D2. Of all the compounds, noradrenaline, is the potential candidate to interact with a receptor.

The specific binding affinity of noradrenaline to D1 and D2 receptors may be crucial for PD treatment, as noradrenaline is essential for motor control and neuronal function.[240] In PD, the deficiency of noradrenaline contributes to worsening symptoms and dyskinesia, which are commonly observed in PD patients during DA replacement therapy.[157] Previous studies have extensively explored noradrenaline as a dopamine receptor agonist, with both *in vitro* and *in silico* investigations reporting its binding interactions and affinities with DA receptors.[241,242,243] These studies have shown that noradrenaline can activate DA receptors, enhancing DA signalling pathways and compensating for DA deficiencies.

By stimulating both D1 and D2 receptors, noradrenaline may boost DA cell activity and mitigate the effects of DA deficiencies. Additionally, the restoration of noradrenergic activity has been shown to reduce dyskinesia, a common side effect of PD treatment.[240] Given these effects, noradrenaline's strong affinity for these receptors supports additional research into its therapeutic

potential in regulating motor activities and potentially alleviating some of the side effects associated with current treatments.

Table 8. Binding affinity of compounds identified in *Datura stramonium* for dopamine receptors (D1 and D2)

Dopamine receptor	Ligand	Ligand-interaction	Common residues	Other residues	Affinity (KJ/mol)
D1 receptor	Apomorphine	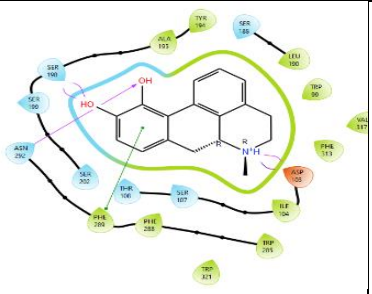	ASN292, ASP103, PHE289, and SER198	-	-
	Atropine	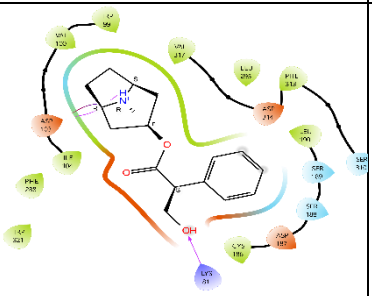	ASP103	LYS81	-4.55
	Hyoscyamine	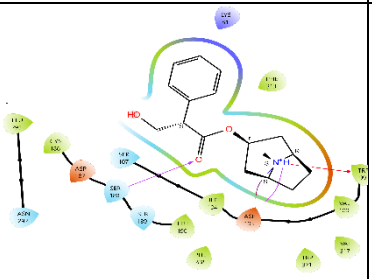	ASP103	SER188 and TRP99	-5.54
	Noradrenaline	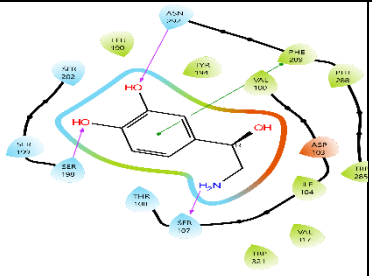	ASN292, PHE289, and SER198	SER107	-6.73
D2 receptor	Risperidone	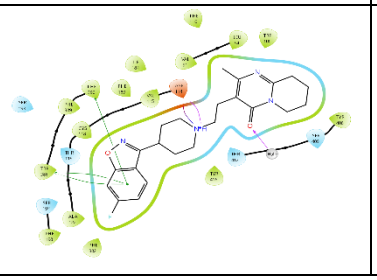	ASP114, H_2O, PHE390, and TRP386	-	-

	Atropine	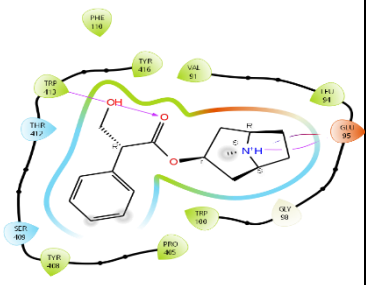	-	GLU95 and TRP413	-4.31
	Hyoscyamine	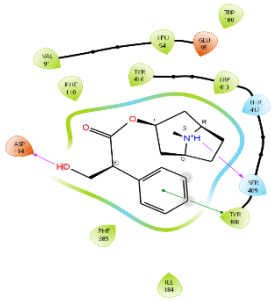	ASP114	SER409 and TYR408	-4.34
	Noradrenaline	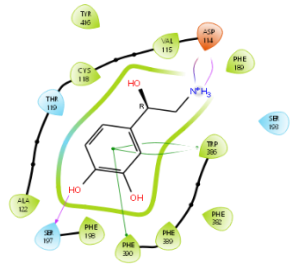	ASP114, PHE390, and TRP386	SER197	-7.43

All compounds formed interactions with the receptor binding site through π-π stacking, hydrogen bonding, and salt bridges (**Table 8**), which are critical for stabilising ligand-receptor complexes, as demonstrated by the reference compound, apomorphine.[244] Atropine and hyoscyamine both formed salt bridge interactions, while noradrenaline demonstrated multiple interactions, including hydrogen bonding and π-π stacking, with several amino acid residues. This similarity in binding mechanisms highlights noradrenaline's strong affinity for the D1 receptor, suggesting its potential to achieve receptor activation comparable to that of the reference ligand.

Atropine formed a distinct hydrogen bond to the receptor binding site, while hyoscyamine formed both a hydrogen bond and a π-cation interaction stabilised by specific amino acid residues. Similarly, noradrenaline exhibited a hydrogen bond with a specific amino acid residue, potentially enhancing its binding affinity. These interactions highlight the unique binding mechanisms of each compound, which could play an important role in determining their efficacy in modulating D1 receptor activity.[245]

Similar to the D1 receptor, interactions with the D2 receptor were mediated by π-π stacking, hydrogen bonding, and salt bridges. Hyoscyamine formed a hydrogen bond interaction, while noradrenaline formed a π-π stacking interaction and a salt bridge, both stabilised by key amino

acid residues. These interactions suggest that these compounds may bind to the D2 receptor in a manner similar to risperidone. The close resemblance of noradrenaline's binding mode to that of risperidone likely explains its higher binding affinity and supports its potential role as a D2 receptor modulator. Noradrenaline has higher affinity for D1 and D2 receptors because of its structural similarity with DA.[246] Both compounds are catecholamines and share a common core structure; a catechol group and an amine group.[247] The main difference between the two is the additional hydroxyl group on the β-carbon of noradrenaline. This similarity in the structural framework allows noradrenaline to interact with DA receptors more effectively than other compounds.

In contrast, atropine formed both hydrogen bond and salt bridge interactions, while hyoscyamine formed a hydrogen bond and a π-π stacking interaction, stabilized by unique amino acid residues. Noradrenaline, on the other hand, formed a hydrogen bond with a specific amino acid residue. These specific interactions suggest that, although hyoscyamine and noradrenaline share general binding features, their exact positioning and interaction with the receptor differ, potentially influencing their therapeutic outcomes and receptor modulation capabilities.[245]

Norephedrine and noradrenaline were identified as the most promising compounds from *C. edulis* and *D. stramonium*, respectively, demonstrating the highest binding affinities for D1 and D2 receptors. This suggests their potential as dual-acting agonists of DA receptors. The distinct interactions observed for each compound indicate variations in their binding modes, which could influence their pharmacological response and therapeutic applications. These findings contribute to the growing body of research on noradrenaline's therapeutic potential in PD and highlight the need for further exploration of its efficacy in combination with other therapeutic strategies.

Chapter 4: Conclusion

C. edulis and *D. stramonium* extracts may have considerable therapeutic potential for PD as indicated by the activity noted. The minimal cytotoxicity observed, together with the cytoprotective properties in both plant extracts, suggests that they may play a role in protecting against neuronal damage in PD. This is notable considering the significant role of OS in PD advancement, as both extracts have been proven to decrease ROS levels, thus, mitigating oxidative damage to cells.

Furthermore, the observed reduction in caspase 3/7 activity suggests that the plant extracts may provide neuroprotection by inhibiting apoptosis, an important mechanism of neuronal death in PD. Their ability to maintain mitochondrial integrity further highlights their therapeutic potential, as mitochondrial dysfunction is a key characteristic of PD and contributes significantly to neurodegeneration. By maintaining mitochondrial function these extracts may help slow the progression of neurodegeneration.

In addition, the strong affinity of norephedrine and noradrenaline for DA receptors indicates their potential to restore DA function, which is essential for alleviating motor symptoms in PD. While consistent with prior studies on noradrenaline as a dopamine receptor agonist, the current findings provide new insight into its dual-acting mechanism and binding modes, suggesting its potential to complement existing therapies by addressing non-motor symptoms and reducing dyskinesia. However, noradrenaline's poor BBB permeability remains a challenge. Future research should focus on strategies like prodrug development or nanocarrier formulations to enhance its CNS delivery, paving the way for novel PD treatments.

In conclusion, *C. edulis* and *D. stramonium* extracts demonstrate potential as sources of bioactive compounds that could help mitigate key aspects of PD, including OS, apoptosis, and mitochondrial dysfunction. These results highlight the need for further investigation, particularly *in vivo* studies, to elucidate their underlying mechanisms and fully assess their therapeutic potential.

4.1 Limitations and recommendations

One of the major limitations of this study is the lack of sufficient literature on the neuroprotective effects of *C. edulis* and *D. stramonium* extracts specifically in SH-SY5Y cells, making direct comparisons with existing studies challenging. Additionally, while SH-SY5Y cells are frequently used in primary screening assays due to their ability to proliferate, their bioenergetic properties and differences from native neuronal environments may affect the accuracy of the results. These cells may not fully represent the molecular and biological mechanisms associated with PD, highlighting the need for more representative models to study the disease more effectively.

While the current findings suggest some neuroprotective potential, the fundamental molecular mechanisms remain largely unknown, and while *in vitro* models are useful, they might not accurately represent the complexity of living organisms. This limitation may have an impact on the findings' practical relevance, highlighting the necessity for more comprehensive studies.

In future studies, it is recommended to use SH-SY5Y cells as a more physiologically relevant model due to their similarities to dopaminergic neurons affected in PD. Retinoic acid has been shown to stimulate neurite growth and branching, hallmark characteristics of differentiated neurons.[112,113] It also plays a key role in the differentiation and proliferation of various cell types by activating RA nuclear receptors, which regulate critical aspects of gene expression.[115,116] Using differentiated cells increases the reproducibility of findings by more closely mimicking the cellular environment of PD, thereby allowing for a more accurate evaluation of potential therapeutic agents.

Furthermore, given the degenerative nature of PD, evaluating the long-term safety of these extracts through chronic toxicity studies is important. Incorporating *in vivo* investigations and animal models will allow for a more thorough knowledge of their effects in complex biological systems. Further research into the role of important enzymes, such as cholinesterase and MAO A, could give unique perspectives into the therapeutic potential and usefulness of these extracts in PD.

References

1. Canter RG, Penney J, Tsai L-H. The road to restoring neural circuits for the treatment of Alzheimer's disease. Nature. 2016;539(7628):187-196. doi:10.1038/nature20412
2. Chen C, Turnbull DM, Reeve AK. Mitochondrial dysfunction in Parkinson's disease: cause or consequence. Biology. 2019; 8(2):38. doi:10.3390/biology802003
3. Pringsheim T, Fiest K, Jette N. The international incidence and prevalence of neurologic conditions: How common are they? Neurology. 2014;83(18):1661-1664. doi:10.1212/WNL.0000000000000929
4. Armstrong R. What causes neurodegenerative disease? Folia Neuropathologica. 2020; 58(2):93-112. doi:10.5114/fn.2020.96707
5. Stoker TB, Barker RA. Recent developments in the treatment of Parkinson's disease. F1000Research. 2020; 9:862. doi:10.12688/f1000research.25634.1
6. Dugger BN, Dickson DW. Pathology of neurodegenerative diseases. Cold Spring Harbor Perspectives in Biology. 2017; 9(7):1-22. doi:10.1101/cshperspect.a028035
7. Gómez-Río M, Caballero MM, Gorriz Saez JM, Mínguez-Castellanos A. Diagnosis of neurodegenerative diseases: The clinical approach. Current Alzheimer Research. 2016; 13(5):469-474. doi:10.2174/1567205013666151116141603
8. Feigin VL, Vos T, Nichols E, Owolabi MO, Carroll WM, Dichgans M, Deuschl G, Parmar P, Brainin M, Murray C. The global burden of neurological disorders: Translating evidence into policy. The Lancet Neurology. 2020; 19(3):255-265. doi:10.1016/S1474-4422(19)30411-9
9. De Lau LM, Breteler MM. Epidemiology of Parkinson's disease. The Lancet Neurology. 2006; 5(6):525-535. doi:10.1016/S1474-4422(06)70471-9
10. [Internet]. Parkinson disease. World Health Organization; 2022 [18 April 2023]. Available from: https://www.who.int/news-room/fact-sheets/detail/parkinson-disease.
11. Kalia LV, Lang AE. Parkinson's disease. The Lancet. 2015; 386(9996):896-912. doi:10.1016/S0140-6736(14)61393-3
12. Jankovic J, Stacy M. Medical management of levodopa-associated motor complications in patients with Parkinson's disease. CNS drugs. 2007; 21:677-692. doi:10.2165/00023210-200721080-00005
13. Smeyne RJ, Jackson-Lewis V. The MPTP model of Parkinson's disease. Molecular Brain Research. 2005; 134(1):57-66. doi:10.1016/j.molbrainres.2004.09.017
14. Rodriguez-Oroz MC, Jahanshahi M, Krack P, Litvan I, Macias R, Bezard E, Obeso JA.

Initial clinical manifestations of Parkinson's disease: Features and pathophysiological mechanisms. The Lancet Neurology. 2009; 8(12):1128-1139. doi:10.1016/S1474-4422(09)70293-5

15. Obeso JA, Rodriguez-Oroz MC, Stamelou M, Bhatia KP, Burn DJ. The expanding universe of disorders of the basal ganglia. The Lancet. 2014; 384(9942):523-531. doi:10.1016/S0140-6736(13)62418-6
16. Chaudhuri KR, Schapira AH. Non-motor symptoms of Parkinson's disease: Dopaminergic pathophysiology and treatment. The Lancet Neurology. 2009; 8(5):464-474. doi:10.1016/S1474-4422(09)70068-7
17. Modi P, Mohamad A, Phom L, Koza Z, Das A, Chaurasia R, Samadder S, Achumi B, Muralidhara, Pukhrambam RJ, Yenisetti CS. Understanding pathophysiology of sporadic Parkinson's disease in drosophila model: Potential opportunities and notable limitations [Internet]: InTechOpen; 2016. Available from: https://dx.doi.org/10.5772/63767.
18. McCormack AL, Thiruchelvam M, Manning-Bog AB, Thiffault C, Langston JW, Cory-Slechta DA, Di Monte DA. Environmental risk factors and Parkinson's disease: Selective degeneration of nigral dopaminergic neurons caused by the herbicide paraquat. Neurobiology of Disease. 2002; 10(2):119-127. doi:10.1006/nbdi.2002.0507
19. Uversky VN. Neurotoxicant-induced animal models of Parkinson's disease: Understanding the role of rotenone, maneb and paraquat in neurodegeneration. Cell and Tissue Research. 2004; 318(1):225-241. doi:10.1007/s00441-004-0937-z
20. Dhillon AS, Tarbutton GL, Levin JL, Plotkin GM, Lowry LK, Nalbone JT, Shepherd S. Pesticide/environmental exposures and Parkinson's disease in East Texas. Journal of Agromedicine. 2008; 13(1):37-48. doi:10.1080/10599240801986215
21. Ritz BR, Manthripragada AD, Costello S, Lincoln SJ, Farrer MJ, Cockburn M, Bronstein J. Dopamine transporter genetic variants and pesticides in Parkinson's disease. Environmental Health Perspectives. 2009; 117(6):964-969. doi:10.1289/ehp.0800277
22. Kim SW, Ko HS, Dawson VL, Dawson TM. Recent advances in our understanding of Parkinson's disease. Drug Discovery Today: Disease Mechanisms. 2005; 2(4):427-433. doi:10.1016/j.ddmec.2005.11.015
23. Rizek P, Kumar N, Jog MS. An update on the diagnosis and treatment of Parkinson disease. Canadian Medical Association Journal. 2016; 188(16):1157-1165. doi:10.1503/cmaj.151179
24. Pagano G, Ferrara N, Brooks DJ, Pavese N. Age at onset and Parkinson disease phenotype. Neurology. 2016; 86(15):1400-1407. doi:10.1212/WNL.0000000000002461
25. Wakabayashi K, Tanji K, Mori F, Takahashi H. The Lewy body in Parkinson's disease:

Molecules implicated in the formation and degradation of α-synuclein aggregates. Neuropathology. 2007; 27(5):494-506. doi:10.1111/j.1440-1789.2007.00803.x

26. Bose A, Beal MF. Mitochondrial dysfunction in Parkinson's disease. Journal of Neurochemistry. 2016; 139:216-31. doi:10.1111/jnc.13731
27. Selvaraj S, Piramanayagam S. Impact of gene mutation in the development of Parkinson's disease. Genes and Diseases. 2019; 6(2):120-28. doi:10.1016/j.gendis.2019.01.004
28. Plotegher N, Berti G, Ferrari E, Tessari I, Zanetti M, Llanelli L, Greggio E, Bisaglia M, Veronesi M, Girotto S, Serra MD, Perego C, Casella L, Bubacco L. DOPAL derived alpha-synuclein oligomers impair synaptic vesicles physiological function. Scientific Reports. 2017; 7(1):1-16. doi:10.1038/srep40699
29. Weng M, Xie X, Liu C, Lim K-L, Zhang C-w, Li L. The sources of reactive oxygen species and its possible role in the pathogenesis of Parkinson's disease. Parkinson's Disease. 2018; 2018(1):1-9. doi:10.1155/2018/9163040
30. Wang X, Yan MH, Fujioka H, Liu J, Wilson-Delfosse A, Chen SG, Perry G, Casadesus G, Zhu X. LRRK2 regulates mitochondrial dynamics and function through direct interaction with DLP1. Human Molecular Genetics. 2012; 21(9):1931-1944. doi:10.1093/hmg/dds003
31. Van der Merwe C, Van Dyk HC, Engelbrecht L, van der Westhuizen FH, Kinnear C, Loos B, Bardien S. Curcumin rescues a PINK1 knock down SH-SY5Y cellular model of Parkinson's disease from mitochondrial dysfunction and cell death. Molecular Neurobiology. 2017; 54:2752-2762. doi:10.1007/s12035-016-9843-0
32. Valente EM, Abou-Sleiman PM, Caputo V, Muqit MM, Harvey K, Gispert S, Ali Z, Del Turco D, AR Bentivoglio, Healy DG Albanese A, Nassbaum R, González-Maldonado R, Deller T, Salvi S, Cortelli P, Gilks WP, Latchman SD, Harvey RJ, Dallapiccola B, Auburger G, Wood NW. Hereditary early-onset Parkinson's disease caused by mutations in PINK1. Science. 2004; 304(5674):1158-1160. doi:10.1126/science.1096284
33. Clark IE, Dodson MW, Jiang C, Cao JH, Huh JR, Seol JH, Yoo SJ, Hay BA, Guo M. Drosophila PINK1 is required for mitochondrial function and interacts genetically with parkin. Nature. 2006; 441(7097):1162-1166. doi:10.1038/nature04779
34. Abou-Sleiman PM, Muqit MM, McDonald NQ, Yang YX, Gandhi S, Healy DG, Harvey K, Harvey RJ, Deas E, Bhatia K, Quinn N, Lees A, Latchman SD, Wood NW. A heterozygous effect for PINK1 mutations in Parkinson's disease? Annals of Neurology. 2006; 60(4):414-419. doi:10.1002/ana.20960
35. Huang M, Chen S. DJ-1 in neurodegenerative diseases: Pathogenesis and clinical application. Progress in Neurobiology. 2021; 204:102-114. doi:10.1016/j.pneurobio.2021.102114

36. Pankratz N, Pauciulo MW, Elsaesser VE, Marek DK, Halter CA, Wojcieszek J, Rudolph A, Shults CW, Foroud T, Nichols WC. Mutations in DJ-1 are rare in familial Parkinson disease. Neuroscience Letters. 2006; 408(3):209-213. doi:10.1016/j.neulet.2006.09.003
37. Anderson PC, Daggett V. Molecular basis for the structural instability of human DJ-1 induced by the L166P mutation associated with Parkinson's disease. Biochemistry. 2008; 47(36):9380-9393. doi:10.1021/bi800677k
38. Malgieri G, Eliezer D. Structural effects of Parkinson's disease linked DJ-1 mutations. Protein Science. 2008; 17(5):855-868. doi:10.1110/ps.073411608
39. Kouli A, Torsney KM, Kuan W-L. Parkinson's disease: Etiology, neuropathology, and pathogenesis. Exon Publications. 2018:3-26. doi:10.15586/codonpublications. parkinsonsdisease.2018.ch1
40. Bloem BR, Okun MS, Klein C. Parkinson's disease. The Lancet. 2021; 397(10291):2284-2303. doi:10.1016/S0140-6736(21)00218-X
41. Dexter DT, Jenner P. Parkinson disease: From pathology to molecular disease mechanisms. Free Radical Biology and Medicine. 2013; 62:132-144. doi:10.1016/j.freeradbiomed.2013.01.018
42. Taylor JM, Main BS, Crack PJ. Neuroinflammation and oxidative stress: Co-conspirators in the pathology of Parkinson's disease. Neurochemistry international. 2013; 62(5):803-819. doi:10.1016/j.neuint.2012.12.016
43. Block M, Hong J-S. Chronic microglial activation and progressive dopaminergic neurotoxicity. Biochemical Society Transactions. 2007; 35(5):1127-1132. doi:10.1042/BST0351127
44. Brieger K, Schiavone S, Miller Jr FJ, Krause K-H. Reactive oxygen species: From health to disease. Swiss Medical Weekly. 2012; 142(3334):w13659. doi:10.4414/smw.2012.13659
45. Krause K-H, Bedard K. NOX enzymes in immuno-inflammatory pathologies. Seminars in Immunopathology. 2008; 30(3):193-194. doi:10.1007/s00281-008-0127-2
46. Moore DJ, West AB, Dawson VL, Dawson TM. Molecular pathophysiology of Parkinson's disease. Annual Review of Neuroscience. 2005; 28:57-87. doi:10.1146/annurev.neuro.28.061604.135718
47. Lim K-L, Zhang C-W. Molecular events underlying Parkinson's disease: An interwoven tapestry. Frontiers in Neurology. 2013; 4:33. doi:10.3389/fneur.2013.00033
48. Miller RL, James-Kracke M, Sun GY, Sun AY. Oxidative and inflammatory pathways in Parkinson's disease. Neurochemical Research. 2009; 34:55-65. doi:10.1007/s11064-008-9656-2

49. Blesa J, Trigo-Damas I, Quiroga-Varela A, Jackson-Lewis VR. Oxidative stress and Parkinson's disease. Frontiers in Neurochemistry. 2015; 9:91. License URL: https://creativecommons.org/licenses/by/4.0/. doi:10.3389/fnana.2015.0009
50. Hauber W. Involvement of basal ganglia transmitter systems in movement initiation. Progress in Neurobiology. 1998; 56(5):507-540. doi:10.1016/s0301-0082(98)00041-0
51. Hastings TG. The role of dopamine oxidation in mitochondrial dysfunction: Implications for Parkinson's disease. Journal of Bioenergetics and Biomembranes. 2009; 41(6):469-472. doi:10.1007/s10863-009-9257-z
52. Zhou X. Molecular toxicological mechanisms of new psychoactive substances "*in vitro*". Doctoral Thesis, University of Basel. 2020. URL: http://edoc.unibas.ch/diss/DissB_13653
53. Keane P, Kurzawa M, Blain P, Morris C. Mitochondrial dysfunction in Parkinson's disease. Parkinson's Disease. 2011; 2011:1-18. doi:10.4061/2011/716871
54. Zuo L, Motherwell MS. The impact of reactive oxygen species and genetic mitochondrial mutations in Parkinson's disease. Gene. 2013; 532(1):18-23. doi:10.1016/j.gene.2013.07.085
55. Michel PP, Hirsch EC, Hunot S. Understanding dopaminergic cell death pathways in Parkinson disease. Neuron. 2016; 90(4):675-691. doi:10.1016/j.neuron.2016.03.038
56. Moon HE, Paek SH. Mitochondrial dysfunction in Parkinson's disease. Experimental Neurobiology. 2015; 24(2):103. doi:10.5607/en.2015.24.2.103
57. Narendra D, Walker JE, Youle R. Mitochondrial quality control mediated by PINK1 and Parkin: Links to Parkinsonism. Cold Spring Harbor Perspectives in Biology. 2012; 4(11):1-19. doi:10.1101/cshperspect.a011338
58. Ding WX, Yin XM. Mitophagy: Mechanisms, pathophysiological roles, and analysis. Biological Chemistry. 2012; 393(7):547-564. doi:10.1515/hsz-2012-0119
59. Park JS, Davis RL, Sue CM. Mitochondrial dysfunction in Parkinson's disease: New mechanistic insights and therapeutic perspectives. Current Neurology and Neuroscience Reports. 2018; 18:1-11. License URL: https://creativecommons.org/licenses/by/4.0/. doi:10.1007/s11910-018-0829-3
60. Albarracin SL, Stab B, Casas Z, Sutachan JJ, Samudio I, Gonzalez J, Gonzalo L, Capani F, Morales L, Barreto GE. Effects of natural antioxidants in neurodegenerative disease. Nutritional Neuroscience. 2012; 15(1):1-9. doi:10.1179/1476830511Y.0000000028
61. Bhat AH, Dar KB, Anees S, Zargar MA, Masood A, Sofi MA, Ganie SA. Oxidative stress, mitochondrial dysfunction and neurodegenerative diseases; a mechanistic insight. Biomedicine and Pharmacotherapy. 2015; 74:101-110. doi:10.1016/j.biopha.2015.07.025
62. Jin H, Kanthasamy A, Ghosh A, Anantharam V, Kalyanaraman B, Kanthasamy AG.

Mitochondria-targeted antioxidants for treatment of Parkinson's disease: Preclinical and clinical outcomes. BBA-Molecular Basis of Disease. 2014; 1842(8):1282-1294. doi:10.1016/j.bbadis.2013.09.007

63. Olajuyigbe OO, Afolayan AJ. Phenolic content and antioxidant property of the bark extracts of *Ziziphus mucronata* willd. Subsp. *mucronata* willd. BMC Complementary and Alternative Medicine. 2011; 11:1-8. doi:10.1186/1472-6882-11-130
64. Sutachan JJ, Casas Z, Albarracin SL, Stab BR, Samudio I, Gonzalez J, Morales L, Barreto GE. Cellular and molecular mechanisms of antioxidants in Parkinson's disease. Nutritional Neuroscience. 2012; 15(3):120-126. doi:10.1179/1476830511Y.0000000033
65. Storch A, Jost WH, Vieregge P, Spiegel J, Greulich W, Durner J, Müller T, M, Kupsch A, Henningsen H, Oertel WH, Fuchs G, Kuhn W, Niklowitz P, Koch R, Herting B, Reichmann H. Randomized, double-blind, placebo-controlled trial on symptomatic effects of coenzyme Q10 in Parkinson disease. Archives of Neurology. 2007; 64(7):938-944. doi:10.1001/archneur.64.7.nct60005
66. Ahlemeyer B, Krieglstein J. Neuroprotective effects of *Ginkgo biloba* extract. Cellular and Molecular Life Sciences. 2003; 60:1779-1792. License URL: https://creativecommons.org/licenses/by/4.0/. doi:10.1007/s00018-003-3080-1
67. Erekat NS. Apoptosis and its role in Parkinson's disease. Exon Publications. 2018; Chapter 4:65-82. doi:10.15586/codonpublications.parkinsonsdisease.2018.ch4
68. Anglade P, Vyas S, Javoy-Agid F, Herrero Ezquerro MT, Michel P, Marquez J, Mouatt-Prigent A, Ruberg M, Hirsch EC, Agid Y. Apoptosis and autophagy in nigral neurons of patients with Parkinson's disease. Histology and Histopathology. 1997; 12(1):25-31. doi: 10.14670/HH-12.25
69. Wang C, Youle RJ. The role of mitochondria in apoptosis. Annual Review of Genetics. 2009; 43(1):95-118. doi:10.1146/annurev-genet-102108-134850
70. Venderova K, Park DS. Programmed cell death in Parkinson's disease. Cold Spring Harbor Perspectives in Medicine. 2012; 2(8):1-23. doi:10.1101/cshperspect.a009365
71. Kothakota S, Azuma T, Reinhard C, Klippel A, Tang J, Chu K, McGarry TJ, Kirschner MW, Koths K, Kwiatkowski DJ, Williams LT. Caspase-3-generated fragment of gelsolin: effector of morphological change in apoptosis. Science. 1997; 278(5336):294-298. doi:10.1126/science.278.5336.294
72. Lev N, Melamed E, Offen D. Apoptosis and Parkinson's disease. Progress in Neuro-Psychopharmacology and Biological Psychiatry. 2003; 27(2):245-250. doi:10.1016/S0278-5846(03)00019-8
73. Reddy P, Reddy T. Mitochondria as a therapeutic target for aging and neurodegenerative

diseases. Current Alzheimer Research. 2011; 8(4):393-409. doi:10.2174/156720511795745401

74. Elmore S. Apoptosis: A review of programmed cell death. Toxicologic Pathology. 2007; 35(4):495-516. doi:10.1080/01926230701320337
75. Ly JD, Grubb DR, Lawen A. The mitochondrial membrane potential (δψm) in apoptosis; an update. Apoptosis. 2003; 8:115-128. doi:10.1023/A:1022945107762
76. Singh S, Dikshit M. Apoptotic neuronal death in Parkinson's disease: Involvement of nitric oxide. Brain Research Reviews. 2007; 54(2):233-250. doi:10.1016/j.brainresrev.2007.02.001
77. Zou H, Li Y, Liu X, Wang X. An apaf-1· cytochrome c multimeric complex is a functional apoptosome that activates procaspase-9. Journal of Biological Chemistry. 1999; 274(17):11549-11556. doi:10.1074/jbc.274.17.11549
78. Niemann B, Rohrbach S. Metabolically relevant cell biology–role of intracellular organelles for cardiac metabolism. The Scientist's Guide to Cardiac Metabolism. 2016. 19-38. doi:10.1016/B978-0-12-802394-5.00003-0
79. Fink SL, Cookson BT. Apoptosis, pyroptosis, and necrosis: Mechanistic description of dead and dying eukaryotic cells. Infection and Immunity. 2005; 73(4):1907-1916. doi:10.1128/IAI.73.4.1907-1916.2005
80. Hajibabaie F, Abedpoor N, Mohamadynejad P. Types of cell death from a molecular perspective. Biology. 2023; 12(11):1426. doi:10.3390/biology12111426
81. Park W, Wei S, Kim B-S, Kim B, Bae S-J, Chae YC, Ryu D, Ha KT. Diversity and complexity of cell death: A historical review. Experimental & molecular medicine. 2023; 55(8):1573-1594. License URL: https://creativecommons.org/licenses/by/4.0/. doi:10.1038/s12276-023-01078-x
82. Vercammen D, Beyaert R, Denecker G, Goossens V, Van Loo G, Declercq W, Grooten J, Fiers W, Vandenabeele P. Inhibition of caspases increases the sensitivity of L929 cells to necrosis mediated by tumor necrosis factor. The Journal of Experimental Medicine. 1998; 187(9):1477-1485. doi:10.1084/jem.187.9.1477
83. Kawahara A, Ohsawa Y, Matsumura H, Uchiyama Y, Nagata S. Caspase-independent cell killing by Fas-associated protein with death domain. The Journal of Cell Biology. 1998; 143(5):1353-1360. doi:10.1083/jcb.143.5.1353
84. Pasparakis M, Vandenabeele P. Necroptosis and its role in inflammation. Nature. 2015; 517(7534):311-320. doi:10.1038/nature14191
85. Li J, McQuade T, Siemer AB, Napetschnig J, Moriwaki K, Hsiao Y-S, Damko E, Moquin M, Walz T, McDermott A, Chan FM, Wu H. The RIP1/RIP3 necrosome forms a functional

amyloid signaling complex required for programmed necrosis. Cell. 2012; 150(2):339-350. doi:10.1016/j.cell.2012.06.019

86. Wang H, Sun L, Su L, Rizo J, Liu L, Wang L-F, Wang F-S, Wang S. Mixed lineage kinase domain-like protein MLKL causes necrotic membrane disruption upon phosphorylation by RIP3. Molecular Cell. 2014; 54(1):133-146. doi:10.1016/j.molcel.2014.03.003
87. Tait SW, Ichim G, Green DR. Die another way: Non-apoptotic mechanisms of cell death. Journal of Cell Science. 2014; 127(10):2135-2144. doi:10.1242/jcs.093575
88. Dauer W, Przedborski S. Parkinson's disease: Mechanisms and models. Neuron. 2003; 39(6):889-909. doi:10.1016/S0896-6273(03)00568-3
89. Lees AJ, Hardy J, Revesz T. Parkinson's disease. The Lancet. 2009; 373(9680):2055-2066. doi:10.1016/S0140-6736(09)60492-X
90. Kakkar AK, Dahiya N. Management of Parkinson's disease: Current and future pharmacotherapy. European Journal of Pharmacology. 2015; 750:74-81. doi:10.1016/j.ejphar.2015.01.030
91. Tarakad A, Jankovic J. Diagnosis and management of Parkinson's disease. Seminars in Neurology; 2017; 37(2):118-126. doi: 10.1055/s-0037-1601888
92. Khan ST, Ahmed S, Gul S, Khan A, Al-Harrasi A. Search for safer and potent natural inhibitors of Parkinson's disease. Neurochemistry International. 2021; 149:105-135. doi:10.1016/j.neuint.2021.105135
93. Armstrong MJ, Okun MS. Diagnosis and treatment of Parkinson disease: A review. Journal of American Medical Association. 2020; 323(6):548-560. doi:10.1001/jama.2019.22360
94. Ellis JM, Fell MJ. Current approaches to the treatment of Parkinson's disease. Bioorganic and Medicinal Chemistry Letters. 2017; 27(18):4247-4255. doi:10.1016/j.bmcl.2017.07.075
95. Koller WC, Rueda MG. Mechanism of action of dopaminergic agents in Parkinson's disease. Neurology. 1998; 50(6_suppl_6):S4-S11. doi:10.1212/wnl.50.6_suppl_6.s11
96. Oster K, Sorkin S. Effects of intravenous injections of L-dopa upon blood pressure. Proceedings of the Society for Experimental Biology and Medicine. 1942; 51(1):67-70. doi:10.3181/00379727-51-13
97. Gandhi KR, Saadabadi A. Levodopa (L-dopa). Statpearls [internet]: StatPearls Publishing; 2023. Available from: https://www.ncbi.nlm.nih.gov/books/NBK482140/
98. Lepule KH, Cordier W, Steenkamp P, Nell M, Steenkamp V. The ability of three African herbal remedies to offer protection against an *in vitro* model of Parkinson's disease. South African Journal of Botany. 2019; 126:121-131. doi:10.1016/j.sajb.2019.01.033

99. Rezak M. Current pharmacotherapeutic treatment options in Parkinson's disease. Disease-a-Month. 2007; 53(4):214-222. doi:10.1016/j.disamonth.2007.05.002

100. Goldenberg MM. Medical management of Parkinson's disease. Pharmacy and Therapeutics. 2008; 33(10):590-606.

101. Blandini F, Armentero MT. Dopamine receptor agonists for Parkinson's disease. Expert Opinion on Investigational Drugs. 2014; 23(3):387-410. doi:10.1517/13543784.2014.869209

102. Rahman MM, Wang X, Islam MR, Akash S, Supti FA, Mitu MI, Rashid MH, Aktar N, Kali SK, Jahan FI, Singla RK, Shen B, Rauf A, Sharma R. Multifunctional role of natural products for the treatment of Parkinson's disease: At a glance. Frontiers in Pharmacology. 2022; 13:1-23. doi:10.3389/fphar.2022.976385

103. Edmondson DE, Binda C, Mattevi A. Structural insights into the mechanism of amine oxidation by monoamine oxidases A and B. Archives of Biochemistry and Biophysics. 2007; 464(2):269-276. doi:10.1016/j.abb.2007.05.006

104. Bratoeff E, Cabeza M, Ramirez E, Heuze Y, Flores E. Recent advances in the chemistry and pharmacological activity of new steroidal antiandrogens and 5α-reductase inhibitors. Current Medicinal Chemistry. 2005; 12(8):927-943. doi:10.2174/0929867053507306

105. Flockhart DA. Dietary restrictions and drug interactions with monoamine oxidase inhibitors: An update. The Primary Care Companion for CNS Disorders. 2012; 73(Suppl 1):17-24. doi:10.4088/JCP.11096su1c.03

106. Silva AH, Fonseca FN, Pimenta AT, Lima MS, Silveira ER, Viana GS, Vasconcelos SM, Leal LK. Pharmacognostical analysis and protective effect of standardized extract and rizonic acid from *Erythrina velutina* against 6-hydroxydopamine-induced neurotoxicity in SH-SY5Y cells. Pharmacognosy Magazine. 2016; 12(48):307-312. doi:10.4103/0973-1296.19220

107. Engelbrecht I, Petzer JP, Petzer A. Evaluation of selected natural compounds as dual inhibitors of catechol-o-methyltransferase and monoamine oxidase. Central Nervous System Agents in Medicinal Chemistry. 2019; 19(2):133-145. doi:10.2174/1871524919666190619090852

108. Soni P, Siddiqui AA, Dwivedi J, Soni V. Pharmacological properties of *Datura stramonium L*. as a potential medicinal tree: An overview. Asian Pacific Journal of Tropical Biomedicine. 2012; 2(12):1002-1008. doi:10.1016/S2221-1691(13)60014-3

109. Al-Snafi AE. Medical importance of *Datura fastuosa* (syn: *Datura metel*) and *Datura stramonium*-A review. IOSR Journal of Pharmacy. 2017; 7(2):43-58. doi:10.9790/3013-0702014358

110. Chaachouay N, Zidane L. Plant-derived natural products: A source for drug discovery and development. Drugs and Drug Candidates. 2024; 3(1):184-207. doi:10.3390/ddc3010011
111. Balkrishna A, Sharma N, Srivastava D, Kukreti A, Srivastava S, Arya V. Exploring the safety, efficacy, and bioactivity of herbal medicines: Bridging traditional wisdom and modern science in healthcare. Future Integrative Medicine. 2024; 3(1):35-49. doi:10.14218/FIM.2023.00086
112. Samuelsson G. Drugs of natural origin: A textbook of pharmacognosy, 5th swedish pharmaceutical press. Stockholm, Sweden. 2004; 68(4):631. doi:10.1021/np058229l
113. Balick MJ, Cox PA. Plants, people, and culture: The science of ethnobotany: Garland Science; 2020. doi:10.4324/9781003049074
114. Kinghorn AD. Pharmacognosy in the 21st century. Journal of Pharmacy and Pharmacology. 2001; 53(2):135-148. doi:10.1211/0022357011775334
115. Newman DJ, Cragg GM, Snader KM. The influence of natural products upon drug discovery. Natural Product Reports. 2000; 17(3):215-234. doi:10.1039/A902202C
116. Butler MS. The role of natural product chemistry in drug discovery. Journal of Natural Products. 2004; 67(12):2141-2153. doi:10.1021/np040106y
117. Balunas MJ, Kinghorn AD. Drug discovery from medicinal plants. Life Sciences. 2005; 78(5):431-441. doi:10.1016/j.lfs.2005.09.012
118. Hill BG. Čat (*Catha edulis* Forsk). Journal of Ethiopian Studies. 1965; 3(2):13-23.
119. Devi MR, Bawari M, Paul S, Sharma G. Neurotoxic and medicinal properties of *Datura stramonium L*.–review. Assam University Journal of Science and Technology. 2011; 7(1):139-144.
120. Alfaifi H, Abdelwahab SI, Mohan S, Taha MME, Syame SM, Shaala LA, Alsanosy R. *Catha edulis* Forsk.(khat): Evaluation of its antidepressant-like activity. Pharmacognosy Magazine. 2017; 13(50):354. doi:10.4103/pm.pm_442_16
121. Ye S, Hu J, Liu Z, Liang M. Progress and research trends on *Catha edulis* (Vahl) Endl. (*Catha edulis*): A review and bibliometric analysis. Frontiers in Pharmacology. 2021; 12:1-12. doi:10.3389/fphar.2021.705376
122. [Internet]. *Catha edulis*. Plant Book; [27 November 2024]. Available from: https://www.plantbook.co.za/catha-edulis/.
123. Mishra D. *Datura stramonium* (common name: Jimson weed) medicinal uses, side effects and benefits. World Journal of Pharmaceutical Research. 2018; 7(12):1011-1019. doi:10.20959/wjpr201812-12710
124. Bussmann RW, Paniagua-Zambrana NY, Njoroge GN. *Datura stramonium l.* Solanaceae. Ethnobotany of the Mountain Regions of Africa. 2020. 1-9.

125. Sayyed A. Phytochemistry, pharmacological and traditional uses of *Datura stramonium L*. Review. Journal of Pharmacognosy and Phytochemistry. 2014; 2(5):123-125.
126. Setshogo MP. A review of some medicinal and or hallucinogenic solanaceous plants of Botswana: The genus *Datura L*. International Journal of Medicinal Plants and Natural Products. 2015; 1(2):15-23.
127. Gaire BP, Subedi L. A review on the pharmacological and toxicological aspects of *Datura stramonium L*. Journal of Integrative Medicine. 2013; 11(2):73-79. doi:10.3736/jintegrmed2013016
128. [Internet]. Jimsonweed (*Datura stramonium*). Midwest Invasive Species Information Network; [27 November 2024]. Available from: http://www.misin.msu.edu/facts/detail/?project=misin&id=160&cname=Jimsonweed.
129. Falkenburger BH, Saridaki T, Dinter E. Cellular models for Parkinson's disease. Journal of Neurochemistry. 2016; 139:121-130. doi:10.1111/jnc.13618
130. Lázaro DF, Pavlou MAS, Outeiro TF. Cellular models as tools for the study of the role of alpha-synuclein in Parkinson's disease. Experimental neurology. 2017; 298:162-171. doi:10.1016/j.expneurol.2017.05.007
131. Schlachetzki J, Saliba SW, Oliveira ACP. Studying neurodegenerative diseases in culture models. Brazilian Journal of Psychiatry. 2013; 35:92-100. doi:10.1590/1516-4446-2013-1159
132. Cetin S, Knez D, Gobec S, Kos J, Pišlar A. Cell models for Alzheimer's and Parkinson's disease: At the interface of biology and drug discovery. Biomedicine and Pharmacotherapy. 2022; 149:112924. doi:10.1016/j.biopha.2022.112924
133. Kovalevich J, Langford D. Considerations for the use of sh-sy5y neuroblastoma cells in neurobiology. Neuronal Cell Culture: Methods and Protocols. 2013:9-21. doi:10.1007/978-1-62703-640-5_2
134. Blum D, Torch S, Lambeng N, Nissou M-F, Benabid A-L, Sadoul R, Verna JM. Molecular pathways involved in the neurotoxicity of 6-OHDA, dopamine and MPTP: Contribution to the apoptotic theory in Parkinson's disease. Progress in Neurobiology. 2001; 65(2):135-172. doi:10.1016/S0301-0082(01)00003-X
135. Xicoy H, Wieringa B, Martens GJ. The SH-SY5Y cell line in Parkinson's disease research: A systematic review. Molecular Neurodegeneration. 2017; 12:1-11. doi:10.1186/s13024-017-0149-0
136. Sherer TB, Betarbet R, Testa CM, Seo BB, Richardson JR, Kim JH, Miller GW, Yagi T, Matsuno-Yagi A, Greenamyre JT. Mechanism of toxicity in rotenone models of Parkinson's disease. Journal of Neuroscience. 2003; 23(34):10756-10764.

doi:10.1523/JNEUROSCI.23-34-10756.2003

137. Alizadeh S, Anani-Sarab G, Amiri H, Hashemi M. Paraquat induced oxidative stress, DNA damage, and cytotoxicity in lymphocytes. Heliyon. 2022; 8(7). doi:10.1016/j.heliyon.2022.e09895

138. Mazzio EA, Reams RR, Soliman KF. The role of oxidative stress, impaired glycolysis and mitochondrial respiratory redox failure in the cytotoxic effects of 6-hydroxydopamine *in vitro*. Brain Research. 2004; 1004(1-2):29-44. doi:10.1016/j.brainres.2003.12.034

139. Gomez-Lazaro M, Bonekamp NA, Galindo MF, Jordán J, Schrader M. 6-Hydroxydopamine (6-OHDA) induces Drp1-dependent mitochondrial fragmentation in SH-SY5Y cells. Free Radical Biology and Medicine. 2008; 44(11):1960-1969. doi:10.1016/j.freeradbiomed.2008.03.009

140. Ikeda Y, Tsuji S, Satoh A, Ishikura M, Shirasawa T, Shimizu T. Protective effects of astaxanthin on 6-hydroxydopamine-induced apoptosis in human neuroblastoma SH-SY5Y cells. Journal of Neurochemistry. 2008; 107(6):1730-1740. doi:10.1111/j.1471-4159.2008.05743.x

141. Mu X, He G, Cheng Y, Li X, Xu B, Du G. Baicalein exerts neuroprotective effects in 6-hydroxydopamine-induced experimental parkinsonism *in vivo* and *in vitro*. Pharmacology Biochemistry and Behavior. 2009; 92(4):642-648. doi:10.1016/j.neuint.2005.11.008

142. Galindo MF, Jordán J, González-García C, Ceña V. Chromaffin cell death induced by 6-hydroxydopamine is independent of mitochondrial swelling and caspase activation. Journal of Neurochemistry. 2003; 84(5):1066-1073. doi:10.1046/j.1471-4159.2003.01592.x

143. Seth K, Agrawal A, Aziz M, Ahmad A, Shukla Y, Mathur N, Seth PK. Induced expression of early response genes/oxidative injury in rat pheochromocytoma (PC12) cell line by 6-hydroxydopamine: Implication for Parkinson's disease. Neuroscience Letters. 2002; 330(1):89-93. doi:10.1016/S0304-3940(02)00714-0

144. Lopes FM, Schröder R, da Frota Júnior MLC, Zanotto-Filho A, Müller CB, Pires AS, Meurer RT, Colpo GD, Gelain DP, Kapczinski F, Moreira JCF, Fernandes MC, Klamt F. Comparison between proliferative and neuron-like SH-SY5Y cells as an *in vitro* model for Parkinson disease studies. Brain Research. 2010; 1337:85-94. License URL: https://creativecommons.org/licenses/by/4.0/. doi:10.1016/j.brainres.2010.03.102

145. Lehmensiek V, Tan E-M, Liebau S, Lenk T, Zettlmeisl H, Schwarz J, Storch A. Dopamine transporter-mediated cytotoxicity of 6-hydroxydopamine *in vitro* depends on expression of mutant α-synucleins related to Parkinson's disease. Neurochemistry International. 2006; 48(5):329-340. doi:10.1016/j.neuint.2005.11.008

146. Blandini F, Armentero M-T, Martignoni E. The 6-hydroxydopamine model: News from the past. Parkinsonism and Related Disorders. 2008; 14:124-129. doi:10.1016/j.parkreldis.2008.04.015

147. Agu P, Afiukwa C, Orji O, Ezeh E, Ofoke I, Ogbu C, Ugwuja EI, Aja PM. Molecular docking as a tool for the discovery of molecular targets of nutraceuticals in diseases management. Scientific Reports. 2023; 13(1):133-198. doi:10.1038/s41598-023-40160-2

148. Lemos A, Melo R, Preto AJ, Almeida JG, Moreira IS, Dias Soeiro Cordeiro MN. *In silico* studies targeting G-protein coupled receptors for drug research against Parkinson's disease. Current Neuropharmacology. 2018; 16(6):786-848. doi:10.2174/1570159X16666180308161642

149. Kawahata I, Finkelstein DI, Fukunaga K. Dopamine D1–D5 receptors in brain nuclei: Implications for health and disease. Receptors. 2024; 3(2):155-181. doi:10.3390/receptors3020009

150. Mathur N, Sai SC, Shandily S, Santoki KM, Vadhavana NN, Shah S, Chandra M. *In silico* docking: Protocols for computational exploration of molecular interactions. Intech Open. 2024; doi:10.5772/intechopen.1005527

151. De Ruyck J, Brysbaert G, Blossey R, Lensink MF. Molecular docking as a popular tool in drug design, an in silico travel. Advances and Applications in Bioinformatics and Chemistry. 2016:1-11. doi:10.2147/AABC.S105289

152. Strober W. Trypan blue exclusion test of cell viability. Current Protocols in Immunology. 1997; 21(1):1-3. doi:10.1002/0471142735.ima03bs21

153. Vichai V, Kirtikara K. Sulforhodamine B colorimetric assay for cytotoxicity screening. Nature Protocols. 2006; 1(3):1112-1116. doi:10.1038/nprot.2006.179

154. Feola A, Cito L, Di Carlo A, Giovane A, Di Domenico M. Microscopy techniques. Advanced Imaging Techniques in Clinical Pathology. 2016:49-63. doi:10.1007/978-1-4939-3469-0_4

155. Yan X, Chen X, Fu C, Jing C, Zhao D, Sun L. Ginseng oligosaccharides protect neurons from glutamate-induced oxidative damage through the Nrf2/HO-1 signaling pathway. Food and Function. 2022; 13(16):8605-1865. doi:10.1039/D2FO01432G

156. McLennan HR, Esposti MD. The contribution of mitochondrial respiratory complexes to the production of reactive oxygen species. Journal of Bioenergetics and Biomembranes. 2000; 32:153-162. doi:10.1023/A:1005507913372

157. Lyublinskaya O, Ivanova JS, Pugovkina N, Kozhukharova I, Kovaleva Z, Shatrova A, Aksenov ND, Zenin VV, Kaulin AY, Gamaley AI, Nikolsky NN. Redox environment in stem and differentiated cells: A quantitative approach. Redox Biology. 2017; 12:758-769.

doi:10.1016/j.redox.2017.04.016

158. Cordier W, Steenkamp V. Bulb extracts of *Boophone disticha* induce hepatotoxicity by perturbing growth, without significantly impacting cellular viability. South African Journal of Botany. 2018; 114:1-8. doi:10.1016/j.sajb.2017.10.005
159. Carrasco RA, Stamm NB, Patel BK. One-step cellular caspase-3/7 assay. Biotechniques. 2003; 34(5):1064-1067. doi:10.2144/03345dd02
160. [Internet]. Mitochondrial staining kit - red fluorescence - cytopainter. Abcam; [27 November 2024]. Available from: https://www.abcam.com/en-us/products/assay-kits/mitochondrial-staining-kit-red-fluorescence-cytopainter-ab112145?srsltid=AfmBOoq-i3TUQUwkhGAkKU2YjH7aCtQv8vYTvcwg8Ij0Asl2P7bvlI#tab=support&drawer=publications.
161. Hardy LW, Malikayil A. The impact of structure-guided drug design on clinical agents. Current Drug Discovery 2003; 3:15-20. URL: https://hod4.net/~hod/papers/General/structure-guided_drug_design.pdf
162. Singh S, Malik BK, Sharma DK. Molecular drug targets and structure based drug design: A holistic approach. Bioinformation. 2006; 1(8):314-320. doi: 10.6026/97320630001314
163. Hughes JP, Rees S, Kalindjian SB, Philpott KL. Principles of early drug discovery. British Journal of Pharmacology. 2011; 162(6):1239-1249. doi: 10.1111/j.1476-5381.2010.01127.x
164. Nieoullon A. Dopamine and the regulation of cognition and attention. Progress in Neurobiology. 2002; 67(1):53-83. doi:10.1016/S0301-0082(02)00011-4
165. Getasetegn M. Chemical composition of *Catha edulis* (khat): A review. Phytochemistry Reviews. 2016; 15:907-920. doi:10.1007/s11101-015-9435-z
166. Sharma M, Dhaliwal I, Rana K, Delta AK, Kaushik P. Phytochemistry, pharmacology, and toxicology of *Datura* species: a review. Antioxidants. 2021; 10(8):1291. doi:10.3390/antiox10081291
167. Dhabbah AM, Badjah-Hadj-Ahmed AY, Alawi AI, Al Angari WA, Alrayes BF. Screening of psychoactive components in fresh khat using direct analysis in real time-time of flight-mass spectrometry. The Saudi Journal of Forensic Medicine and Sciences. 2018; 1(3):45-50. doi:10.4103/sjfms.sjfms_2_19
168. Field CR. Alkaloids of *Catha* spp. Dissertation. University of KwaZulu-Natal; 2001. URL: https://hdl.handle.net/10413/10206
169. Wabe NT. Chemistry, pharmacology, and toxicology of khat (*Catha edulis* Forsk): A review. Addict health. 2011; 3(3-4):137. URL: https://pmc.ncbi.nlm.nih.gov/articles/PMC3905534/

170. Pendl E, Pauritsch U, Kollroser M, Schmid MG. Determination of cathinone and cathine in khat plant material by LC–MS/MS: Fresh vs. dried leaves. Forensic Science International. 2021; 319:1106-1158. doi:10.1016/j.forsciint.2020.110658
171. Kerrigan S, Savage M, Cavazos C, Bella P. Thermal degradation of synthetic cathinones: Implications for forensic toxicology. Journal of Analytical Toxicology. 2016; 40(1):1-11. doi:10.1093/jat/bkv099
172. Ali WM, Al Habib K, Al-Motarreb A, Singh R, Hersi A, Al Faleh H, Asaad N, Al-Saif S, Almahmeed W, Sulaiman K, Amin H, Al-Lawati J, Bustani NA, Al-Sagheer NQ, Al-Qahtani A, Suwaidi JAI. Acute coronary syndrome and khat herbal amphetamine use: An observational report. Circulation. 2011; 124(24):2681-2689. doi:10.1161/CIRCULATIONAHA.111.039768
173. Antoine Lanfranchi D, Tomi F, Casanova J. Enantiomeric differentiation of atropine/hyoscyamine by (13) C NMR spectroscopy and its application to *Datura stramonium* extract. Phytochemical Analysis. 2010; 21(6):597-601. doi:10.1002/pca.1240
174. Yadav B, Singla A, Srivastava N, Gupta P. Pharmacognostic and phytochemical screening of *Datura stramonium* by TLC and GC-MS: A forensic approach. Biomedical and Pharmacology Journal. 2021; 14(4):2221-2226. doi:10.13005/bpj/2320
175. Miraldi E, Masti A, Ferri S, Comparini IB. Distribution of hyoscyamine and scopolamine in *Datura stramonium*. Fitoterapia. 2001; 72(6):644-648. doi:10.1016/S0367-326X(01)00291-X
176. Jakabová S, Vincze L, Farkas Á, Kilár F, Boros B, Felinger A. Determination of tropane alkaloids atropine and scopolamine by liquid chromatography–mass spectrometry in plant organs of *Datura* species. Journal of Chromatography A. 2012; 1232:295-301. doi:10.1016/j.chroma.2012.02.036
177. Leong HS, Philp M, Simone M, Witting PK, Fu S. Synthetic cathinones induce cell death in dopaminergic SH-SY5Y cells via stimulating mitochondrial dysfunction. International Journal of Molecular Sciences. 2020; 21(4):13-70. doi:10.3390/ijms21041370
178. Valente MJ, Bastos ML, Fernandes E, Carvalho Fl, Guedes de Pinho P, Carvalho Mr. Neurotoxicity of β-keto amphetamines: Deathly mechanisms elicited by methylone and mdpv in human dopaminergic SH-SY5Y cells. ACS Chemical Neuroscience. 2017; 8(4):850-859. doi:10.1021/acschemneuro.6b00421
179. Pallavi Sharma PS, Richa Bhardwaj RB, Ankita Yadav AY, Sharma R. Study of antioxidant activity of *Datura stramonium* Linn. Research Journal of Phytochemistry. 2014; 8(3):112-118. doi:=rjphyto.2014.112.118&org=10
180. Vélez-Huerta J, Ramírez-Cabrera MA, González-Santiago O, Favela-Hernández JMdJ,

Arredondo-Espinoza EU, Balderas-Rentería I. Neuroprotective activity of *Datura inoxia* and *Turnera diffusa* extracts in an *in vitro* model of neurotoxicity. Pharmacognosy Magazine. 2022; 18(78). doi:10.4103/pm.pm_543_21

181. Sengupta T, Vinayagam J, Nagashayana N, Gowda B, Jaisankar P, Mohanakumar K. Antiparkinsonian effects of aqueous methanolic extract of *Hyoscyamus niger* seeds result from its monoamine oxidase inhibitory and hydroxyl radical scavenging potency. Neurochemical Research. 2011; 36:177-186. doi:10.1007/s11064-010-0289-x
182. Luo Y, Zhou S, Takeda R, Okazaki K, Sekita M, Sakamoto K. Protective effect of amber extract on human dopaminergic cells against 6-hydroxydopamine-induced neurotoxicity. Molecules. 2022; 27(6):1817. doi:10.3390/molecules27061817
183. Wei L, Ding L, Mo M-s, Lei M, Zhang L, Chen K, Xu P. Wnt3a protects SH-SY5Y cells against 6-hydroxydopamine toxicity by restoration of mitochondria function. Translational Neurodegeneration. 2015; 4(11):1-8. doi:10.1186/s40035-015-0033-1
184. Pasban-Aliabadi H, Esmaeili-Mahani S, Sheibani V, Abbasnejad M, Mehdizadeh A, Yaghoobi MM. Inhibition of 6-hydroxydopamine-induced PC12 cell apoptosis by olive (*Olea europaea L*.) leaf extract is performed by its main component oleuropein. Rejuvenation Research. 2013; 16(2):134-142. doi:10.1089/rej.2012.13
185. Ju MS, Lee P, Kim HG, Lee KY, Hur J, Cho S-H, Sung SH, Oh MS. Protective effects of standardized *Thuja orientalis* leaves against 6-hydroxydopamine-induced neurotoxicity in SH-SY5Y cells. Toxicology *in Vitro*. 2010; 24(3):759-765. doi:10.1016/j.tiv.2009.12.026
186. Xie H-r, Hu L-s, Li G-y. SH-SY5Y human neuroblastoma cell line: *In vitro* cell model of dopaminergic neurons in Parkinson's disease. Chinese Medical Journal. 2010; 123(8):1086-1092. doi:10.3760/cma.j.issn.0366-6999.2010.08.021
187. Silva J, Alves C, Pinteus S, Mendes S, Pedrosa R. Neuroprotective effects of seaweeds against 6-hydroxydopamine-induced cell death on an *in vitro* human neuroblastoma model. BMC Complementary and Alternative Medicine. 2018; 18:1-10. doi:10.1186/s12906-018-2103-2
188. Engidawork E. Pharmacological and toxicological effects of *Catha edulis* f. (khat). Phytotherapy Research. 2017; 31(7):1019-1028. doi:10.1002/ptr.5832
189. Paz-Ramos MI, Cruz SL, Violante-Soria V. Amphetamine-type stimulants: Novel insights into their actions and use patterns. Clinical and Translational Investigation. 2023; 75(3):143-157. doi:10.24875/ric.23000110
190. Umarudeen AM, Modibbo MR. Evaluation of the neurobehavioural toxicity potential of aqueous ethanol extracts of leaf/seed of *Datura metel*, *Mucuna pruriens,* and *Tapinanthus globiferus* growing on *Azadirachta indica* host tree in mice. International Journal of

Biochemistry Research and Review. 2023; 32(8):13-27. doi:10.9734/ijbcrr/2023/v32i8831

191. Latchoumycandane C, Anantharam V, Jin H, Kanthasamy A, Kanthasamy A. Dopaminergic neurotoxicant 6-ohda induces oxidative damage through proteolytic activation of PKCδ in cell culture and animal models of Parkinson's disease. Toxicology and Applied Pharmacology. 2011; 256(3):314-323. doi:10.1016/j.taap.2011.07.021
192. Susin SA, Lorenzo HK, Zamzami N, Marzo I, Snow BE, Brothers GM, Mangion J, Jacotot E, Costantini M, Loeffler M, Larochette N, Goodlett DR, Aebersold R, Siderovski DP, Penninger JM, Kroemer G. Molecular characterization of mitochondrial apoptosis-inducing factor. Nature. 1999; 397(6718):441-446. doi:10.1038/17135
193. Gomez-Lazaro M, Galindo MF, Concannon CG, Segura MF, Fernandez-Gomez FJ, Llecha N, Comella JX, Prehn JHM, Jordan J. 6-hydroxydopamine activates the mitochondrial apoptosis pathway through p38 MAPK-mediated, p53-independent activation of BAX and PUMA. Journal of Neurochemistry. 2008; 104(6):1599-1612. doi:10.1111/j.1471-4159.2007.05115.x
194. Moosavi M, Farrokhi MR, Tafreshi N. The effect of curcumin against 6-hydroxydopamine induced cell death and Akt/GSK disruption in human neuroblastoma cells. Physiology and Pharmacology. 2018; 22(3):163-171.
195. Lochner M, Thompson AJ. The muscarinic antagonists scopolamine and atropine are competitive antagonists at 5-HT3 receptors. Neuropharmacology. 2016; 108:220-228. doi:10.1016/j.neuropharm.2016.04.027
196. Suthprasertporn N, Mingchinda N, Fukunaga K, Thangnipon W. Neuroprotection of SAK3 on scopolamine-induced cholinergic dysfunction in human neuroblastoma SH-SY5Y cells. Cytotechnology. 2020; 72:155-164. doi:10.1007/s10616-019-00366-7
197. Papadimitriou M, Hatzidaki E, Papasotiriou I. Linearity comparison of three colorimetric cytotoxicity assays. Journal of Cancer Therapy. 2019; 10(7):580-590. doi:10.4236/jct.2019.107047
198. Hanrott K, Gudmunsen L, O'Neill MJ, Wonnacott S. 6-hydroxydopamine-induced apoptosis is mediated via extracellular auto-oxidation and caspase 3-dependent activation of protein kinase Cδ. Journal of Biological Chemistry. 2006; 281(9):5373-5382.
199. Ali A, Martins AMC, Alam W, Khan H. Neuroprotective effects of alkaloids. Phytonutrients and Neurological Disorders. 2023. 245-257.
200. Jaisin Y, Ratanachamnong P, Prachayasittikul S, Watanapokasin R, Kuanpradit C. Protective effects of ethyl acetate extract of *Eclipta prostrata* against 6-hydroxydopamine-induced neurotoxicity in SH-SY5Y cells. Science Asia. 2016; 42:259. doi:10.2306/scienceasia1513-1874.2016.42.259

201. Luo Y, Sakamoto K. Ethyl pyruvate protects SH-SY5Y cells against 6-hydroxydopamine-induced neurotoxicity by upregulating autophagy. Plos one. 2023; 18(2):1-10. doi:10.1371/journal.pone.0281957

202. Yoshioka Y, Negoro R, Kadoi H, Motegi T, Shibagaki F, Yamamuro A, Ishimaru Y, Maeda S. Noradrenaline protects neurons against H_2O_2-induced death by increasing the supply of glutathione from astrocytes via β3-adrenoceptor stimulation. Journal of Neuroscience Research. 2021; 99(2):621-637. doi:10.1002/jnr.24733

203. Chen X, Guo C, Kong J. Oxidative stress in neurodegenerative diseases. Neural Regeneration Research. 2012; 7(5):376-385. doi:10.3969/j.issn.1673-5374.2012.05.009

204. Mohd Sairazi NS, Sirajudeen K. Natural products and their bioactive compounds: Neuroprotective potentials against neurodegenerative diseases. Evidence-Based Complementary and Alternative Medicine. 2020; 2020(1):1-30. doi:10.1155/2020/6565396

205. Carpa R, Dumitru D-V, Burtescu RF, Maior MC, Dobrotă C, Olah N-K. Bio-chemical analysis of *Datura stramonium* extract. Studia Universitatis Babes-Bolyai Biologia. 2017; 62(2):5-19. doi:10.24193/subbbiol.2017.2.01

206. Atlabachew M, Chandravanshi BS, Redi M. Selected secondary metabolites and antioxidant activity of khat (*Catha edulis* forsk) chewing leaves extract. International Journal of Food Properties. 2014; 17(1):45-64. doi:10.1080/10942912.2011.614367

207. Abdelwahab SI, Alsanosy R, Mohamed Elhassan Taha M, Mohan S. Khat induced toxicity: Role on its modulating effects on inflammation and oxidative stability. BioMed Research International. 2018; 2018(1):1-7. doi:10.1155/2018/5896041

208. Vinokur Y. Hydrophilic and lipophilic antioxidant capacity and content of phenolic compounds in fresh khat leaves (*Catha edulis* forsk.). Ethnobotanical Leaflets. 2008; 2008(1):73.

209. Hailu YM, Atlabachew M, Chandravanshi BS, Redi-Abshiro M. Composition of essential oil and antioxidant activity of khat (*Catha edulis* forsk), Ethiopia. Chemistry International. 2017; 3(1):25.

210. Noui A, Boudiar T, Boulebd H, Gali L, del Mar Contreras M, Segura-Carretero A, Nieto G, Akkal S. HPLC–DAD–ESI/MS profiles of bioactive compounds, antioxidant and anticholinesterase activities of ephedra alata subsp. Alenda growing in Algeria. Natural Product Research. 2022; 36(22):5910-5915. doi:10.1080/14786419.2021.2024184

211. Nataraj J, Manivasagam T, Thenmozhi AJ, Essa MM, Khan MA. Antiparkinsonic effect of black tea and its components. Food and Parkinson's disease: Nova Science Publishers, Inc.; 2016. 115-131.

212. Matcha R, Saride GK, Ranjan S. *In vitro* anti-inflammatory and antioxidant activity of leaf extracts of *Datura metal*. Asian Journal of Pharmaceutical and Clinical Research. 2013; 6(4):146-149.

213. Roy S, Pawar S, Chowdhary A. Evaluation of *in vitro* cytotoxic and antioxidant activity of *Datura metel* Linn. and *Cynodon Dactylon* Linn. extracts. Pharmacognosy Research. 2016; 8(2):123. doi:10.4103/0974-8490.175610

214. Forman HJ, Zhang H, Rinna A. Glutathione: Overview of its protective roles, measurement, and biosynthesis. Molecular aspects of medicine. 2009; 30(1-2):1-12. doi:10.1016/j.mam.2008.08.006

215. Tatton WG, Chalmers-Redman R, Brown D, Tatton N. Apoptosis in Parkinson's disease: Signals for neuronal degradation. Annals of Neurology: Official Journal of the American Neurological Association and the Child Neurology Society. 2003; 53(3):61-72. doi:10.1002/ana.10489

216. Hartmann A, Hunot S, Michel PP, Muriel M-P, Vyas S, Faucheux BA, Mouatt-Prigent A, Turmel H, Srinivasan A, Ruberg M, Evan GI, Agid Y, Hirsch EC. Caspase-3: A vulnerability factor and final effector in apoptotic death of dopaminergic neurons in Parkinson's disease. Proceedings of the National Academy of Sciences. 2000; 97(6):2875-2880. doi:10.1073/pnas.040556597

217. Liu Y, Guo Y, An S, Kuang Y, He X, Ma H, Li J, Lu J, Zhang N, Jiang C. Targeting caspase-3 as dual therapeutic benefits by RNAi facilitating brain-targeted nanoparticles in a rat model of Parkinson's disease. Plos One. 2013; 8(5):e62905. doi:10.1371/journal.pone.0062905

218. Saito Y, Nishio K, Ogawa Y, Kinumi T, Yoshida Y, Masuo Y, Niki E. Molecular mechanisms of 6-hydroxydopamine-induced cytotoxicity in PC12 cells: Involvement of hydrogen peroxide-dependent and-independent action. Free Radical Biology and Medicine. 2007; 42(5):675-685. doi:10.1016/j.freeradbiomed.2006.12.004

219. Rathinam R, Ghosh S, Neumann WL, Jamesdaniel S. Cisplatin-induced apoptosis in auditory, renal, and neuronal cells is associated with nitration and downregulation of LMO4. Cell death discovery. 2015; 1(1):1-8. doi:10.1038/cddiscovery.2015.52

220. White JB, Beckford J, Yadegarynia S, Ngo N, Lialiutska T, d'Alarcao M. Some natural flavonoids are competitive inhibitors of caspase-1,-3, and-7 despite their cellular toxicity. Food Chemistry. 2012; 131(4):1453-1459. doi:10.1016/j.foodchem.2011.10.026

221. Smith MP, Cass WA. Oxidative stress and dopamine depletion in an intrastriatal 6-hydroxydopamine model of Parkinson's disease. Neuroscience. 2007; 144(3):1057-1066. doi:10.1016/j.neuroscience.2006.10.004

222. Kannan K, Jain SK. Oxidative stress and apoptosis. Pathophysiology. 2000; 7(3):153-163. doi:10.1016/S0928-4680(00)00053-5

223. Roy A, Khan A, Ahmad I, Alghamdi S, Rajab BS, Babalghith AO, Alshahrani MY, Islam S , Islam MR. Flavonoids a bioactive compound from medicinal plants and its therapeutic applications. BioMed Research International. 2022; 2022(1):1-9. doi:10.1155/2022/5445291

224. Alum EU, Famurewa AC, Orji OU, Aja PM, Nwite F, Ohuche SE, Ukasoanya SC, Nnaji LO, Joshua D, Igwe KU, Chima SF. Nephroprotective effects of *Datura stramonium* leaves against methotrexate nephrotoxicity via attenuation of oxidative stress-mediated inflammation and apoptosis in rats. Avicenna Journal of Phytomedicine. 2023; 13(4):377. doi:10.22038/AJP.2023.21903

225. Shih Y-T, Chen I-J, Wu Y-C, Lo Y-C. San-Huang-Xie-Xin-Tang protects against activated microglia-and 6-ohda-induced toxicity in neuronal SH-SY5Y cells. Evidence-Based Complementary and Alternative Medicine. 2011; 2011(1):429384. doi:10.1093/ecam/nep025

226. Guo S, Bezard E, Zhao B. Protective effect of green tea polyphenols on the SH-SY5Y cells against 6-ohda induced apoptosis through ROS–NO pathway. Free Radical Biology and Medicine. 2005; 39(5):682-695. doi:10.1016/j.freeradbiomed.2005.04.022

227. Zorov DB, Juhaszova M, Sollott SJ. Mitochondrial reactive oxygen species (ROS) and R4OS-induced ROS release. Physiological Reviews. 2014; 94(3):909-950. doi:10.1152/physrev.00026.2013

228. Korshunov SS, Skulachev VP, Starkov AA. High protonic potential actuates a mechanism of production of reactive oxygen species in mitochondria. FEBS letters. 1997; 416(1):15-18. doi:10.1016/S0014-5793(97)01159-9

229. Norat P, Soldozy S, Sokolowski JD, Gorick CM, Kumar JS, Chae Y, Yağmurlu K, Prada F, Walker M, Levitt MR, Price RJ, Tvrdik P, Kalani MYS. Mitochondrial dysfunction in neurological disorders: Exploring mitochondrial transplantation. NPJ Regenerative Medicine. 2020; 5(1):22. doi:10.1038/s41536-020-00107-x

230. Koklesova L, Liskova A, Samec M, Zhai K, Al-Ishaq RK, Bugos O, Šudomová M, Biringer K, Pec M, Adamkov M, Hassan STS, Saso L, Giordano FA, Büsselberg D, Kubatka P, Golubnitschaja O. Protective effects of flavonoids against mitochondriopathies and associated pathologies: Focus on the predictive approach and personalized prevention. International Journal of Molecular Sciences. 2021; 22(16):1-29. doi:10.3390/ijms22168649

231. Du X, Li Y, Xia Y-L, Ai S-M, Liang J, Sang P, Ji X-L, Liu SQ. Insights into protein–ligand

interactions: Mechanisms, models, and methods. International Journal of Molecular Sciences. 2016; 17(2):144. doi:10.3390/ijms17020144

232. Isaacson SH, Hauser RA, Pahwa R, Gray D, Duvvuri S. Dopamine agonists in Parkinson's disease: Impact of D1-like or D2-like dopamine receptor subtype selectivity and avenues for future treatment. Clinical Parkinsonism and Related Disorders. 2023:100-212. doi:10.1016/j.prdoa.2023.100212
233. Lees A. Dopamine agonists in Parkinson's disease: A look at apomorphine. Fundamental and Clinical Pharmacology. 1993; 7(3-4):121-128. doi:10.1111/j.1472-8206.1993.tb00226.x
234. Zhuang Y, Krumm B, Zhang H, Zhou XE, Wang Y, Huang X-P, Liu Y, Cheng X, Jiang Y, Jiang H, Zhang C, Yi W, Roth BL, Zhang Y, Xu HE. Mechanism of dopamine binding and allosteric modulation of the human D1 dopamine receptor. Cell Research. 2021; 31(5):593-596. doi:10.1038/s41422-021-00482-0
235. Wang S, Che T, Levit A, Shoichet BK, Wacker D, Roth BL. Structure of the D2 dopamine receptor bound to the atypical antipsychotic drug risperidone. Nature. 2018; 555(7695):269-273. doi:10.1038/nature25758
236. Kalyanasundar B, Perez CI, Arroyo B, Moreno MG, Gutierrez R. The appetite suppressant D-norpseudoephedrine (Cathine) acts via D1/D2-like dopamine receptors in the nucleus accumbens shell. Frontiers in Neuroscience. 2020; 14:572328. doi:10.3389/fnins.2020.572328
237. Aoyama S, Kase H, Borrelli E. Rescue of locomotor impairment in dopamine D2 receptor-deficient mice by an adenosine a2a receptor antagonist. Journal of Neuroscience. 2000; 20(15):5848-5852. doi:10.1523/JNEUROSCI.20-15-05848.2000
238. Fox S, Lang AE. Therapy of the motor features of Parkinson's disease. Movement Disorders. 2010. 252-272. doi:10.1016/b978-1-4160-6641-5.00015-5
239. Jenner P. The rationale for the use of dopamine agonists in Parkinson's disease. Neurology. 1995; 45(3):6-12. doi:10.1212/wnl.45.3_suppl_3.s6
240. Fornai F, di Poggio AB, Pellegrini A, Ruggieri S, Paparelli A. Noradrenaline in Parkinson's disease: From disease progression to current therapeutics. Current medicinal chemistry. 2007; 14(22):2330-4. doi:10.2174/092986707781745550
241. Delaville C, Deurwaerdère PD, Benazzouz A. Noradrenaline and Parkinson's disease. Frontiers in Systems Neuroscience. 2011; 5(31). doi:10.3389/fnsys.2011.00031
242. Lanau F, Zenner MT, Civelli O, Hartman DS. Epinephrine and norepinephrine act as potent agonists at the recombinant human dopamine D4 receptor. Journal of Neurochemistry. 1997;68(2):804-812. doi:10.1046/j.1471-4159.1997.68020804.x

243. Gaskill PJ, Khoshbouei H. Dopamine and norepinephrine are embracing their immune side and so should we. Current opinion in neurobiology. 2022; 77:102626. doi: 10.1016/j.conb.2022.102626

244. Durdagi S, Salmas RE, Stein M, Yurtsever M, Seeman P. Binding interactions of dopamine and apomorphine in D2 high and D2 low states of human dopamine D2 receptor using computational and experimental techniques. ACS Chemical Neuroscience. 2016; 7(2):185-195. doi:10.1021/acschemneuro.5b00271

245. Jóźwiak K, Płazińska A. Structural insights into ligand—receptor interactions involved in biased agonism of G-protein coupled receptors. Molecules. 2021; 26(4):851. doi:10.3390/molecules26040851

246. Senior T, Botha MJ, Kennedy AR, Calvo-Castro J. Understanding the contribution of individual amino acid residues in the binding of psychoactive substances to monoamine transporters. ACS Omega. 2020; 5(28):17223-17231. doi:10.1021/acsomega.0c01370

247. Axelrod J, Weinshilboum R. Catecholamines. New England Journal of Medicine. 1972; 287(5):237-242. doi:10.1056/NEJM197208032870508

Appendix I: Faculty of Health Sciences Research Ethics committee approval letter

UNIVERSITEIT VAN PRETORIA
UNIVERSITY OF PRETORIA
YUNIBESITHI YA PRETORIA
Faculty of Health Sciences

Institution: The Research Ethics Committee, Faculty Health Sciences, University of Pretoria complies with ICH-GCP guidelines and has US Federal wide Assurance.
- FWA 00002567, Approved dd 18 March 2022 and Expires 18 March 2027.
- IORG #: IORG0001762 OMB No. 0990-0279 Approved for use through June 30, 2025 and Expires 07/28/2026.

Faculty of Health Sciences **Research Ethics Committee**

20 August 2024

Approval Certificate
Annual Renewal

Dear Miss T Mogale,

Ethics Reference No.: 359/2023 – Line 2
Title: Assessing the effects of two plants containing psychoactive compounds on the SH-SY5Y Parkinson's disease neuroblastoma cell model

The **Annual Renewal** as supported by documents received between 2024-07-10 and 2024-08-13 for your research, was approved by the Faculty of Health Sciences Research Ethics Committee on 2024-08-13 as resolved by its quorate meeting.

Please note the following about your ethics approval:
- Renewal of ethics approval is valid for 1 year, subsequent annual renewal will become due on 2025-08-20.
- The Research Ethics Committee (REC) must monitor your research continuously. To this end, you must submit as may be applicable for your kind of research:
  a) annual reports;
  b) reports requested *ad hoc* by the REC;
  c) all visitation and audit reports by a regulatory body (e.g. the HPCSA, FDA, SAHPRA) within 10 days of receiving one;
  d) all routine monitoring reports compiled by the Clinical Research Associate or Site Manager within 10 days of receiving one.
- The REC may select your research study for an audit or a site visitation by the REC.
- The REC may require that you make amendments and take corrective actions.
- The REC may suspend or withdraw approval.
- Please remember to use your protocol number (359/2023) on any documents or correspondence with the Research Ethics Committee regarding your research.

Ethics approval is subject to the following:
- The ethics approval is conditional on the research being conducted as stipulated by the details of all documents submitted to the Committee. In the event that a further need arises to change who the investigators are, the methods or any other aspect, such changes must be submitted as an Amendment for approval by the Committee.

We wish you the best with your research.

Yours sincerely

On behalf of the FHS REC, Dr R Sommers
MBChB, MMed (Int), MPharmMed, PhD
Deputy Chairperson *of the Faculty of Health Sciences Research Ethics Committee, University of Pretoria*

The Faculty of Health Sciences Research Ethics Committee complies with the SA National Act 61 of 2003 as it pertains to health research and the United States Code of Federal Regulations Title 45 and 46. This committee abides by the ethical norms and principles for research, established by the Declaration of Helsinki, the South African Medical Research Council Guidelines as well as the Guidelines for Ethical Research: Principles Structures and Processes, Second Edition 2015 (Department of Health).

Research Ethics Committee
Room 4-60, Level 4, Tswelopele Building
University of Pretoria, Private Bag X323
Gezina 0031, South Africa
Tel +27 (0)12 356 3084
Email: deepeka.behari@up.ac.za
www.up.ac.za

Fakulteit Gesondheidswetenskappe
Lefapha la Disaense tša Maphelo

Appendix II: Reagents and their preparation

1. Solvents

β-mercaptoethanol, acetic acid, acetonitrile, dichloromethane, dimethyl sulfoxide, ethyl acetate, formic acid, methanol, and methyl tert butyl ether was purchased from Sigma Aldrich (St Louis, USA) and were used without further purification.

2. Cellular cytotoxicity and cytoprotection assays

2.1 Cell culture

2.1.1 Ham's F12 medium and Dulbecco's modified Eagle's medium (DMEM)

Dulbecco's Modified Eagle's Medium/Ham's Nutrient Mixture F12 (1:1) was purchased from Sigma-Aldrich (St Louis, USA), and was supplemented with 1% penicillin/streptomycin, and 10% FCS prior to use.

2.1.2 Foetal calf serum

FCS was purchased from Sigma Aldrich (St Louis, USA). Solutions were inactivated through heating at 56°C for 45 min and stored at -20°C.

2.1.3 Penicillin/streptomycin

Penicillin/streptomycin was purchased from Sigma Aldrich (St Louis, USA) at 10 000 units penicillin and 10 000 µg streptomycin per 1 mL.

2.1.4 Trypan blue

Trypan blue was made up at (0.1% w/v) solution by dissolving 500 mg trypan blue powder in 50 mL PBS and subsequently the solution was filtered through a 0.45 µm syringe filter to remove any insoluble particles. The solution was stored at room temperature in the dark.

2.1.5 TrypLE

TrypLE solution was purchased from Thermo Fisher Scientific (Waltham, USA) in liquid form and used undiluted. The solution was stored at room temperature.

2.2 Cytotoxicity and cytoprotection assays

2.2.1 6-Hydroxydopamine (6-OHDA)

6-Hydroxydopamine powder was obtained from Sigma-Aldrich (St Louis, USA), and stock solutions were made up to concentrations identified in 1% ascorbic acid. Aliquots will be stored at -80°C and working solutions will be freshly prepared before Use.

2.2.2 Acetic acid solution

A 1% acetic acid solution was prepared by diluting 1 mL of glacial acetic acid (Sigma Aldrich, St Louis) with distilled water to a final volume of 100 mL. The stock solution was stored at room temperature.

2.2.3 Trichloroacetic acid (TCA)

Trichloroacetic acid solution (50% w/v) was made up by dissolving 50 g in 100mL of distilled water.

2.2.4 Tris-Base

Tris-Base powder was purchased from Merck Chemicals (Darmstadt, Germany). The solution was prepared by dissolving 2.42 g in 1 L of distilled water, and was stored at 4°C. The pH was adjusted to 7.4 using sodium hydroxide and hydrochloric acid.

2.2.5 Saponin

Saponin powder was obtained from Sigma Aldrich (St. Louis, USA). A 1% solution was prepared by dissolving 1 g into 100 mL of distilled water and subsequently stored at 4 ℃.

2.2.6 Sulforhodamine B (SRB) dye

The SRB dye was prepared by dissolving 57 mg of the SRB powder (Sigma Aldrich, St Louis) in 100 mL of a 1% (v/v) acetic acid solution and stored at 4°C until use.

3. Intracellular ROS assay

3.1 Dihydro dichlorofluorescein diacetate (H_2DCFDA)

Dihydro dichlorofluorescein diacetate substrate solution was prepared by dissolving 3.90 mg H_2DCFDA powder with DMSO to a final volume of 800 µL.

3.2 Phosphate-buffered saline (PBS) buffer

Phosphate-buffered saline was made by dissolving 9.23 g of the FTA haemagglutinin powder (BD Bioscience, New Jersey, USA) in distilled water, to make a final volume of 1L. The solution will be sterilised by autoclaving, at 120°C/2 bar for 30 min.

3.3 Potassium persulfate

Potassium persulfate was purchased from Sigma Aldrich (St Louis, USA). A stock solution (10 mM) was prepared by dissolving 27.03 mg powder with PBS buffer to a final volume of 10 mL. To make 1 mM solution, 200 µL of potassium persulfate solution was diluted with 800 µL of FCS-negative media.

4. Caspase 3/7 activity

4.1 Acetyl-Asp-Glu-Val-Asp-7-amido-4-methylcoumarin (Ac-DEVD-AMC)

Ac-DEVD-AMC was purchased from Sigma-Aldrich (St. Louis, USA). A 5 mM stock solution was prepared by dissolving 5.07 mg in 2 mL DMSO and stored at -80°C in 25 µL aliquots.

4.2 Cold lysis buffer

HEPES, 3-[(3-cholamidopropyl)-dimethylammonio]-1-propanesulfonate (CHAPS), EDTA and PMSF were purchased from Sigma-Aldrich (St. Louis, USA), while β-mercaptoethanol (4.3 mM) was purchased from Merck Chemicals (South Africa). A solution of 10 mM HEPES, 2 mM CHAPS, 5 mM EDTA, 0.5 mM PMSF and 4.3 mM β-mercaptoethanol was prepared by dissolving 70.06 mg EDTA, 61.49 mg CHAPS, and 119.15 mg HEPES in 2.984 mL distilled water. The incomplete buffer was stored at 4°C. Thirty minutes prior to experimentation 15 µL PMSF (0.5 mM) and 1 µL β-mercaptoethanol (4.3 mM) was added to make up 3 mL cold assay buffer.

4.3 Substrate buffer

A solution of 10 mM HEPES, 5 mM EDTA, was prepared by dissolving 238.30 mg HEPES and 146.12 mg EDTA in 100 mL distilled water. The incomplete buffer was stored at 4°C. Thirty minutes prior to experimentation 50 µL PMSF (0.5 mM), 3 µL β-mercaptoethanol (4.3 mM) and 20 µL Ac-DEVD-AMC (10 µM) was added to make up 10 mL substrate buffer.

4.4 Cisplatin

Cisplatin was prepared by diluting 10 µL of stock solution (20 mM) with 6.99 mL FCS negative media to make up 29.85 µM.

5. Mitochondrial integrity

5.1 Cytopainter red dye

The dye was prepared by diluting 6 µL of dye in FCS negative media to make up 10 mL solution.

6. Pure compounds

6.1 Atropine

Atropine powder was purchased from Thermo Fisher Scientific (Waltham, USA). A stock solution (1 mM) was prepared by dissolving 5.6 mg in 8 mL DMSO and stored at -80°C in 150 µL aliquots.

6.2 Scopolamine

Scopolamine powder was purchased from Thermo Fisher Scientific (Waltham, USA). A stock solution (1 mM) was prepared by dissolving 3.51 mg in 8 mL DMSO and stored at -80°C in 150 µL aliquots.